SNOW HYDROLOGY OF A MOUNTAINOUS RAIN-ON-SNOW ENVIRONMENT - THE WAIMAKARIRI CATCHMENT, NEW ZEALAND

A thesis

presented for the degree of

Doctor of Philosophy in Geography

in the University of Canterbury,

Christchurch, New Zealand

by

R.D. Moore

University of Canterbury

1984

ACKNOWLEDGMENTS

Many individuals and organizations contributed to this project. I was financially supported by a Commonwealth Scholarship and the project was funded by the Ministry of Works and Development for the National Water and Soil Conservation Organization.

My supervisor, Dr Ian Owens, administered the research contract and read drafts of the thesis. In addition, Ian assisted in the carrying of what eventually became several hundred kilograms of equipment from Arthur's Pass to Temple Basin.

My colleague, Glenn McGregor, also carried a few loads in the interests of science. More importantly, Glenn introduced me to the concept of rock and roll snow science. Glenn and the other PhD students generated a supportive work environment.

The technical staff of the University of Canterbury Geography Department assisted with many phases of the field work and thesis preparation. I especially acknowledge the craftsmanship of the late Arthur Brown, who designed and built much of the field equipment.

Trev Chinn, John Fenwick and Dr Mauri McSaveney of the Water and Soil Science Centre, MWD, assisted with equipment loans. Graeme Davenport processed the Camp Stream precipitation and streamflow data. Mark Rogers deserves special thanks for carrying out the first phases of a multi-media data transfer. Dave Duffield and Mike Bowden of the North Canterbury Catchment Board cooperated with some aspects of field work and supplied streamflow data.

Assistance with data processing came from Paul Gorman

and Jackie Owens. Martin Bakker of the Canterbury University Ski Club and Robyn Harrington of the University Computing Centre carried out the latter phases of a data transfer. Special commendation goes to Charles Brown and John Roper-Lyndsay of the Computing Centre for their patience in extricating me from computational snags.

Others who provided valuable discussion include Professors Hans Panofsky and Tony Raynor and Drs M.H. Smith, Andy Bowen, Peter Jackson, Andy Sturman and Sten Bergström. Drs Andy Pearce and Blair Fitzharris thoughtfully commented on some early chapter drafts. My former colleagues from U.B.C. - Ludwig Braun, Garry Barrett and Dr Thom Gallie - supplied encouragement and criticism at a crucial point of the project.

Steve Anderson and Kath Armon of Arthur's Pass generously accommodated me during field work, and their open friendship helped me survive some trying times. The staff of Arthur's Pass National Park freely cooperated in any way they could. The community of Arthur's Pass is thanked for their Thursday beer and social nights, which drowned many a sorrow. The staff and members of the Canterbury University and Christchurch Ski Clubs are thanked for cooperation. I thank my compatriot Hamish Kassa for his perseverance in trying to teach me to ski like him.

Finally, I thank Drs Michael Church and Garry K.C. Clarke for the inspiration to continue in academics, and Julie Gardner, who encouraged and debated, amongst other things.

TABLE OF CONTENTS

LIST OF FIGURES

PAGE

LIST OF TABLES

PAGE

LIST OF APPENDICES

PAGE

LIST OF SYMBOLS

Note: The units given below are usually the appropriate SI units. Where other units are used for convenience, for example for precipitation intensity, an example of a non-SI unit is also given. Only the operational units are given for empirical parameters such as the degree-day factor. No units are given for statistical quantities such as regression coefficients or for dimensionless quantities.

a	5,470,000 m^{-1} s^{-1}
A	intercept of regression line; ablation (kg m^{-2} s^{-1})
B	slope of regression line; base of transfer function (d)
BETA	infiltration parameter
BMAX	maximum value of B (d)
c	fractional total cloud cover
c_i	cloud cover of type i
c_{pa}	specific heat of air (J kg^{-1} $°C^{-1}$)
c_{pi}	specific heat of ice (J kg^{-1} $°C^{-1}$)
c_{pw}	specific heat at water (J kg^{-1} $°C^{-1}$)
C	flux wave celerity ($m \cdot s^{-1}$; $m \cdot h^{-1}$)
C_c	celerity of concentrated flow ($m \cdot s^{-1}$; $m \cdot h^{-1}$)
C_d	shock wave celerity in dry snow ($m \cdot s^{-1}$; $m \cdot h^{-1}$)
C_p	psychrometric constant (mb/°C)
C_s	shock front celerity ($m \cdot s^{-1}$; $mm \cdot h^{-1}$)
C_u	celerity of uniform flow ($m \cdot s^{-1}$; $mm \cdot h^{-1}$)
C_v	coefficient of variation
CF	Craigieburn Forest
CL	soil moisture evaporative threshold (mm)

CMI	convective melt index ($°C \cdot m \cdot s^{-1}$)
CRF	refreezing coefficient ($mm \cdot d^{-1} °C^{-1}$)
CRT	channel routing coefficient ($d \cdot s \cdot L^{-1}$)
C1	wind function coefficient ($W \cdot m^{-2} mb^{-1}$)
C2	wind function coefficient ($W \cdot m^{-2} mb^{-2}$)
D_E	bulk exchange coefficient for water vapour ($m \cdot s^{-1}$)
D_H	bulk exchange coefficient for sensible heat ($m \cdot s^{-1}$)
D_M	bulk exchange coefficient for momentum ($m \cdot s^{-1}$)
D_N	neutral case bulk exchange coefficient ($m \cdot s^{-1}$)
D_S	stable case bulk exchange coefficient ($m \cdot s^{-1}$)
D_U	unstable case bulk exchange coefficient ($m \cdot s^{-1}$)
DDF	degree-day factor ($mm \cdot d^{-1} °C^{-1}$)
DP	Auckland-Invercargill pressure difference (mb)
DUZ	input to upper zone storage (mm)
e	vapour pressure at 850 mb (mb)
e_a	vapour pressure at level z_a (mb)
e_s	vapour pressure at snow surface (mb)
e*(T)	saturation vapour pressure at temperature T (mb)
e'	vapour pressure adjusted to sea level (mb)
E	evaporation (m; mm);
	model efficiency
f	percolation concentration factor
F^2	sum of squared difference between two series
F_o^2	variance of observed series
FC	field capacity (mm)
g	gravitational acceleration ($m \cdot s^{-2}$)
G_i	concentration of ice in snow ($kg \cdot m^{-3}$)
G_{ih}	concentration of ice at snow surface ($kg \cdot m^{-3}$)
G_w	concentration of liquid water in snow ($kg \cdot m^{-3}$)
G_{wh}	concentration of liquid water at snow surface ($kg \cdot m^{-3}$)

h	snow depth (m; mm)
H	horizon angle (deg)
IEB	Index Energy Budget
k	von Karman's constant (0.4)
k_{ci}	cloud radiative coefficients
K	intrinsic permeability (m^2; mm^2)
K_G	ground thermal conductivity ($W \cdot m^{-1} \cdot °C^{-1}$)
K0	upper zone recession coefficient (d^{-1})
K1	upper zone recession coefficient (d^{-1})
K2	lower zone recession coefficient (d^{-1})
$K\downarrow$	incoming shortwave radiation ($W \cdot m^{-2}$)
$K\uparrow$	reflected shortwave radiation ($W \cdot m^{-2}$)
L_f	latent heat of fusion ($J \cdot kg^{-1}$)
L_v	latent heat of vaporization ($J \cdot kg^{-1}$)
$L\downarrow$	incoming longwave radiation ($W \cdot m^{-2}$)
$L\uparrow$	outgoing longwave radiation ($W \cdot m^{-2}$)
M	melt rate ($m \cdot s^{-1}$; $mm \cdot d^{-1}$)
M_F	melt rate in forest ($m \cdot s^{-1}$; $mm \cdot d^{-1}$)
n	sample size; gravity flow theory exponent
p	atmospheric pressure (mb)
P	precipitation intensity or total ($m \cdot s^{-1}$; $mm \cdot d^{-1}$)
P_F	net precipitation in forest ($m \cdot s^{-1}$; $mm \cdot d^{-1}$)
PERC	lower zone recharge (mm)
PET	potential evapotranspiration ($mm \cdot d^{-1}$)
PW	fraction of catchment which evaporates freely
Q_E	latent heat transfer ($W \cdot m^{-2}$)
Q_G	ground heat transfer ($W \cdot m^{-2}$)
Q_H	sensible heat transfer ($W \cdot m^{-2}$)
Q_M	rate of energy involved in fusion ($W \cdot m^{-2}$)
Q_P	precipitation heat transfer ($W \cdot m^{-2}$)
Q0	upper zone runoff component ($mm \cdot d^{-1}$)

Q1	upper zone runoff component ($mm \cdot d^{-1}$)
Q2	lower zone runoff component ($mm \cdot d^{-1}$)
Q*	net radiation ($W \cdot m^{-2}$)
Rb	bulk Richardson number
RFR	rate of refreezing ($mm \cdot d^{-1}$)
RH	relative humidity (%)
RMF	radiation melt factor ($mm \cdot d^{-1} °C^{-1}$)
S_w	water saturation (fraction of pore volume)
S_{wi}	irreducible water saturation
SB	Ski Basin
SCA	snow-covered area (km^2)
SL	snow-line elevation (m)
SLZ	lower zone storage (mm)
SM	soil moisture storage (mm)
S*	effective water saturation
t	time (s; d)
T	air temperature at 850 mb (°C)
T'	air temperature adjusted to sea level (K)
T_a	air temperature at level z_a (°C)
T_a'	air temperature deviation from mean (°C)
T_d	dry bulb temperature (°C)
T_K	mean temperature of near-surface air layer (K)
T_r	rain temperature (°C)
T_s	snow surface temperature (°C);
	mean snow pack temperature (°C);
$T_s(z)$	depth-dependent snow pack temperature (°C)
T_t	temperature of surrounding terrain (K)
T_w	wet bulb temperature (°C)
TB	Temple Basin
Th	1000-500 mb layer thickness (gpm)
u	wind speed at 15 m or 850 mb ($m \cdot s^{-1}$)
u_a	wind speed at level z_a ($m \cdot s^{-1}$)

u_a'	deviation from mean wind speed ($m \cdot s^{-1}$)
UZL	upper zone storage threshold (mm)
v	percolation flux rate ($m \cdot s^{-1}$; $mm \cdot h^{-1}$)
VF	view factor
W	unit mass of snow ($kg \cdot m^{-2}$)
WIN	input to soil moisture routine (mm)
WRG	gravimetric water retention capacity ($kg \cdot kg^{-1}$)
WRV	volumetric water retention capacity ($m \cdot m^{-1}$)
X_i	observed series
$\overline{X}$	mean of X_i
Y_i	modelled series
z	vertical coordinate (m; mm)
z_a	measurement height (m; mm)
z_o	roughness length (m; mm)
z/L	Monin-Obukhov stability parameter
α	albedo
ΔL	change in liquid water storage ($kg \cdot m^{-2}$; m)
ε_a	apparent atmospheric emissivity
ε_{ao}	apparent clear-sky emissivity
ε_s	emissivity of snow surface
ε_t	emissivity of surrounding terrain
ρ_a	density of air ($kg \cdot m^{-3}$)
ρ_s	density of snow ($kg \cdot m^{-3}$)
ρ_{sd}	density of dry snow ($kg \cdot m^{-3}$)
ρ_{sw}	density of wet snow ($kg \cdot m^{-3}$)
ρ_w	density of water ($kg \cdot m^{-3}$)
ϕ	porosity
ϕ_e	effective porosity
σ	Stefan-Boltzman constant (5.67×10^{-8} $W \cdot m^{-2} K^{-4}$)

ABSTRACT

Studies were carried out in the Waimakariri catchment on the east side of the South Island, to contribute to the general understanding of the inter- and intra-regional variations of snow hydrological phenomena and to the practical needs of hydrologists in New Zealand.

Turbulent exchange of sensible and often latent heat can produce rapid melt because of the exposed, alpine nature of the seasonal snow zone and the dominance of maritime air masses and strong westerly air flow. Regional air mass and circulation characteristics provide stronger controls on turbulent exchange than local advection and locally-generated winds at a site near the Main Divide. Estimates of turbulent exchange at a site 20 km in the lee of the Main Divide show weaker correlations with large scale indices than at the Main Divide site. Air flow-terrain interactions cause a variation in snowmelt climate across the South Island. The spatial patterns of snow surface lowering in a 71 ha catchment suggest that melt patterns vary with weather type, with exposure to wind being the main control during advective melt situations.

Field observations, climatic considerations and theoretical calculations indicate that snow cover should not have an important impact upon water routing near the Main Divide, where mid-winter rain-on-snow is common. In the drier climate of the eastern ranges, ice layers may significantly impede percolation. Movement of water at the base of the pack is difficult to predict because of the variability in runoff mechanisms and lack of knowledge about superimposed and ground ice.

A simple model using daily climate data satisfactorily reproduced snow accumulation at a snow course at 1750 m elevation when temperatures measured at 1550 m and low elevation precipitation were used. Simulation quality was unsatisfactory when low elevation temperatures were used, because of the deviations of the assumed from the actual lapse rates. A runoff model using a lumped transformation routine and a distributed snow routine performed poorly when applied to a 94 ha catchment ranging from 1020 to 1730 m elevation. The model overestimated runoff, possibly because of subsurface losses. Snow accumulation was reasonably reproduced above 1500 m, but below 1500 m many snow events were misclassified because of the inadequacy of daily temperature as a discriminator. A spring melt period was simulated using observed snow lines rather than simulated snow cover. A melt routine incorporating a regional air flow index reproduced runoff variations better than a simple temperature index. The lumped transformation routine is inadequate in situations where runoff sources and mechanisms vary between events.

The magnitude of seasonal snow storage varies between years, but is great enough to require inclusion in streamflow models of mountainous catchments. The contribution of melt in the seasonal snow zone to flood runoff is difficult to assess given the available data, but may vary across the South Island because of systematic geographic variations in storm types producing heavy rain during rain-on-snow events. Melt in the transient snow zone is limited by wind speed, not air temperature, but can augment short term runoff during intense rain events.

CHAPTER ONE

INTRODUCTION

This thesis describes investigations into the nature of seasonal snow hydrology in the Waimakariri catchment in the central South Island of New Zealand. In this chapter, aspects of snow hydrology, both specific to New Zealand and general, are reviewed to provide the background to and justification for the present study. These reviews are followed by statements of the objectives of the present study and the approaches taken to achieve these objectives.

1.1 SNOW HYDROLOGY

Much of the early work in snow hydrology was directed toward developing tools for quantifying the snow resource. Examples of such studies are the pioneering work in snow surveying by Church (1933) and Collins' (1934) application of the degree-day approach to runoff volumes. One of the earliest successful process studies was carried out by Sverdrup (1936) as part of meteorological and glaciological investigations in Spitzbergen. Sverdrup used the energy balance framework to investigate turbulent exchange over melting snow, and his formulation of the aerodynamic approach has been used almost unaltered ever since for calculating sensible and latent heat exchanges.

Studies of snowmelt runoff generation processes continued through the 1940's and 1950's. These studies were

used to develop methods of analysis and synthesis for use in water resources planning. A major portion of the American research effort was carried out as part of the Cooperative Snow Investigations, and is summarized by USACE (1956; 1960). Russian work from the same period is reviewed by Kuz'min (1972). European and Asian workers, particularly the Japanese, carried out studies concurrently.

Technological advances following World War Two created new avenues of research. Advances in digital computers allowed the development of models for simulating snow accumulation, ablation and runoff. Modelling continues to be an active topic in snow hydrology (WMO, 1982). Information available through remote sensing from satellites and aircraft has found use in many aspects of snow hydrology. Research into peace-time uses of nuclear technology made possible the development of profiling snow gauges.

Several papers since 1978 have reviewed state-of-the-art of aspects of snowmelt runoff processes (Price et al., 1979; Wankiewicz, 1979; Colbeck et al., 1979; Male and Granger, 1981; Obled and Harder, 1979; Dunne, 1983). The consensus from these papers with respect to snowmelt is that the processes acting at a point are well understood, and can be modelled satisfactorily given adequate instrumentation. However, methods for characterizing the energy available for snowmelt over an area are lacking. Male and Granger (1981) have noted that modelling the turbulent exchanges of sensible and latent heat over snow is particularly problematic. Although radiation is normally the dominant energy source for

snowmelt in most environments, the sensible and latent heat fluxes dominate the snowmelt energy budget and produce high rates of melt under conditions characterized by warm, humid air, moderate to strong winds and low insolation (Light, 1941; Hendrick et al., 1971) - conditions which are often encountered during rain-on-snow events.

Snowmelt and rain inputs at the top of a snow pack can become streamflow via several pathways. The movement of water through ripe, homogeneous snow is reasonably well understood, and a theory of this movement has been successfully applied to predicting outflow from runoff plots by Dunne et al. (1976). However, departures from either ripeness or homogeneity present problems that are not totally resolved. Wankiewicz (1979) presented a qualitative model of water flow through layered snow, and Colbeck (1975; 1979a) has developed quantitative theories. The main problem in applying these theories is the lack of knowledge of the characteristics of the inhomogeneities influencing the flow. Colbeck (1976) developed a theory of water movement in dry homogeneous snow. Anderson (1979) discussed the importance of deep, dry snow packs in routing water inputs during rain-on-snow events. However, Colbeck's (1976) theory appears not to have been tested against field data. The movement of water once it reaches the base of the snow pack is understood only for some restrictive cases, such as snow overlying impermeable frozen ground (Dunne et al., 1976). Dunne (1983) has outlined some fruitful avenues of research on snow-soil-water interactions.

In addition to studies of processes and technology applications, some research has concentrated on regional

aspects of snow hydrology. This research focuses on one or more of the ensemble of snow hydrology processes operating in a location, with consideration of the environmental constraints on the processes. As Colbeck (1979b) observed, the laws of physics are universal but the magnitudes of processes vary; therefore, care must be taken in transposing models and concepts to new environments. For example, Woo (1982) discussed how snowmelt runoff models which were developed in temperate climates have not worked well in the Arctic. Examples of regional studies include those of Fitzgibbon (1977), Granger and Male (1978), Jordan (1978), Woo (1982) and Braun (in prep.).

Christner and Harr (1982) and Cooley and Robertson (1983) have noted that many of the techniques in the snow hydrologist's "tool kit" were developed for regions having deep and/or continuous snow packs. Transient snow covers, which can form and ablate several times in a winter, are hydrologically significant in several parts of the world. The influence on flooding and erosion of the melting of shallow snow covers during rain has been reported in Great Britain (Johnson and Archer, 1973), in the lowland and low alpine zones of Switzerland (Braun and Zuidema, 1982) and in the Pacific Northwest and Intermountain areas of the United States of America (Harr, 1981; Christner and Harr, 1982; Cooley and Robertson, 1983). Interest in the dynamics of transient snow covers and rain-on-snow events appears to have grown in recent years. For example, the theme of the 1983 Western Snow Conference was "Hydrology in a rain-on-snow environment". New Zealand's mountain regions are characterized by unreliable snow cover which "thaws,

recedes and reforms at intervals" (Gillies, 1964), and could appropriately be called a rain-on-snow environment. The next section reviews New Zealand snow hydrology in some detail.

1.2 NEW ZEALAND SNOW HYDROLOGY

Fitzharris, in 1979, described New Zealand snow hydrology research as being in its "infancy". Despite some work since then, notably that of Prowse (1981), much of which is also reported by Prowse and Owens (1982; 1984), knowledge of New Zealand's snow hydrology has not yet reached the stage where potentially operational models have been applied successfully. Fitzharris (1979) attributed much of the lack of knowledge to disagreement amongst water managers and engineers as to the significance of the seasonal snow resource. This disagreement, in turn, can be traced to the problems involved with quantifying the seasonal snow resource in the New Zealand setting.

The topography in the South Island mountains can be generally characterized as steep and rugged. Consequently, most New Zealanders live in the lowlands, and very few meteorological stations have been maintained in the snow zones. In addition, the topography makes access to the snow zones difficult, and snow surveys involve great effort (Gillies, 1964). The fluctuations of the freezing level throughout the winter and the great spatial variability of snow accumulation due to the topography minimize the utility of the index snow course concept, which is a valuable tool in other parts of the world (Fitzharris, 1978). Another

problem is that snowmelt often coincides with heavy rain along the Main Divide; without rainfall information, hydrographs can yield little information on snowmelt.

Several workers have used the water balance framework to estimate the magnitude of seasonal snow storage. Fitzharris (1979) summarized estimates which have been made for the catchments developed for hydro-electric generation. These estimates put the average seasonal snow storage between fourteen and thirty percent of the annual streamflow. Since Fitzharris' (1979) review, Fitzharris and Grimmond (1982) have estimated that seasonal snow storage is thirty-three percent of annual runoff in the Fraser catchment in Central Otago (see Fig. 1.1), an IHD representative basin with an area of 120 km^2. Bowden (1983) calculated that seasonal snowmelt accounts for thirty-six percent of streamflow in the Rakaia River during the months October to January, or sixteen percent of annual runoff.

Although the inter-annual variability of seasonal snow storage is an important management consideration, few investigations have been made. O'Loughlin (1969a) reported snow course measurements made in the Waimakariri catchment at an elevation of 1750 m. The peak measured water equivalent ranged from 220 to 1020 mm, while the mean peak measured value for the years 1962 to 1973 is approximately 470 mm, implying a variability of over one hundred percent. Fitzharris and Grimmond (1982) estimated the variation in peak storage in the Fraser catchment to be fifty-seven percent of the mean.

The available evidence shows clearly that seasonal snow storage is an important but variable component in the

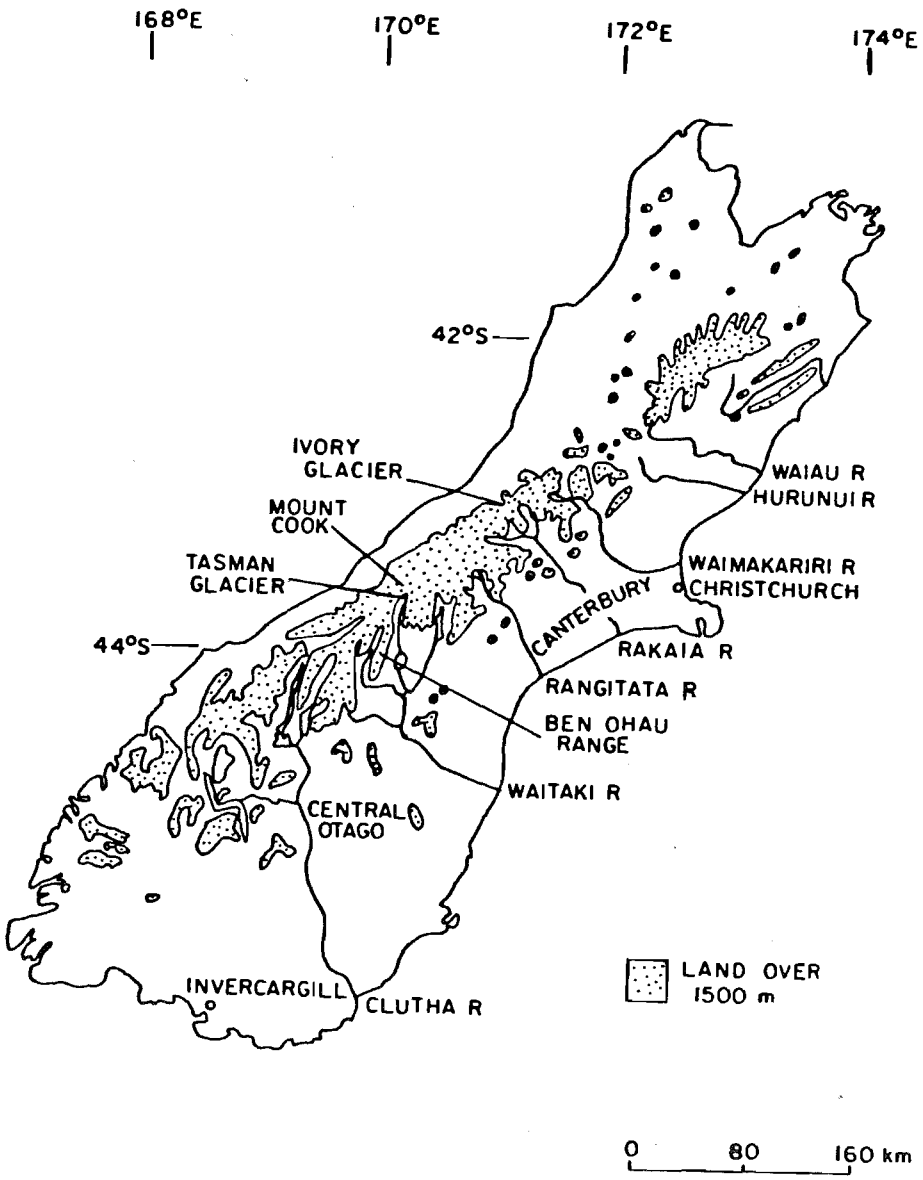

Fig. 1.1. Map of the South Island.

hydrology of many South Island catchments. However, the release of snow storage occurs when requirements for irrigation and other uses are low, particularly since the release often coincides with heavy rain in the headwaters. Therefore, the management implications of seasonal snow storage are important mainly in the hydro-power catchments, the Waitaki and the Clutha. Flooding is a problem in many areas of New Zealand, and some efforts are being made to develop flood forecasting models for real-time application (for example, Goring, 1984). These models presently deal with rain floods, although snowmelt can contribute significantly to generation of storm runoff. For example, Fitzharris et al. (1980) estimated that snowmelt contributed thirty-seven percent of the water input to the Fraser River during a storm which produced a 170 year flood in an adjacent catchment. The National Water and Soil Conservation Organisation recognizes the need to understand the influences of seasonal snowmelt on flood generation in the large snow-fed South Island catchments (M.E. Yates, pers. comm.).

Very little research on snowmelt runoff processes has been carried out in New Zealand compared to overseas. Gillies (1964), O'Loughlin (1969a) and Archer (1970) noted that rapid ablation coincides with north-westerly storms, which are most frequent during spring. Energy exchange over a glacier surface during summer was investigated by Harding (1972), but these results are not totally applicable to seasonal snow. Fitzharris et al. (1980) estimated that during the 1978 Otago floods, the turbulent exchanges supplied fifty-eight percent of the energy used for melt,

net radiation twenty-three percent and the sensible heat of rain nineteen percent. Prowse (1981) and Prowse and Owens (1982) estimated energy exchanges over seasonal snow in the Craigieburn Range in the Waimakariri catchment from meteorological observations. They reported that sensible heat is the dominant source of energy under most weather situations and in all seasons, with the contributions from net radiation and latent heat depending upon the atmospheric conditions.

Fitzharris (1979) noted that very little was known about the structure and hydrological properties of New Zealand snow packs. O'Loughlin (1969a) reported measurements of liquid water contents and dye experiments of percolation rates; but these were not related systematically to weather conditions or streamflow response. Since 1979, McNulty and Fitzharris (1980), Weir and Owens (1981), Prowse (1981) and Prowse and Owens (1984) have described snow pack structure and the spatial and/or temporal variability of the characteristics. These studies indicate that New Zealand snow packs are stratigraphically complex, with ice layers being an ubiquitous feature, and are relatively warm. Prowse (1981) reported that the greatest observed heat deficit in the Craigieburn Range was equivalent to 12 mm of melt. No studies of snow-soil-water interactions have been made in the context of runoff generation, and the only discussion of the effect of snow on streamflow generation was O'Loughlin's (1969a, b) descriptions of the responses of a mountain catchment to rain during light and heavy snow years.

Several investigations have been made of methods for

monitoring snow cover in New Zealand. Gillies (1964), Morris and O'Loughlin (1965), Chinn (1969), O'Loughlin (1969a) and Archer (1970) carried out snow course measurements, but the data does not appear to have been used for management purposes. Fitzharris (1976; 1977) used snow surveys to investigate the spatial variation of snow accumulation in Central Otago, and to estimate the snow storage in the Clutha catchment. Gillies (1964) and Chinn and Whitehouse (1980) discussed the utility of fixed-wing aircraft inspection. The advantage of this approach is the ability to assess coverage over an extensive area, but aircraft inspections cannot yet shed any light on the magnitude of snow storage (Fitzharris, 1979). Hickman (1972) estimated snow line elevations from satellite imagery, but again, this data does not appear to have been applied. A snow pillow is operating in the Fraser catchment, and this data was the key information used by Fitzharris et al. (1980) to assess snowmelt during the 1978 Otago floods.

Models of snow accumulation, melt and runoff have not yet been successfully applied in New Zealand. Conceptual runoff models applied in New Zealand catchments in the 1960's and 1970's did not account for snow. Bowden (1974) suggested that snow influences were responsible for the overestimation of winter flows and the underestimation of spring flows when Taylor's (1972) model was applied in the Waiau catchment. Grimmond (1980) and Fitzsimmons (1983) applied versions of Martinec's (1975) model using ground-based observations of snow cover; problems encountered in both efforts were possibly caused by

inadequate input data.

1.3 OBJECTIVES AND APPROACH

As noted previously, more research is required on the processes operating in rain-on-snow environments, particularly with respect to approaches to modelling the snow surface energy exchange and the influence of snow cover on basin response. Seasonal snow cover is an important but poorly-understood component in the hydrology of many catchments draining the mountainous zones of New Zealand's South Island, in which rain-on-snow events occur frequently. Therefore, this study of snow hydrology in a catchment draining the Southern Alps is intended to contribute to two spheres of knowledge: the field of applied knowledge of use to water managers in New Zealand, and the general understanding of the inter- and intra-regional variations of snow hydrological phenomena. The major objectives of this study can be summarized as follows:

(1) to investigate the spatial and temporal variability of snow surface energy exchange during snowmelt, with particular reference to the sensible and latent heat fluxes;

(2) to evaluate in a New Zealand context the role of snow cover as a control on runoff generation;

(3) to develop and test models of snow accumulation, melt and runoff that could be applied operationally; and

(4) to define the nature of the seasonal snow resource in a New Zealand catchment.

The approach adopted here is to study in the field the processes operating and the controls on these processes. Appropriate models are formulated on the basis of the process studies, and are then applied to existing hydroclimatic data, both to test the appropriateness of the models and to extend the time scale of the study. Efforts are made to describe, using the results of the present and previous investigations, the characteristics of snow storage and release in a New Zealand catchment at different spatial and temporal scales.

Research was focussed upon the Waimakariri catchment for three main reasons. First, the geology, vegetation and range of climatic characteristics are representative of many east coast South Island rivers such as the Hurunui and Rakaia, although differences in hypsography may play an important hydrological role (Bowden, 1977). Second, access to the snow zones is relatively easy. A railway and a highway run more or less through the centre of the catchment, and ski fields are located in the high rainfall areas near the Main Divide, as well as in the drier eastern portions of the catchment. Most of the ski fields are reached by walking, but the huts run by the various ski clubs provide a reasonable base for field operations. Third, the Ministry of Works and Development (MWD) and the Forest Research Institute (FRI) have maintained hydrometeorological data collection programmes within the catchment since the early 1960's, including climate stations, streamflow gauging sites and snow surveys. These data comprise the longest and most comprehensive for any mountain location in New Zealand, and reduce the

requirements for data collected specifically for this study.

1.4 PRESENTATION FORMAT

Six chapters comprise the remainder of this thesis. The first of these describes the environment of the Waimakariri catchment and the field sites, outlines the methods of data collection and discusses the accuracy of field data. Chapter two also briefly describes the nature of the field seasons in terms of data collection and representativeness.

Chapters three, four, five and six each address one of the four objectives of the study. Chapter three focuses on snowmelt processes and the implications for modelling. The routing of rain and snowmelt from the snow surface to a stream channel is discussed in chapter four. Chapter five describes the development of models for predicting snow accumulation, melt and runoff with reference to the results of chapters three and four. These models are then applied to snow survey and streamflow data. In chapter six, an attempt is made to define the nature of the seasonal snow resource in the Waimakariri catchment by synthesizing the results of the present and previous investigations. Some attempt is made to generalize the results to other South Island catchments.

The final chapter reviews the main findings of the study. The implications of the results for understanding hydrological behaviour in New Zealand and for snowmelt runoff modelling are discussed, and possible areas for future research are identified.

CHAPTER TWO

FIELD AREA AND DATA COLLECTION

The reasons for selecting the Waimakariri catchment for study are outlined in chapter one. In this chapter, the physical environment of the Waimakariri catchment, the data collection sites and instrumentation, and the study period are described.

2.1 THE WAIMAKARIRI CATCHMENT

The Waimakariri catchment is located in the central South Island of New Zealand. The river drains the eastern slopes of the Southern Alps from the Main Divide and flows into the South Pacific Ocean a few kilometres north of Christchurch (Fig. 2.1). The total catchment area is 3670 km^2; the catchment area above the Otarama Gorge and including the Kowai catchment is 2340 km^2. In the following discussion "catchment" refers to the catchment above the Gorge, and unreferenced facts are generally from Hayward (1967).

2.1.1 Geology and Physiography

The present topography of the catchment is chiefly the result of the Kaikoura orogeny during the Middle and Late Tertiary to Pleistocene and subsequent glacial and post-glacial activity. Ridgetop and peak elevations range

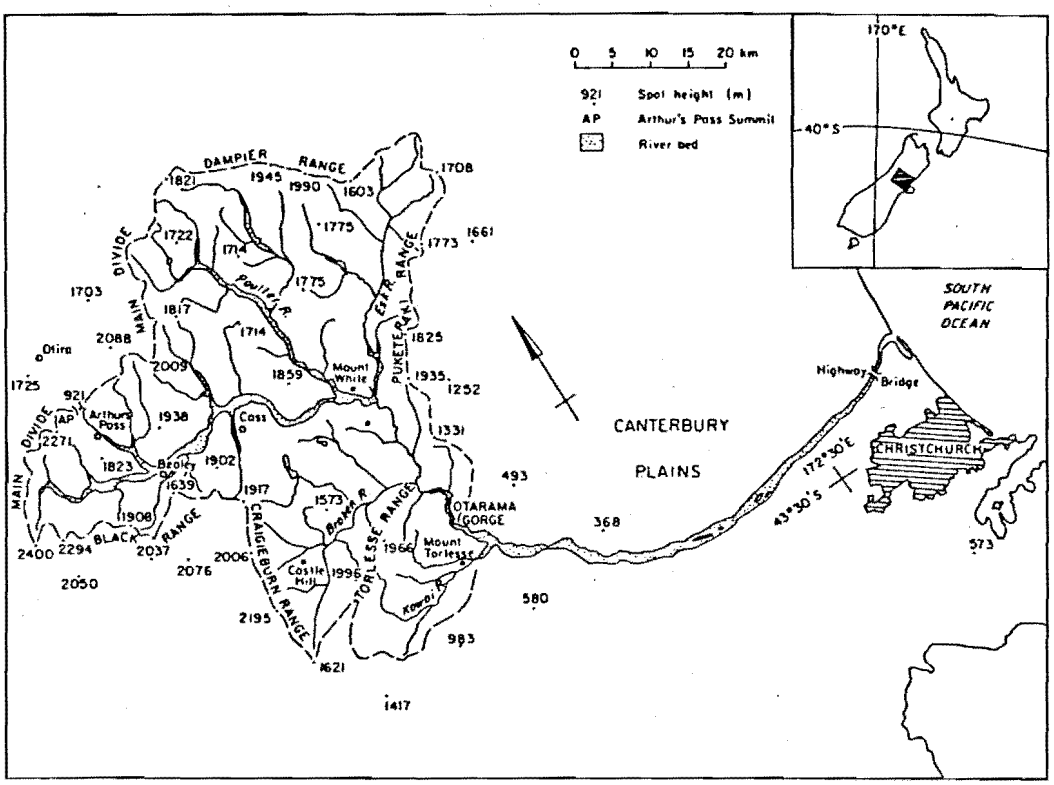

Fig. 2.1. Map of the Waimakariri catchment.

from 1500 to 2400 m, while valley bottoms are at about 600 to 800 m. The highest summits and steepest slopes are located close to the Main Divide, with the eastern portions of the catchment being composed of lower, more rounded mountains. The highest summit in the catchment is Mount Murchison at 2400 m, and the median elevation of the catchment is 1040 m (Fig. 2.2).

The bedrock geology is dominated by strongly indurated sandstones and siltstones of Triassic and Jurassic age, which are often referred to as greywacke and argillite. The beds have been extensively tilted, folded and faulted. The bedrock is readily erodible, and incised streams and gorges are common, particularly in the higher rainfall areas close to the Main Divide. The Tertiary inlier in the valley between the Craigieburn and Torlesse Ranges consists mainly of limestone and covers five percent of the area of the catchment. Surficial deposits derived from the dominant siltstone and sandstone lithologies cover fifteen percent of the catchment, generally at lower elevations. These deposits include moraines, kame terraces, alluvial/colluvial fans and glacio-fluvial and fluvial materials. Extensive portions of the upper mountain slopes are mantled by scree deposits, which are derived from the underlying greywacke and argillite.

The most recent glaciation ended ca 15000 B.P. Fluvial and colluvial processes have extensively modified much of the post-glacial landscape, which comprised cirque basins and wide valleys with steep valley walls. Present glaciation is restricted to remnant cirque glaciers along the east flank of the Main Divide, which cover an area of

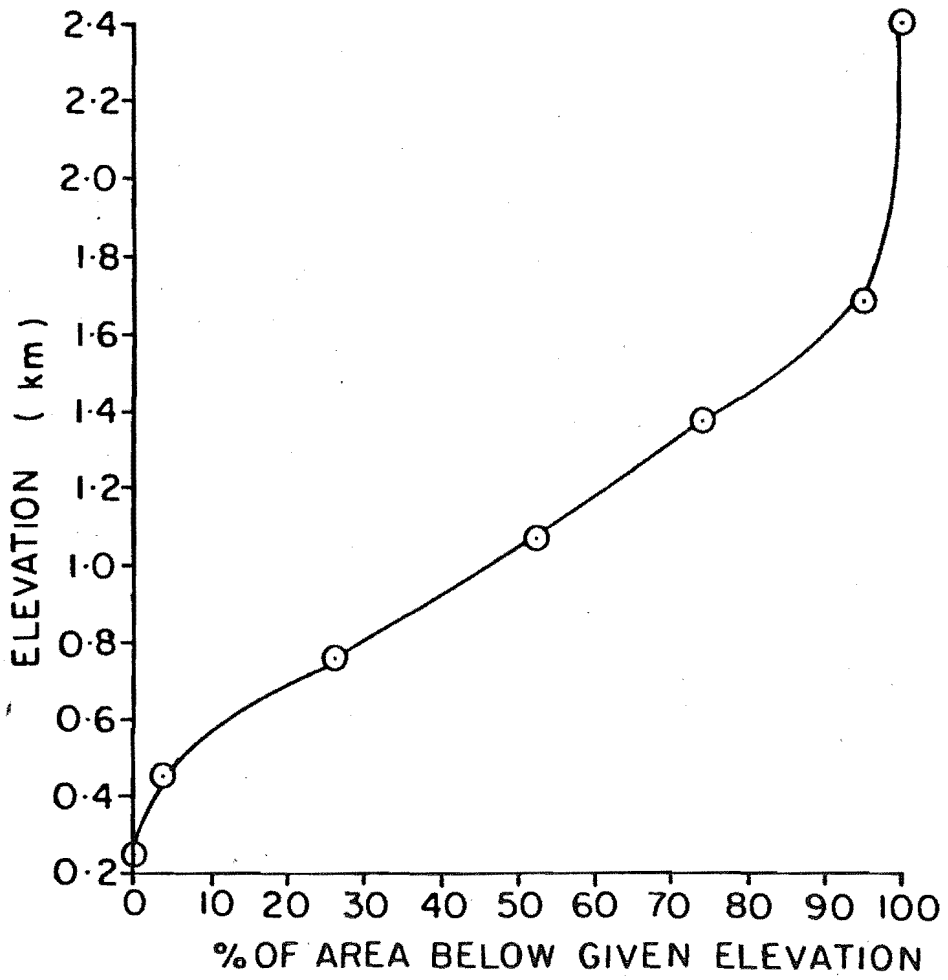

Fig. 2.2. Hypsometric curve of the Waimakariri catchment (adapted from Hayward, 1967).

4.3 km^2 (Anderton, 1973). The permanent snow-line elevation is presently 1900 m (Chinn and Whitehouse, 1980).

2.1.2 Climatology

New Zealand's South Island lies in the latitudes known as the "roaring forties". Weather situations are dominated by cyclonic, anticyclonic and frontal systems generally moving from west to east over the Tasman Sea, producing a typical "west coast mid-latitude" climate (Fitzharris, 1978).

2.1.2.1 Temperature and Humidity

The Waimakariri catchment is dominated by oceanic air masses, producing a moderate temperature climate. Fig. 2.3 illustrates the long term monthly temperature characteristics of two stations in Craigieburn Forest Park. Ski Basin (SB) has an elevation of 1550 m, while Craigieburn Forest (CF) is at 914 m. Even at 1550 m, the mean daily temperature is below freezing only three months of the year, with the lowest mean daily temperature, -1.4°C, in July. The lowest recorded temperature is -14.5°C at SB and -9.6°C at CF. The annual range in monthly means of daily temperature is 11°C at SB and 11.8°C at CF. The average daily range is 6.8°C at SB and 10.7°C at CF.

The long term mean values of relative humidity recorded during morning observations are 73 % at SB and 76 % at CF, reflecting the maritime influences. However, relative humidities as low as 30 % can occur during some westerly

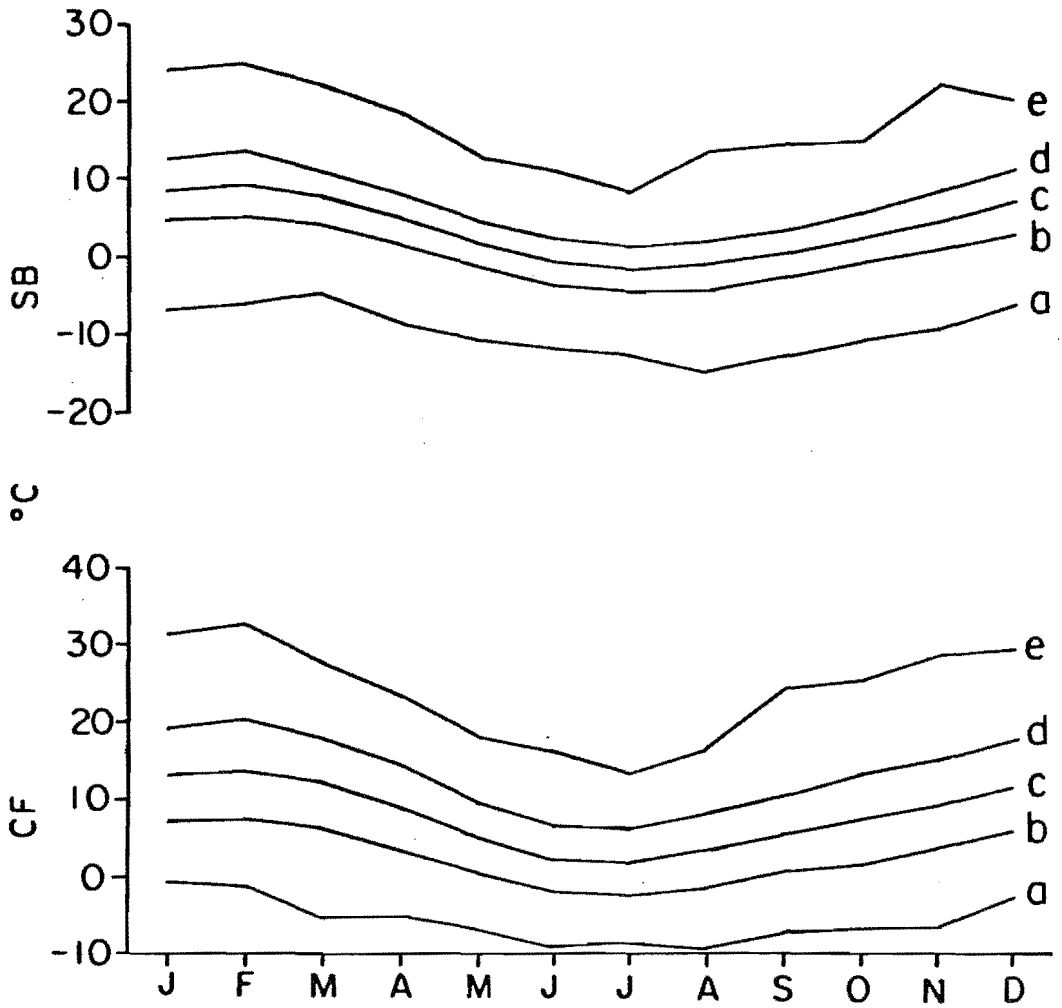

Fig. 2.3. Long term monthly temperature characteristics at CF and SB.
a) lowest recorded
b) average daily minimum
c) mean
d) average daily maximum
e) highest recorded

situations, presumably as a result of a foehn effect (McCracken, 1980).

Comparable long term temperature and humidity statistics are not available for any stations in the western portions of the catchment such as Arthur's Pass. However, it is expected that temperatures in the areas closer to the Main Divide would be more moderate and humidities higher than in the Craigieburn area, because of the greater exposure to maritime infuences.

2.1.2.2 Precipitation

Fig. 2.4 shows the distribution of 1941 to 1970 normals of mean annual precipitation over the Waimakariri catchment. From this figure it appears that mean annual precipitation is largely a function of proximity to the Main Divide and elevation, reflecting the dominance of precipitation events associated with westerly winds. Hayward (1967) estimated that during one north-westerly storm, sixty percent of the total basin precipitation fell on thirty percent of the catchment, the band within 10 to 15 km of the Main Divide. Precipitation associated with southerly winds does not have so great an influence on precipitation patterns. Localized convective storms produce short-lived high intensity events in the central parts of the catchment (for example, in the vicinities of Cass, Mount White and Grasmere) (Sturman and Soons, 1983).

Monthly precipitation normals for 1941 to 1970 at six stations in the Waimakariri catchment are shown in Fig. 2.5. At Arthur's Pass, rainfall is greater during autumn

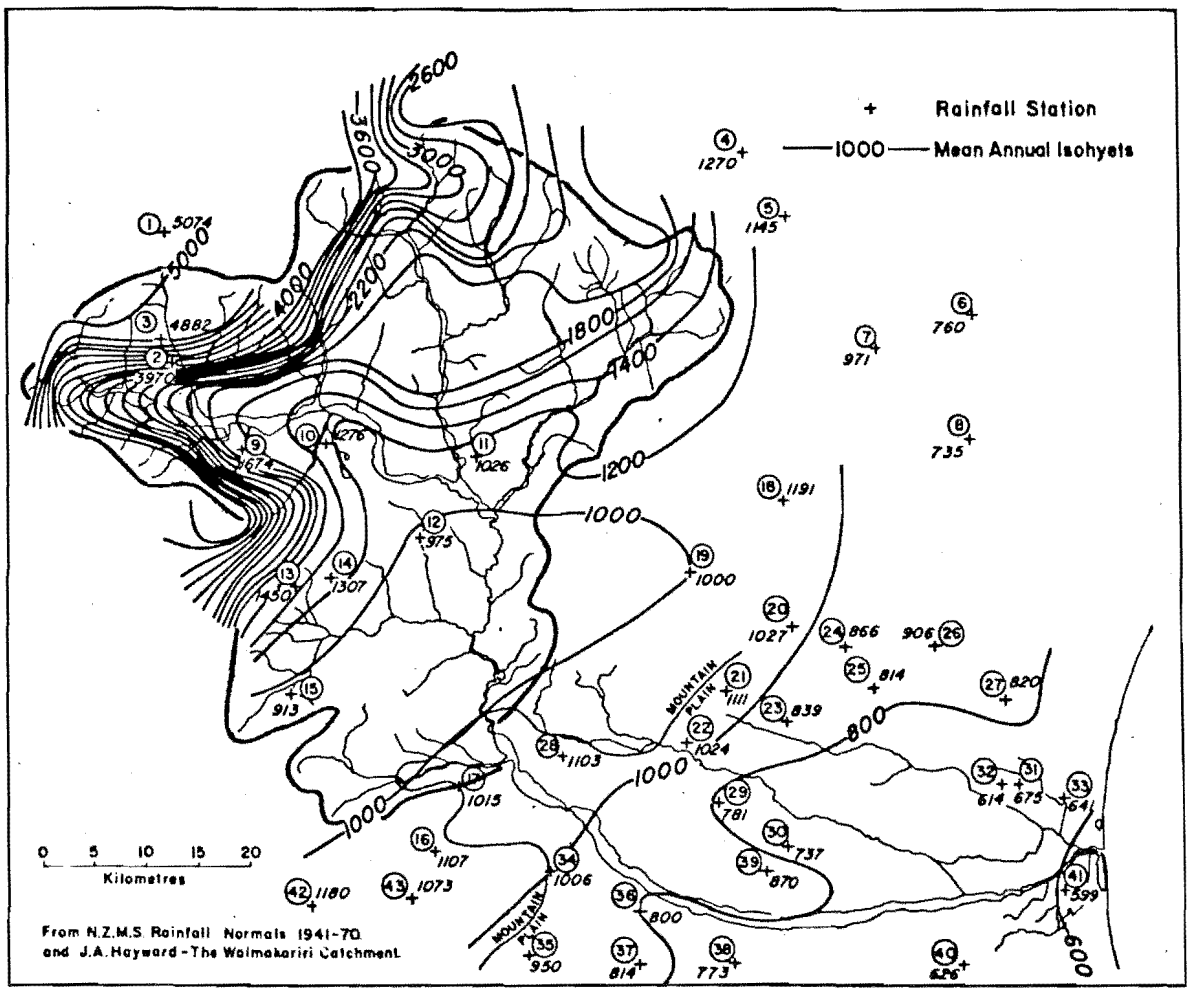

Fig. 2.4. Mean annual precipitation over the Waimakariri catchment (compiled by Dr A.P. Sturman).

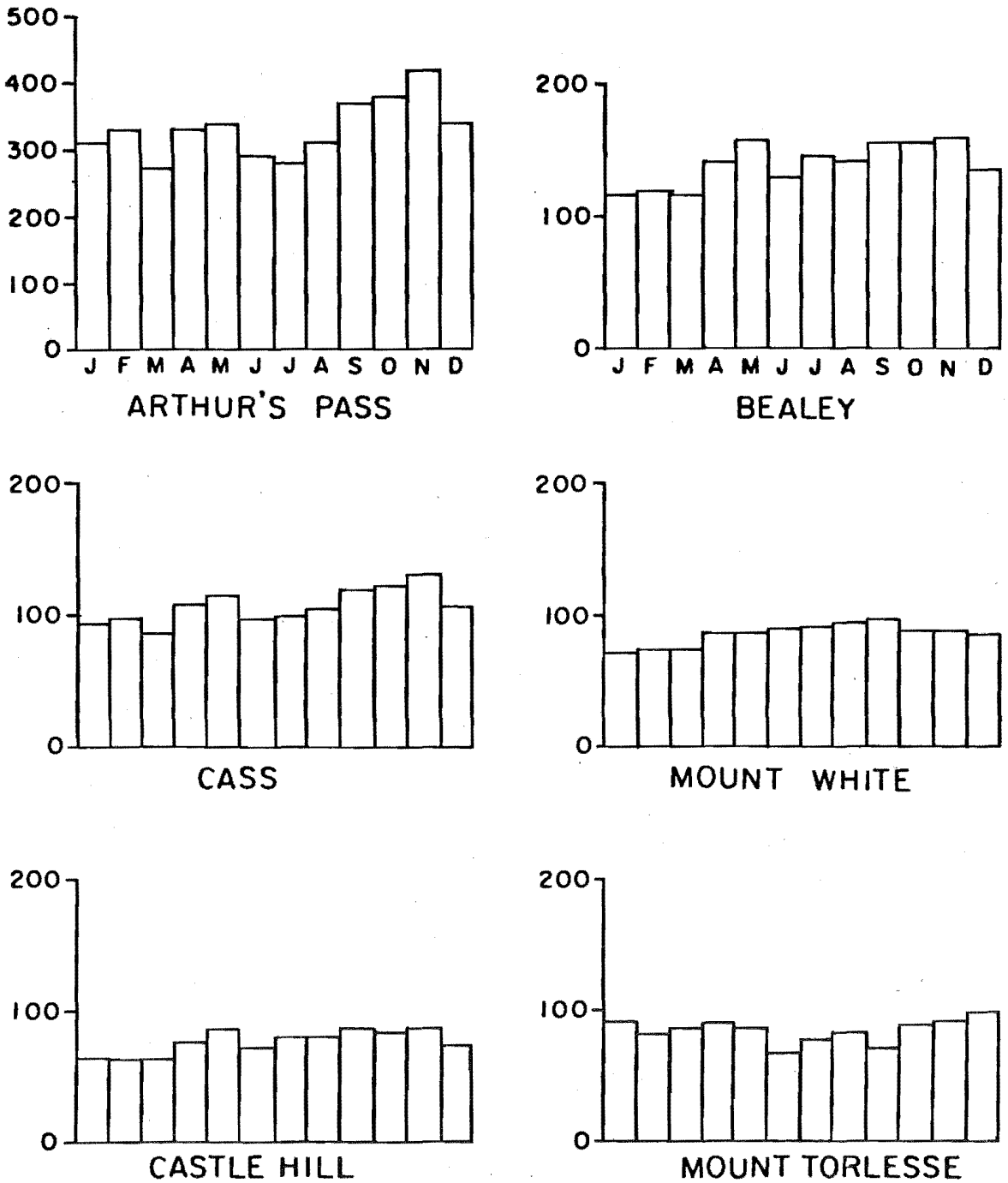

Fig. 2.5. Mean monthly precipitation (mm) (1941 to 1970 normals) for six stations in the Waimakariri catchment.

and spring than during the solstices. These peaks are associated with the increased frequency of westerly storms which coincide with seasonal circulation changes. However, thirty year normals in New Zealand are unstable; only one or two exceptionally dry or wet months can mask a true seasonal pattern (A.I. Tomlinson, pers. comm.). The other stations exhibit the spring and autumn peaks to varying degrees, depending upon their distance from the Main Divide, exposure to southerly precipitation and influence of convective rainfall.

2.1.2.3 Snow

Snow can fall at any time of year, but the main snow season normally begins in May or June and ends between September and December. Morris and O'Loughlin (1965) estimated that above 1500 m elevation snowfall accounts for thirty-five percent of the annual precipitation; this percentage decreases with elevation such that snowfall below 900 m is negligible. However, occasional exceptional snowstorms can produce heavy snowfalls at low elevations, disrupting transportation and agriculture (Tomlinson, 1970). Prowse (1981) noted that seventy-five percent of all snowstorms in the Craigieburn Range between 1975 and 1980 produced less than 25 mm of precipitation at SB. Archer (1970) similarly found in the Ben Ohau Range, which lies two ranges east of the Main Divide, that snow accumulated slowly, in a series of low intensity storms. No systematic studies of snowstorm characteristics appear to have been carried out in the western portions of the Southern Alps,

but this author's observations indicate that snowstorm magnitudes and frequencies are greater near and west of the Main Divide than in the eastern ranges.

Both the length and timing of the snow season and the magnitude of snow accumulation vary greatly from year to year (Fig. 2.6). This variability appears to be due more to the height of the freezing level during precipitation events than to variations in precipitation quantities: Prowse (1981) found a poor correlation between winter precipitation totals and peak snow course water equivalents in the Craigieburn Range. Variability in snow accumulation operates on longer time scales as well. Burrows (1976) and Tomlinson (1970) have discussed the concentrations of severe snowfalls during the periods 1860 to 1880 and 1920 to 1940, and ski runs down the road from Arthur's Pass to Otira (elevation ca 500 m) are described in issues of the Australia-New Zealand Ski Year Book from the 1930's. Oscar Coberger, a long-time resident of Arthur's Pass village until his death in 1982, gave skiing lessons near the summit of Arthur's Pass (950 m) in the 1920's and 1930's. In contrast, the 1960's and 1970's were characterized by generally light snow accumulation in the South Island (LaChapelle, 1979; Hessel, 1983), and this author has not witnessed in the last three years the development of a ski-able snow cover at the summit of Arthur's Pass, much less down to Otira.

The seasonal snow-line lies at approximately 1300 m in the Craigieburn Range (O'Loughlin, 1969a; Prowse, 1981). Transient snow covers develop below the seasonal snow-line down to 700 m, but often disappear within a few days. In

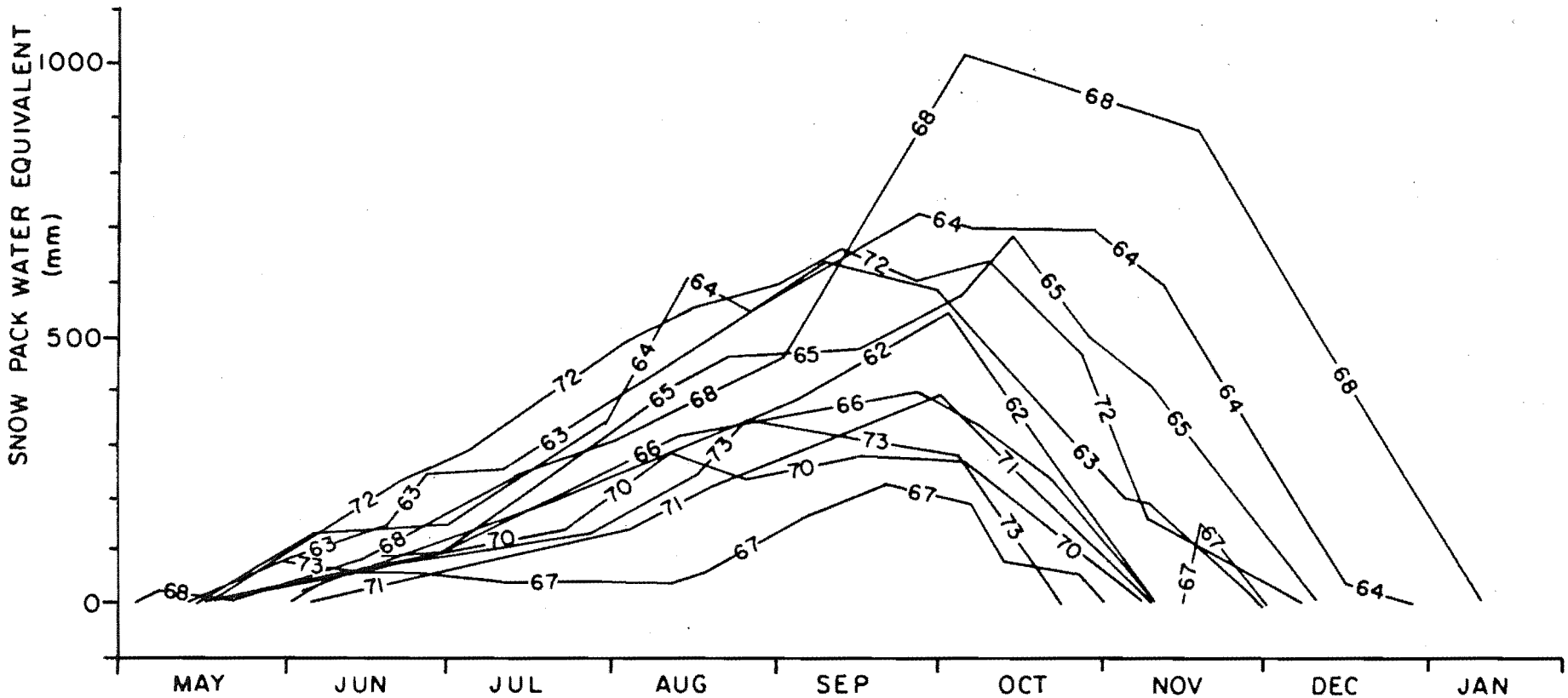

Fig. 2.6. Snow course data at Allan's Basin (updated from O'Loughlin, 1969a).

the Craigieburn Range, the average number of days with snow lying (half of site covered) varied in the period from 1965 to 1968 from 33 d a^{-1} at 914 m to 226 d a^{-1} at 1680 m (O'Loughlin, 1969a).

Westerly weather systems, which can result in the advection of warm, moist air into the South Island region along with strong winds, can occur at any time of the year and produce rapid ablation. However, the frequency of these systems is greatest in spring, when most of the seasonal snow accumulation melts. Gillies (1964), Archer (1970) and O'Loughlin (1969a) all noted the rapid spring thaw in the eastern South Island, and the rareness of snow cover persisting into the summer.

2.1.3 Hydrology

Hydrological investigations in the Waimakariri catchment are hampered by the lack of good gauging sites. All sites, particularly the gorge, have unstable beds. The Highway Bridge site (Fig. 2.1) is somewhat better, but up to twenty percent or more of the instantaneous flow is lost to groundwater as the river flows through the Canterbury Plains (Dalmer, 1971). For these reasons, Hayward's (1967) discussion on streamflow refers to stage heights at the gorge, not discharge. The Highway Bridge gauging site is maintained by the North Canterbury Catchment Board, and records extend back to 1967.

Fig. 2.7 illustrates the seasonal flow variability in the Waimakariri catchment. The flow regime is marked by a peak in the spring months, which Bowden (1977) has

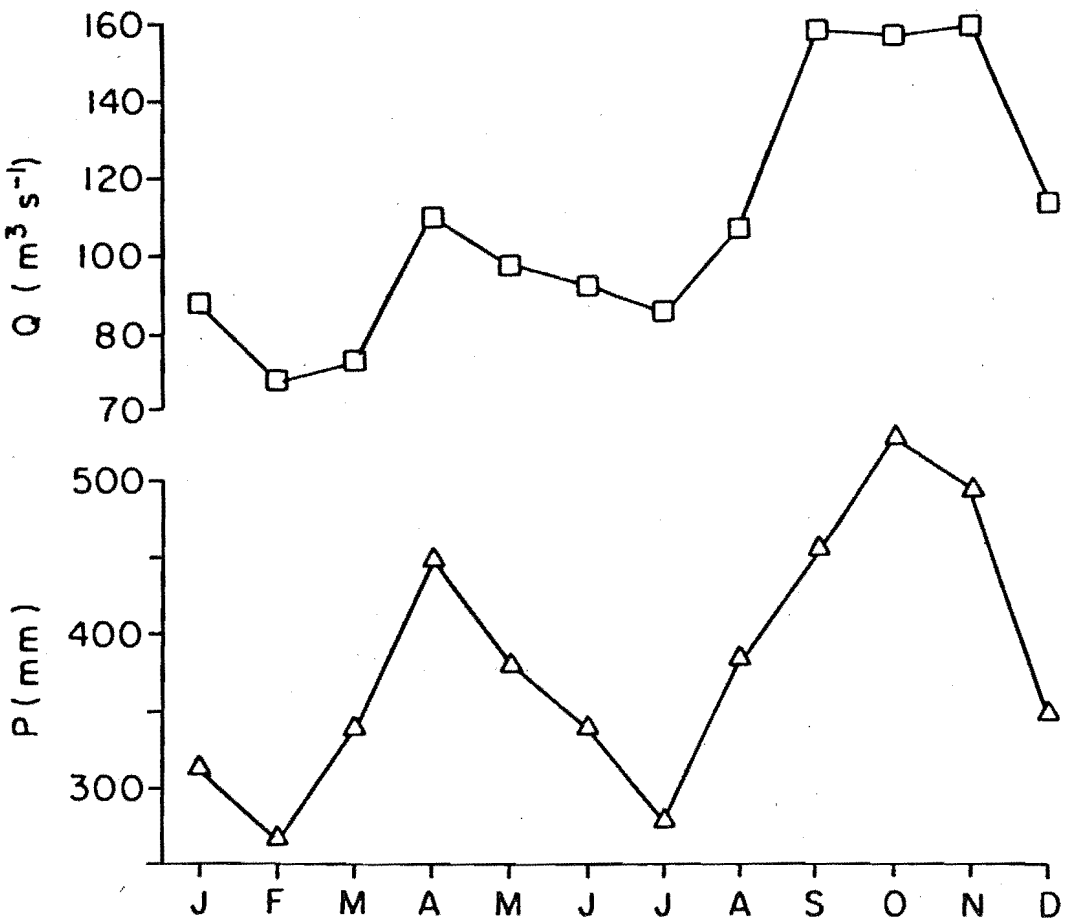

Fig. 2.7. Mean monthly discharge at Highway Bridge and mean monthly precipitation at Arthur's Pass 1967 to 1977.

attributed to snowmelt, but which also coincides with the seasonal peak in precipitation along the Main Divide. A secondary peak in the autumn coincides with the other peak in precipitation at Arthur's Pass and West Coast sites. Low flows occur in February, when precipitation is low and evaporative losses high, and in July, when a portion of precipitation enters snow storage.

Floods in the Waimakariri can occur at any time of the year, and are generally associated with north-westerly storms. An analysis of 273 floods or freshes between 1954 and 1964 indicates that only twelve could be attributed to southerly storms (Hayward, 1967). Hayward (1967) compared stage hydrographs at Waimakariri Gorge with Arthur's Pass rainfall, and found that peak stages occurred within twenty-four hours of the commencement of heavy rain. From this evidence, Hayward (1967) concluded that the upper Waimakariri catchment has low storage potential and that much of the streamflow comes from surface runoff and rapid subsurface runoff.

2.1.4 Vegetation

The vegetation in the Waimakariri catchment has been considerably altered by man. Fires in pre-European times cleared extensive portions of the eastern catchment of their forest cover. Forest has not regenerated, and much of this cleared land is presently used for sheep runs. In the following discussion, montane refers to the elevations between 300 and 914 m, upper montane or subalpine to the zone from 914 to 1370 m, and alpine to elevations above 1370

m. Figures given below are from Hayward (1967).

Indigenous evergreen beech forest (Nothofagus spp.) extends to 1370 m, and occupies thirty-nine percent of the montane and upper montane zones, or twenty-nine percent of the upper catchment. Scrub species, predominantly matagouri (Discaria toumatou), manuka (Leptospermum scoparium) and tauhinu (Cassinia fulvida), cover three percent of the catchment, or seven percent of the montane zone. A further one percent of the catchment is covered by subalpine scrub. Grassland vegetation comprises forty-three percent of the catchment. Montane grassland covers thirty percent of the catchment or seventy-five percent of the montane zone, while upper montane and alpine grasslands cover thirteen percent of the catchment. Twenty-four percent of the catchment is unvegetated, being composed of bare rock, scree, riverbed or lakes.

2.2 FIELD SITES AND INSTRUMENTATION

Data used in this study were collected at Temple Basin (TB) and in the northern portion of the Craigieburn Range. Temple Basin was instrumented specifically for this study and represents conditions in the high rainfall portion of the catchment near the Main Divide. Data collection sites in the Craigieburn Range represent the more continental conditions prevailing in the eastern portion of the catchment (Prowse, 1981) and were maintained by the Forest Research Institute (FRI) and/or the Ministry of Works and Development (MWD).

2.2.1 Temple Basin

Temple Basin is shown in Fig. 2.8. It is an old cirque basin of greywacke lithology. Tussock grassland on thin soils covers the lower portions of the basin up to ca 1500 m; exposed bedrock, screes and two small tarn lakes make up the remainder of the basin. The permanent stream channel is incised into the bedrock to depths of up to 10 m.

Temple Basin was initially instrumented with a Foxboro water level recorder at the basin outlet, and a Stevenson screen containing a thermohygrograph and a propane-heated precipitation gauge at the meteorological station (Fig. 2.8). The meteorological station was located at the flattest site in the basin which could be accessed in all weather with relative freedom from avalanche hazard. The precipitation gauge performed poorly and was later replaced with a Lambrecht siphon rain gauge. The bulk of the meteorological instrumentation was not installed until the end of September 1982, owing to unforeseen delays in the construction of instrument stands and some electronic components. This instrumentation consisted of two Munro cup counter anemometers, two sets of shielded wet and dry bulb thermistors, two albedometers and a net radiometer.

One anemometer and one set of wet and dry bulb thermistors were each set at one of two levels on a stand. The radiometers were set on a separate stand, several metres from the rest of the instrumentation. The Stevenson screen was set up at approximately the same level as the upper anemometer and thermistors.

The anemometers were fitted with switches that closed

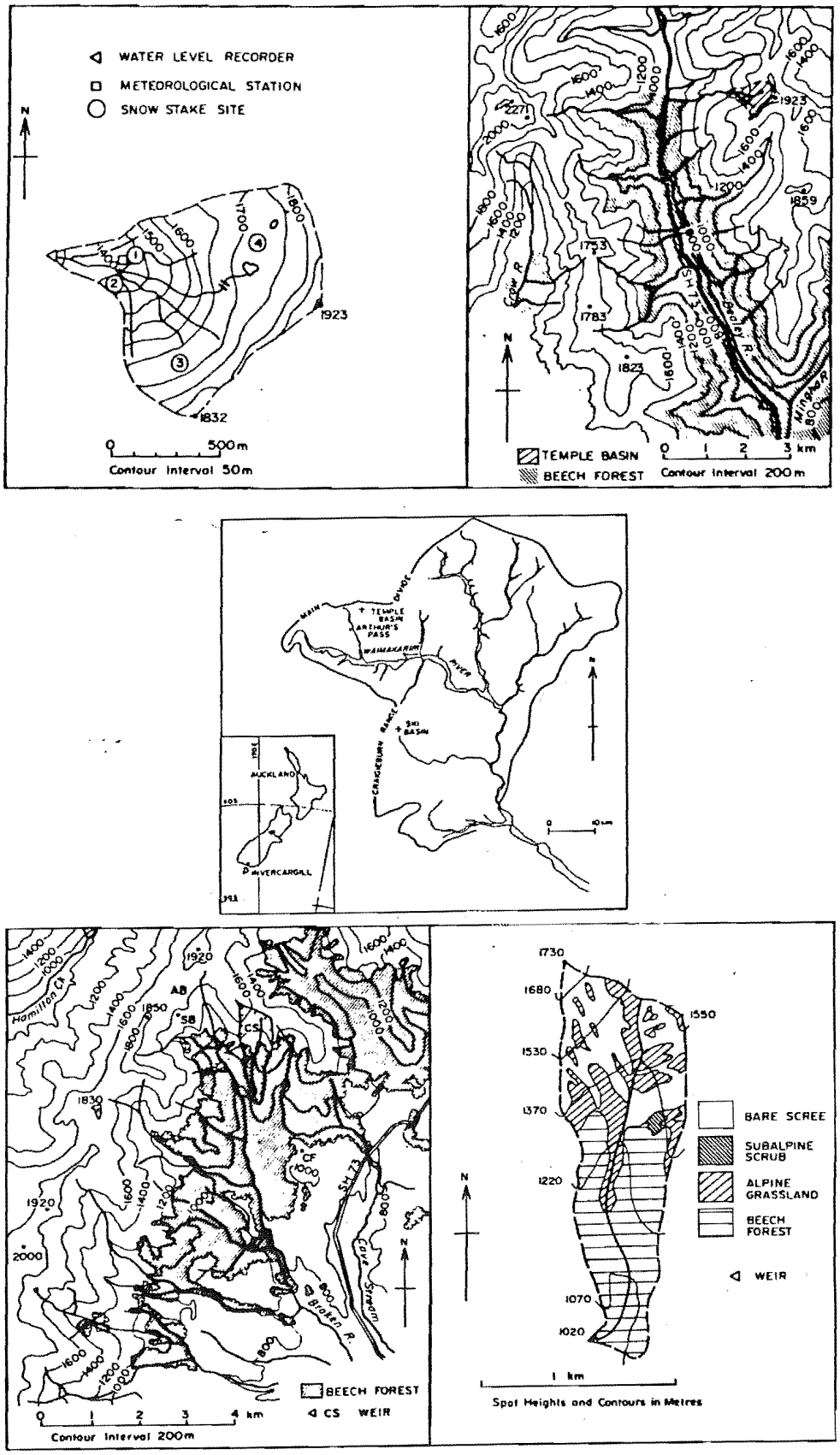

Fig. 2.8. Maps of field sites (top, Temple Basin; bottom, Craigieburn Range and Camp Stream).

every 100 m wind run. Output from the radiometers and thermistors were recorded every ten minutes as an analogue signal in mV by a Solid State Pacific data logger. Output from the anemometers was recorded by the data logger as the number of switch closings in each ten minute interval. The data logger was stored in a refrigerator from which the motor and wiring had been removed. The instrumentation used in 1983 was essentially the same as in 1982, except that a Campbell Scientific CR-21 data logger replaced the Solid State machine.

In addition to the instrumentation just described, a snowboard was installed at the meteorological site for measuring the water equivalent of new snow. Six snow depth stakes were set at each of four sites. The stakes were made from 10 mm diameter white fibreglass rods, and ranged from 2 to 3 m in height, depending upon the expected total snow depth at a site.

2.2.2 Craigieburn Range

The Craigieburn Range lies 20 km east of the Main Divide (Fig. 2.1). In the 1960's, FRI installed several climate stations with a variety of elevations and exposures (Morris, 1965). Two of these stations, SB and CF (see Fig. 2.8), have been continued as daily visited stations, although SB was degraded to weekly visits in 1983. Each site was equipped with a thermohygrograph, maximum and minimum thermometers and Belfort weighing bucket precipitation gauges. Instrumentation at CF also includes a Lambrecht recording anemograph (height 6.1 m) and a Feuss

bimetallic actinograph. At SB, instrumentation includes a totalizing anemometer set at 2.7 m above the ground, and a Feuss actinograph was installed over the years 1969 to 1974. Daily climate observations included cloud type and amount and wet and dry bulb temperatures. At CF, daily precipitation was read from a manual rain gauge, and total snow depth was recorded at SB.

Camp Stream (CS) is a first order stream draining a V-shaped basin with an area of 0.94 km^2. Its location, topography and vegetative cover are shown in Fig. 2.8. The elevational distribution of cover types and area are given in Table 2.1. Camp Stream was established as a representative basin for the International Hydrological Decade. The Forest Research Institute installed an H-flume weir at the basin outlet and several climate stations in the basin. The Ministry of Works and Development took over the maintenance of Camp Stream in the 1970's, and presently maintain the stream gauging site and a Fischer and Porter raingauge within the catchment. The raingauge is located just above treeline at an elevation of 1370 m.

Streamflow is also recorded at Hut Creek (informal name), which is a north-facing catchment of 21.7 ha. The catchment is located adjacent to the CF climate site, and ranges in elevation from 880 to 1085 m. Vegetative cover comprises a mixture of tussock, introduced short grasses and scrub patches (seventy percent), pockets of mountain beech (ten percent), trial plantings of exotic conifers (ten percent) and bare ground (ten percent). Mean annual precipitation and runoff are approximately 1500 and 750 mm, respectively.

Table 2.1 - Characteristics of Camp Stream basin by elevation zone.

Elevation Range (m)	1020-1070	1070-1220	1220-1370	1370-1530	1530-1680	1680-1730
Area (km^2)	.06	.25	.26	.26	.09	.02
% Forest	100	90	63	0	0	0
% Tussock	0	10	18	25	20	0
% Scrub	0	0	5	0	0	0
% Scree	0	0	14	75	80	100

(Derived from Ministry of Works, 1968)

In addition to the climate and streamflow investigations, snow investigations were carried out in the Craigieburn Range by FRI. Snow courses were established in Allan's Basin (AB) (Fig. 2.8) at an elevation of 1750 m and in Camp Stream at 1450 m. Physical characteristics of the snow cover such as density, temperature and free water content were studied, and were summarized by O'Loughlin (1969a).

2.3 DATA PROCESSING AND ACCURACY

A variety of data collected via several media were used in this study. The processing and accuracy of most of the field data are discussed in this section. However, the accuracy of some measurements, such as snow surveys, are discussed in association with the results of the measurements.

2.3.1 Thermistor Data

The channels monitoring the lower level thermistors malfunctioned during 1982, so wet and dry bulb temperatures were available for only the upper level. The resolution of the thermistor-data logger system is $\pm$ 0.1°C. Tests involving constant temperature water baths indicate that the accuracy of the thermistors compared to mercury-in-glass thermometers is $\pm$ 0.3°C with no apparent bias. However, during calm periods with bright sunshine, the thermistors warmed up despite the radiation shields. This warming was on the order of 2°C compared to sling psychrometer and

thermohygrograph readings. The thermohygrograph data were used whenever strong radiative heating or cooling appeared to affect the thermistors.

The ten minute readings of wet and dry bulb temperatures were averaged over hourly periods, and the mean hourly vapour pressure was calculated from

$$e_a = e^*(T_w) - C_p\ (T_d - T_w) \qquad (2.1)$$

where e_a is the vapour pressure (mb), $e^*(T_w)$ is the saturation vapour pressure at the wet bulb temperature, C_p is the psychrometric constant ($mb \cdot °C^{-1}$) and T_d and T_w are the dry and wet bulb temperatures (°C). Saturation vapour pressures were calculated according to the Tetens formula:

$$e^*(T) = \begin{cases} 6.11\ \text{antilog}_{10}\,[7.5 \cdot T/(T + 237.3)] & T>0°C \\ 6.11\ \text{antilog}_{10}\,[9.5 \cdot T/(T + 265.5)] & T\leq 0°C \end{cases} \qquad (2.2)$$

Lowe (1977) showed that Eq. (2.2) gives values which deviate from the Goff-Gratch values by less than 0.1% for temperatures above -5°C. Temperatures and humidities did not change greatly within the hourly periods, so the non-linearity of Eq. (2.2) should not significantly perturb the hourly averages of e_a computed from averages of T_d and T_w.

2.3.2 Thermohygrograph Data

Clock drives occasionally deviate from the desired speed, particularly under extreme temperature and humidity conditions, producing chart time irregularities of up to several hours over several days. The temporal resolution of weekly thermohygrograph charts is approximately 15 min. The accuracy of any time reading from a chart should be about 30

min if the time is corrected to occasional time checks.

The accuracy of the bimetallic temperature sensor is within $\pm$ 1°C compared to mercury-in-glass thermometers placed in the Stevenson screen. The error can exceed this value when the mechanism response is damped due to low temperatures or icing within the screen. Neither of these conditions is important during rapid melt events, in which air temperatures are several degrees above freezing and wind speeds are high.

The accuracy of the hygrograph was generally about 5% relative humidity compared to sling psychrometer readings in the range from 30% to 80%. At higher humidities the hygrometer drifted, often recording humidities greater than 100%. Inaccuracies were greater at low air temperatures, when small changes in air temperature create large changes in relative humidity. Low temperatures and icing can affect the mechanical response of the sensor.

Data were manually extracted from the thermohygrograph charts from both TB and SB and were corrected whenever time, temperature or humidity readings deviated from observed values at check points. Hourly averages were estimated visually because the temporal resolution does not permit numerical averaging of several values. Vapour pressures were calculated as

$$e_a = e^*(T_a)\ RH/100$$

where RH is the relative humidity (%).

2.3.3 Wind Speed

The response characteristics of the anemometers used at CF, SB and TB are not known. However, the main periods of interest were characterized by strong winds which would have greatly and consistently exceeded the stall speeds of the instruments. The resolution of hourly wind run at TB is 100 m, corresponding to 0.03 $m \cdot s^{-1}$.

2.3.4 Radiation

The data logger channels which recorded the output from the albedometers in 1982 malfunctioned, so net radiation was the only radiative exchange available. The resolution of the net radiometer-data logger system is approximately 2 $W \cdot m^{-2}$, while the accuracy of the net radiometer is $\pm$ 10% under good conditions (manufacturer's information). However, moisture on the domes under rainy conditions and heating of the domes under sunny conditions affect the measurements (Anderson, 1976).

2.3.5 Precipitation

Precipitation measurement is subject to both sampling and instrument error. Sampling problems and some implications will be discussed further in chapter five. A major source of error in precipitation measurements is gauge catch deficiency, which is well documented (for example, Dreaver and Hutchinson, 1974). Catch deficiency is particularly problematic for solid precipitation; the

extreme case occurs when snow "caps" the gauge orifice, preventing precipitation form entering the gauge. Problems with gauge operation in cold weather and snow bridging have resulted in missing periods of record from the higher elevation precipitation gauges in the Craigieburn Range.

Siphon raingauges such as the Lambrecht become inoperative if the water in the float chamber freezes. This problem occurred at TB, so the winter precipitation record is unreliable. During the spring melt period in 1982, the gauge operated well. However, catch deficiency was probably important because of the windy, exposed nature of the site. Hourly rainfall totals were extracted manually from the charts. The resolution of the charts is 0.1 mm, which is probably much smaller than the catch errors.

2.4 STUDY PERIOD

The field portion of this study was conducted during 1982 and 1983. In this section, the nature of the field seasons and problems with data collection will be discussed.

2.4.1 The 1982 Field Season

The snow season during 1982 appeared to be typical at TB, compared with the reports of snow conditions reported in the Canterbury University Ski Club's hut book through the years. The first snows at 1450 m fell at the end of April, but the main accumulation began towards the end of June. Several snowfalls occurred in July: one storm resulted in 1.23 m of new snow being drifted and deposited at the

meteorological site. Several rain-on-snow and snow events occurred during August and September. Because of malfunctions of the propane-heated precipitation gauge, very little precipitation data was collected.

The data logging system and the Lambrecht rain gauge were installed 30 September. Some fresh snow fell during the first two weeks of October, and a rain-on-snow event occurred from 18 to 20 October. The data from this period suffered from the interferences of keas (Nestor notabilis), native mountain parrots which are renowned for their destructive tendencies. Several other researchers have commented on the data collection problems associated with keas (Anderton and Chinn, 1978; Harding, 1972; Marcus et al., in prep.). The keas tore the polyethylene domes from the net radiometer, defecated on the snow below the radiometers and tore apart some of the wires connecting the instruments to the data logger. Fortunately, the novelty of the instrumentation must have worn off, and the keas did not significantly molest the equipment after 20 October. The bulk of the snow accumulation in TB melted between 28 October and 9 November and the meteorological record for this period is complete and reliable. The melt period is described in more detail in chapter three.

Streamflow at TB was meant to be included in the field data. The water level recorder operated satisfactorily through the winter, but, unfortunately, malfunctioned during the major runoff events which occurred while the meteorological instrumentation was operating. The ink occasionally stopped flowing and the clock stopped three times in one week.

2.4.2 The 1983 Field Season

The start of the 1983 snow season was not atypical. Complete snow cover was established in TB by early July; the snow depth around the Stevenson screen was approximately 500 mm. However, through July and August the freezing level during precipitation events was often around 1600 m. Consequently, very little snow accumulation or melt occurred at the elevation of the meteorological site, but a reasonable snow pack accumulated above 1500 m. The ski clubs at TB were only able consistently to ski on slopes higher than 1500 m.

A major snow storm which turned to a warm rain-on-snow event occurred in mid-August. Unfortunately, during the heavy, driving rain, water got into the refrigerator and disrupted the data logger's operation. Several snowfalls occurred in late September. Rapid melt conditions obliterated most of the snow cover in TB by 12 October. Because of data logger malfunctions most of the record during the melt period is missing and much of the record preceeding the melt contains bad signals. Consequently, the meteorological record at TB for 1983 contains large gaps.

CHAPTER THREE

SNOWMELT PROCESSES

The magnitude and timing of snowmelt are among the most important factors in snow hydrology. In this chapter, snowmelt processes operating in the Waimakariri catchment are investigated. Particular attention is paid to the controls on the spatial and temporal variability of the turbulent fluxes. Some implications of the process studies for snowmelt modelling are discussed.

3.1 METHODOLOGY

There exist no direct means of measuring snowmelt, either at a point or over an area. Therefore, water and energy balance approaches are used to determine snowmelt. A disadvantage of water balance approaches is that they cannot be used directly for snowmelt prediction for modelling and forecasting purposes. The energy balance approach can be used for prediction because it directly relates snowmelt to measurable climatic variables. A further advantage of energy balance approaches is that they provide a means for explaining the variability of snowmelt rates (Fitzgibbon and Dunne, 1983). In this study, a combination of energy balance and water balance approaches was used to study snowmelt. The details of the methods used are given in this section.

3.1.1 Water Balance Approach

Hubley (1954) expressed the mass balance of a unit area of snow cover for which wind deposition/erosion and evaporation/condensation are negligible as

$$\frac{dW}{dt} = G_{ih}\frac{dh}{dt} + \int_0^h \frac{\partial G_i}{\partial t}dz + G_{wh}\frac{dh}{dt} + \int_0^h \frac{\partial G_w}{\partial t}dz \qquad (3.1)$$

where W is the mass of snow in the column (kg m^{-2}), G_i and G_w are the concentrations of the ice and liquid water in the snow (kg m^{-3}), G_{ih} and G_{wh} are the concentrations of ice and water at the snow surface, h is the snow pack depth (m), and z and t are the vertical (m) and temporal (s) coordinates. The sum of the first two terms on the right hand side is the melt and the sum of the third and fourth terms is the net change in liquid water storage. Hence, (3.1) can be expressed for a finite time interval as

$$A = M - \Delta L$$

where A is the ablation, M is the melt and ΔL is the change in liquid water content, all of which can be expressed in units of kg m^{-2} or m of water equivalent. If evaporation/condensation is negligible, the ablation is equal to the outflow from the snow column.

Ablation can be evaluated fairly readily by four methods: (1) sampling of changes in snow depth and density at a site (Work et al., 1965); (2) measurement of snowpack outflow from lysimeters (Anderson, 1976; USACE, 1956) or runoff plots (Price, 1977); (3) in-situ measurements of depth and density using radioactive probes (Smith and Halverson, 1969; Föhn, 1973); and (4) snow pillows (Beaumont, 1965). To calculate snowmelt, these methods must be coupled with measurements of liquid water content,

changes in which can be significant compared to melt for time periods of a day or less, as rain and/or meltwater move through the snowpack. Unfortunately, melting calorimetric determination of liquid water content, which appears to be the most commonly applied method in the field (Bernard and Wilson, 1941; Yosida, 1960; O'Loughlin, 1969a; Jordan, 1978) is subject to instrument bias (Colbeck, 1978b; Jordan, 1983). Even accurate methods of measuring water content will be subject to considerable sampling error, due to the great spatial and temporal variability in liquid water content (Wankiewicz and de Vries, 1978).

In this study, ablation was calculated from depth and density measurements. Snow depth changes were measured at stakes which were set to the ground surface. To help eliminate bias due to the uneven snow surface, the stakes were read from the top down to a sheet aluminum disk, which was 500 mm in diameter with a 12 mm hole drilled in the centre, and which was inserted over the stake. Density was measured with a Mount Rose sampler. Unfortunately, the sampler was not calibrated with a density pit because the spring scale in the snowpit kit gave unreliable readings. Studies by Work et al. (1965) and Jordan (1978) show that for ripe snow the sampler overestimates density by about nine percent, so this figure was used to correct densities obtained from the Mount Rose sampler. Ablation measurements are discussed further in section 3.2.2.

3.1.2 Energy Balance Approach

The energy balance of a snow pack can be expressed as

$$d\Theta/dt + Q_M = Q^* + Q_H + Q_E + Q_P + Q_G \qquad (3.2)$$

where $(d\Theta/dt)$ is the rate of change of heat content referenced to 0°C per unit area, Q_M is the energy involved in the fusion process, Q^* is the net radiative exchange, Q_H is the sensible heat flux, Q_E is the latent heat flux, Q_P is the precipitation heat flux and Q_G is the ground heat flux. All terms on the right hand side of Eq. (3.2) are expressed in W m^{-2} or MJ m^{-2} d^{-1}, and are considered positive if directed toward the pack, and negative if directed away from the pack. The terms on the left hand side are considered positive if they act as sinks for the energy fluxes and negative if sources.

A snow pack undergoing active melt is usually isothermal at 0°C, which is the maximum temperature of ice under normal conditions, and the heat content is constant. Therefore, all of the net energy gained by the pack is used for melt, and snowmelt rates can be calculated by assessing all of the exchanges in Eq. (3.2) and using the relationship

$$M = Q_M/(\rho_w \cdot L_f)$$

where M is the melt rate in m s^{-1}, ρ_w is the density of water (kg m^{-3}) and L_f is the latent heat of fusion in J kg^{-1}. If the net energy exchange represents a loss of heat to the pack, melting ceases, and the total heat loss must be subtracted from the heat gains when calculating average melt rates over the following melt period. By calculating melt rates over time frames in which the net

change in heat content is negligible, explicit calculation of $d\Theta/dt$ can be avoided. Internal energy changes are discussed further in chapter four. The following sections discuss the methods used for evaluating each of the exchanges in Eq. (3.2). The snow surface was assumed to be melting for the purpose of calculating the exchanges.

3.1.3 Radiative Exchange

The radiation budget at a surface can be written as

$$Q^* = K\downarrow - K\uparrow + L\downarrow - L\uparrow \qquad (3.3)$$

where $K\downarrow$ and $K\uparrow$ are the incoming and reflected shortwave exchanges, and $L\downarrow$ and $L\uparrow$ are the incoming and outgoing longwave exchanges. At Temple Basin (TB), Q^* was measured directly with a net radiometer. Because net radiation has never been measured at Ski Basin (SB), correlative approaches such as that used by Dunne and Price (1975) were precluded. Net radiation at SB therefore had to be calculated by estimating each of the terms in Eq. (3.3)

Net shortwave radiation, K^*, has often been expressed as

$$K^* = K\downarrow(1 - \alpha) \qquad (3.4a)$$

$$\alpha = K\uparrow/K\downarrow \qquad (3.4b)$$

where α is the albedo of the snow, which is a wavelength-integrated reflectivity. Eqs. (3.4) ignore the complexities of the wavelength-dependent processes of transmission, absorption and reflection, but they are adequate for operational applications over deep snow packs, particularly for daily totals (USACE, 1956). Eq. (3.4a) was applied at SB using daily totals of $K\downarrow$ measured at

Craigieburn (CF), which were adjusted for the SB site by monthly ratios of $K\downarrow(SB)/K\downarrow(CF)$. These ratios were derived by Prowse (1981) from the six year period when concurrent measurements were made at the two sites. Following Prowse (1981), the albedo was set at 0.5 for the spring melt period on the basis of the relationship between α and snow surface density given by Anderson (1976).

Snow closely approximates a black body, reflecting only a small portion of incident longwave radiation, so $L\uparrow$ can be simply calculated from

$$L\uparrow = \varepsilon_s \sigma (T_s + 273.16)^4$$

where ε_s is the emissivity of the snow surface, σ is the Stefan-Boltzmann constant (5.67×10^{-8} W m^{-2} K^{-4}) and T_s is the snow surface temperature (°C). The emissivity was set to 0.99 (Male and Granger, 1981).

Incoming longwave radiation comprises contributions from the unobscured sky dome and the surrounding terrain, and according to Male and Granger (1981) can be calculated as

$$L\downarrow = \varepsilon_a \sigma (T_a + 273.16)^4 \cdot VF + (1 - VF) \cdot \varepsilon_t \sigma T_t^4$$

where ε_a is the apparent emissivity of the atmosphere, T_a is screen level temperature (°C), ε_t and T_t are the emissivity and temperature (K) of the surrounding terrain; and VF is the view factor of the measurement site, defined by

$$VF = \cos^2 (90 - H)$$

where H is the average horizon angle from the zenith in degrees. The view factor for the SB site is .958 (Prowse, 1981). The surrounding terrain was assumed to be snow covered, so T_t = 273.16 K and ε_t = 0.99. The atmospheric emissivity was calculated as for clear skies using the

modified Brutsaert formula described by Marks (1979), which is

$$\varepsilon_{ac} = 1.24(e'/T')^{1/7}$$

Here, e' and T' are screen level vapour pressure (mb) and temperature (K) which were calculated by extrapolating the observed T_a to sea level using a lapse rate of $6.5\,^{\circ}C\ km^{-1}$, and assuming constant relative humidity with elevation. This clear sky emissivity was then adjusted for cloud cover using the Bolz formula, which Arnfield (1979) found gave better results than several others. The Bolz formula is

$$\varepsilon_a = \varepsilon_{ac}\cdot[1 + (\sum_{i}^{n} k_{ci}\, c_i)c]$$

where k_{ci} are coefficients depending upon cloud type (Sellers, 1965), c_i is the fractional amount of cloud type i, n is the number of cloud types recorded and c is the total cloud cover.

3.1.4 Sensible and Latent Heat Exchanges

The turbulent fluxes, Q_H and Q_E, were calculated using bulk aerodynamic formulae, which are derived by combining flux-gradient relationships with empirical profile formulations (Deardorff, 1968). This approach has been used over melting snow by many investigators (Anderson, 1976; Price and Dunne, 1976; Prowse and Owens, 1982; Fitzgibbon and Dunne, 1980, 1983; Heron and Woo, 1978). A derivation of the formulae, with a discussion of the underlying assumptions and a review of the success of field applications, is included in appendix A.

The formulae used here are

$$Q_H = \rho_a c_{pa} D_H (T_a - T_s) \quad (3.5a)$$

$$Q_E = \rho_a L_v D_E (.622/p)(e_a - e_s) \quad (3.5b)$$

where ρ_a and c_{pa} are the density (kg m^{-3}) and specific heat (J kg^{-1} $°C^{-1}$) of air; T_a and e_a are the temperature (°C) and vapour pressure (mb) at height z_a (m) above the snow surface; p is atmospheric pressure (mb); T_s and e_s are the temperature and vapour pressure at the snow surface (0°C and 6.11 mb, respectively, for melting snow); L_v is the latent heat of vaporization (J kg^{-1}); and D_H and D_E are the bulk transfer coefficients for sensible and latent heat, respectively (m s^{-1}).

The bulk exchange coefficients are assumed from similarity arguments to equal D_M, the bulk exchange coefficient for momentum transfer. Under neutral conditions, D_M is given by

$$D_M = k^2 u_a / [\ln(z_a/z_o)]^2$$

where k is von Karman's constant, here taken as 0.4, u_a is the wind speed (m s^{-1}) at height z_a and z_o is the aerodynamic roughness length (m). During snowmelt, conditions are generally near-neutral to highly stable (de la Casiniere, 1974), so the exchange coefficients have to be corrected for stability. A stability parameter which can be calculated from one level measurements is the bulk Richardson number, defined by

$$Rb = g(T_a - T_s) z_a / (u_a^2 \cdot T_K)$$

where T_K is the mean absolute temperature of the air layer, and g is the gravitational acceleration (m s^{-2}). Deardorff (1968), Price (1977) and Moore (1983) have shown that a stability correction based upon Rb is equivalent to one

based upon the more complicated Monin-Obukhov parameter z/L.

Deardorff (1968) derived the stability correction for the general case of $D_H \neq D_E \neq D_M$. Anderson (1976) noted that if the exchange coefficients are equal, Deardorff's stability correction, which is the ratio of the stable and neutral case transfer coefficients (D_S/D_N), can be written as

$$D_S/D_N = (1 - 5Rb)^2 \qquad (3.6)$$

Price (1977) related the correction factor suggested by Monteith (1957) to the log-linear profile formulations found by Webb (1970), and derived

$$D_S/D_N = (1 + 10Rb)^{-1} \qquad (3.7a)$$

$$D_U/D_N = (1 - 10Rb) \qquad (3.7b)$$

where D_U is the exchange coefficient for unstable stratification. Eqs. (3.7) are equivalent to Eq. (3.6) for small values of Rb, because Price (1977) assumed that z/L was small in his derivation. The calculation of snowmelt should not be greatly affected by the differences at larger Rb because wind speeds, and consequently Q_H and Q_E, are usually small in the range of Rb for which Eqs. (3.6) and (3.7a) diverge. Eq. (3.7a) was used in this study because turbulent transfer does not in reality vanish abruptly at some degree of stability, as in Eq. (3.6), but over a range of values (Anderson, 1976). Moreover, turbulence occurs in periodic bursts, even at high degrees of stability (Halberstam and Schieldge, 1979).

The roughness length must be specified to apply Eqs. (3.5). At TB, z_o was calculated from Eq. (15) in appendix A for all cases with wind speeds greater than 2 m s^{-1} and Rb less than .012. Eq. (15) is sensitive to errors in the

wind speed, and an average value is required from several observations (Berkowicz and Prahm, 1982). Regression analysis and visual examination of the time series of z_o and ln z_o showed no simple trends with time (compare with Price, 1977), so the median value rounded to the nearest mm was considered representative of the entire period. This value is 4 mm, and agrees with other values found in the literature for similar snow conditions (see Table 1 in appendix A). At SB, z_o = 2.5 mm was used (Prowse, 1981).

3.1.5 Precipitation Heat Flow

The heat input due to the sensible heat of precipitation is given by

$$Q_p = \rho_w c_{pw} (T_r - T_s) P \qquad (3.8)$$

where c_{pw} is the specific heat (J $kg^{-1}°C^{-1}$) of water, T_r is the rain temperature and P is the precipitation rate (m s^{-1}). Rain temperature is difficult to measure, so the near surface wet bulb temperature is used as a surrogate, on the grounds that a falling raindrop acts like a wet bulb (Fletcher, 1962).

When rain moves into a snow pack with sub-freezing temperatures, it may freeze into the snow, releasing its latent of fusion. This process was unimportant during the spring melt period studied, but can be important in some situations, and is discussed further in chapter four.

3.1.6 Ground Heat Flow

The conductive heat flux from the ground can be calculated from Fourier's law,

$$Q_G = -K_G(dT/dz)$$

where z decreases with depth in the soil and K_G is the thermal conductivity of the soil ($W\ m^{-1}\ K^{-1}$). Although Q_G may be important during the winter season, particularly for snow metamorphism, it is small compared to the other heat sources during melt periods (Male and Granger, 1981), and is commonly neglected in energy balance computations of snowmelt (for example, Price, 1977; Heron and Woo, 1978; Jordan, 1978). Prowse (1981) estimated Q_G in the Craigieburn Range using measured soil temperatures and representative conductivities, and confirmed that it can be ignored during snowmelt periods. The ground heat flux was not included in snowmelt computations in this study.

3.2 SNOWMELT CALCULATIONS

Observations of snowmelt and the relevant variables for energy balance computations were made during a spring melt period in 1982. In this section the melt period characteristics are described, the accuracy of the energy balance computations is considered, and the contributions of the energy balance components are discussed. Detailed analysis of the factors controlling snow surface energy exchange is reserved for section 3.3.

3.2.1 Description of the Melt Period

The winter of 1982 was typical in that several mid-winter rain-on-snow and melt events occurred. Alternating snowfalls and melt periods occurred throughout the early spring. Rain fell at the meteorological site between 18 and 20 October, followed by snowfall and accumulation from 21 to 26 October. Melt conditions resumed 27 October, and air temperatures never dropped below freezing at TB or SB after 28 October. The mean snow-line elevation ranged from below 900 m on 25 October to around 1300 m on 9 November. Energy balance calculations are made for the period 28 October to 9 November, by which time twenty-five percent of TB was clear of snow.

A range of weather situations was experienced during the melt period, from calm anticyclonic conditions to frontal passages. Daily summaries of the weather situations are given in Table 3.1 and are illustrated in Fig. 3.1.

3.2.2 Accuracy of the Energy Balance Estimates

At TB, net radiation was measured directly by a net radiometer, and the accuracy of this instrument under good conditions is about ten percent (manufacturer's information), but heating of the polyethylene domes during sunny weather and moisture on the domes during rainy weather can affect the measurement (Anderson, 1976). Both of these conditions occurred at TB, and the net effect on the radiation measurements is not known. The net radiation estimates at SB involve many assumptions, such as the ratio

Table 3.1 - Daily summaries of weather situations.

Oct	28	Initially a high pressure ridge covering South Island; passage of cold front and westerly winds later in day.
	29	Low developing over South Island, passage of cold fronts.
	30	Ridge of high pressure over Tasman Sea, north-westerly wind increasing later in day.
	31	Strong north-westerly winds, frontal passage in afternoon.
Nov	1	Low moving to south-east of New Zealand, north-westerlies weakening, anticyclone extending influence over New Zealand.
	2-3	Anticyclone over New Zealand region.
	4	Depression deepening south of New Zealand, westerlies increasing in afternoon.
	5	Strong west to south-west winds, passage of cold fronts.
	6	Strong west to north-west winds, frontal passage.
	7	Anticyclone north of New Zealand, low to south-west, strong north-west winds.
	8	High moving to north-east, low to south-east, frontal passage, strong north-west winds decreasing in evening.

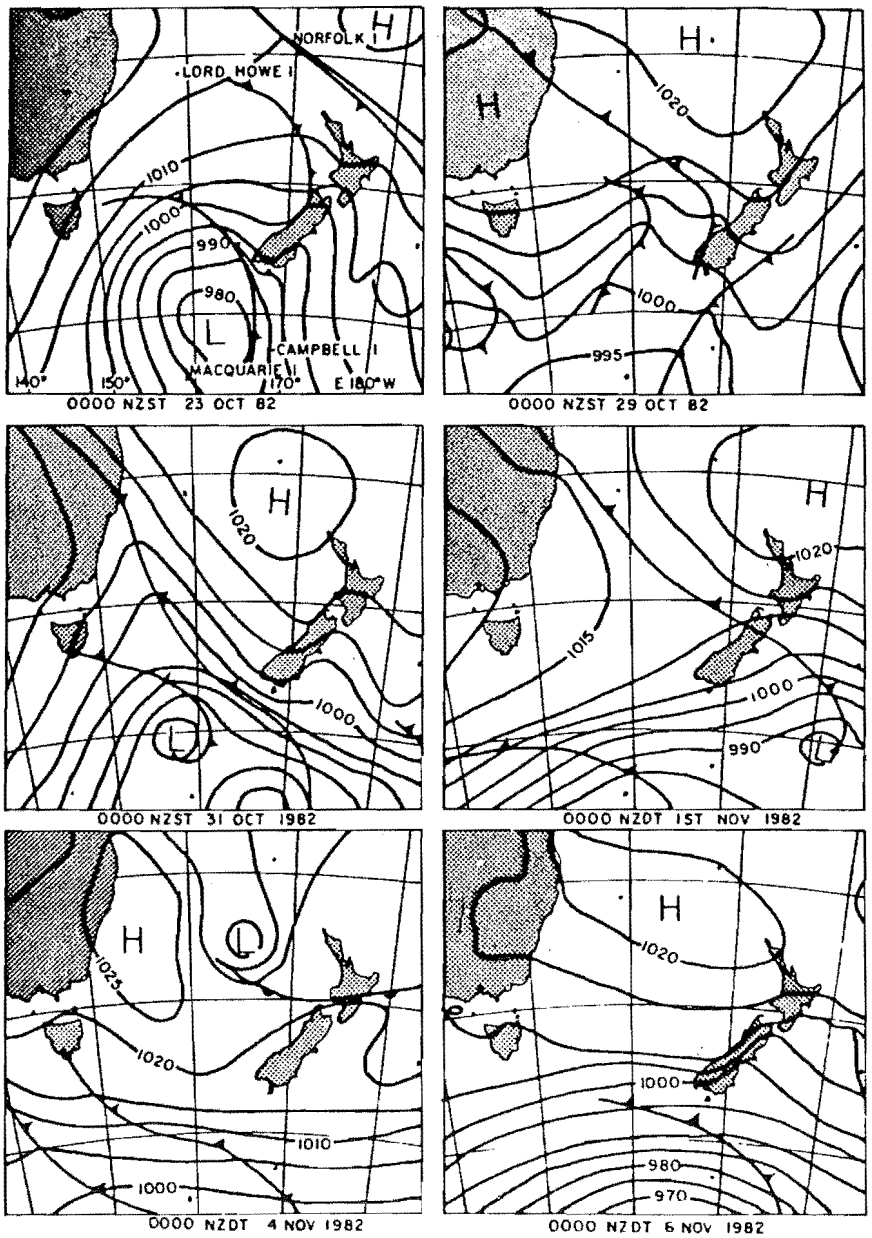

Fig. 3.1. Selected surface charts during spring, 1982.

$K\downarrow(SB)/K\downarrow(CF)$ and $\alpha = 0.5$, so that the estimates carry a high degree of uncertainty.

Error in Q_P is due to rain gauge catch deficiency and differences between T_r and T_w. Neither of these sources of error can be evaluated. However, Q_P contributed only two percent or less of the estimated heat inputs (see next section) so inaccuracies are not critical.

The accuracy of the sensible and latent heat flux estimates is difficult to assess because, although the bulk aerodynamic approach should be reasonably robust to violations of the assumptions (Moore, 1983), such violations will probably have some effect. In addition, the assumption $K_E = K_H$ carries a degree of uncertainty. Other sources of error are assessed below.

One possible source of error is the invalidity of the assumption of a melting snow surface. However, this was not considered to be important because the times that the computed Q_M was negative, and consequently the surface was freezing, were characterised by low wind speeds, and hence low values of Q_H and Q_E. For these conditions of low wind speed (less than 2 m s^{-1}), decreasing T_S would increase the terms $(T_a - T_S)$ and $(e_a - e_S)$ in Eqs. (3.5), but would also increase Rb, thereby decreasing the transfer coefficient and compensating for the increase in the temperature and vapour pressure differences. If the deviations from $T_S = 0°C$ were believed to have produced significant errors, T_S could have been estimated readily by the procedures recommended by Granberg (1979).

Conditions characterised by moderate to strong winds and air temperatures several degrees above freezing are

typical of melt conditions at TB and SB. Under these conditions, the errors in temperature and wind speed should certainly not exceed ten percent, so the maximum possible error in Q_H should be within twenty percent, since Q_H is proportional to the product of u_a and T_a. If these errors are random, they will be compensating over a period of days. The latent heat flux is proportional to $(e_a - 6.11)$ rather than to e_a, so proportional errors in Q_E will be greater than proportional errors in e_a. Again, these errors will average out in the absence of bias. Another source of error is involved in specifying z_o. Moore (1983) showed that bias due to errors in z_o should be within ten to twenty percent.

One further possible source of error in the estimation of Q_H and Q_E at SB is the use of daily averages of T_a, e_a and u_a. The effect of using daily averages can be understood by evaluating the mean of the product of two quantities, say u_a and T_a:

$$\overline{u_a T_a} = \overline{u}_a \cdot \overline{T}_a + \overline{u_a' T_a'} \qquad (3.9)$$

The second term on the right hand side of (3.9) is the covariance of u_a and T_a. Thus, if u_a and T_a are positively correlated, as they are in some situations, the use of daily rather than hourly means will underestimate the true mean of the product (see, for example, Hogg et al., 1982).

To assess the likely magnitude of this source of bias, daily values of Q_H and Q_E were calculated for TB using daily means, and were compared to daily values which were calculated as the sums of hourly means. For the twelve day period, the ratio Q_{HD}/Q_H (where the subscript D denotes the value calculated from daily averages) was 1.03, and Q_{ED}/Q_E = 1.07. For individual days, Q_{HD}/Q_H ranges from 0.67 to 1.20

and Q_{ED}/Q_E from 0.67 to 1.88. The days on which the ratios deviate greatly from unity are days with relatively low wind speeds (less than 3 m s^{-1}) and consequently low inputs of Q_H and Q_E. The low wind speeds occurred on days of weak regional airflow, during which local winds develop. Deviations from unity were generally within ten percent for days with higher wind speeds. The lowest daily mean of u_a at SB was 2.49 m s^{-1} and the daily mean was greater than 3 m s^{-1} on all but three days, so the bias in the daily values of Q_H and Q_E at SB due to the use of daily averages is probably less than ten percent.

The accuracy of the energy balance estimates can be roughly assessed by comparing the energy balance estimate of melt to a water balance estimate. On 1 November, the snow density calculated from the mean of six samples taken at the instrument site with a Mount Rose sampler and corrected for a nine percent bias (see section 3.1.1) was 458 kg m^{-3}, with an unbiased standard error of the estimate of 12 kg m^{-3}. The snow surface was melting, and rain and/or strong melt had been occurring for over a day, so the liquid water content was assumed to be eight percent, after considering measurements made by O'Loughlin (1969a) and Jordan (1978). Thus, the density of the ice matrix was 421 kg m^{-3}. The snow was fully ripe, so the ice density should have been fairly constant through the melt period. Between 30 October and 9 November the observed snow surface lowering was 850 mm, while the lowering computed from the energy balance and ice density estimates is 832 mm, which shows remarkably good agreement. At SB, only snow depth and not density was recorded, so the density was assumed to be the same as at

TB. At SB, observed lowering was 770 mm, while the computed lowering is 830 mm, a difference of eight percent. These comparisons between observed and computed snow surface lowering suggest that the energy balance estimates are reasonable, although biases in estimates of the different fluxes may be compensating.

3.2.3 Energy Balance Results

Table 3.2 shows the mean values of the energy balance components at TB and SB for the twelve day melt period. Sensible heat was the greatest source of energy at both sites, reflecting the generally warm, windy conditions prevailing during the melt period. Net radiation was second in importance at SB, followed by Q_E, while at TB, Q_E was more important than Q*. Precipitation heat flow was relatively unimportant at both sites, but was greater at TB than at SB. The differences in Q* and Q_p are due to the greater maritime exposure of TB: the greater cloud cover decreased $K\downarrow$, while the greater rainfall at TB produced larger inputs of Q_p. The differences in Q_H and Q_E between the sites are discussed in section 3.3.2.2.

Daily values of the energy balance components are shown in Fig. 3.2. It can be seen by referring to Fig. 3.1 and Table 3.1 that days of greatest heat input are characterised by strong north-westerly airflow (for example, 31 October). Days with lesser heat input are characterised by either weak regional airflow or south-westerly airflow, which brings cooler air (for example, 29 October and 4 November). This relationship reflects the dominance of the turbulent

Table 3.2 - Mean values of the melt rates and energy balance components at Temple Basin and Ski Basin during the spring 1982 melt period. All fluxes are in MJ $m^{-2} d^{-1}$ and melt is in $mm \cdot d^{-1}$.

M	Q*	Q_H	Q_E	Q_P	
32	1.7	6.0	2.7	0.2	Temple Basin
40	2.4	10.3	0.5	0.0	Ski Basin

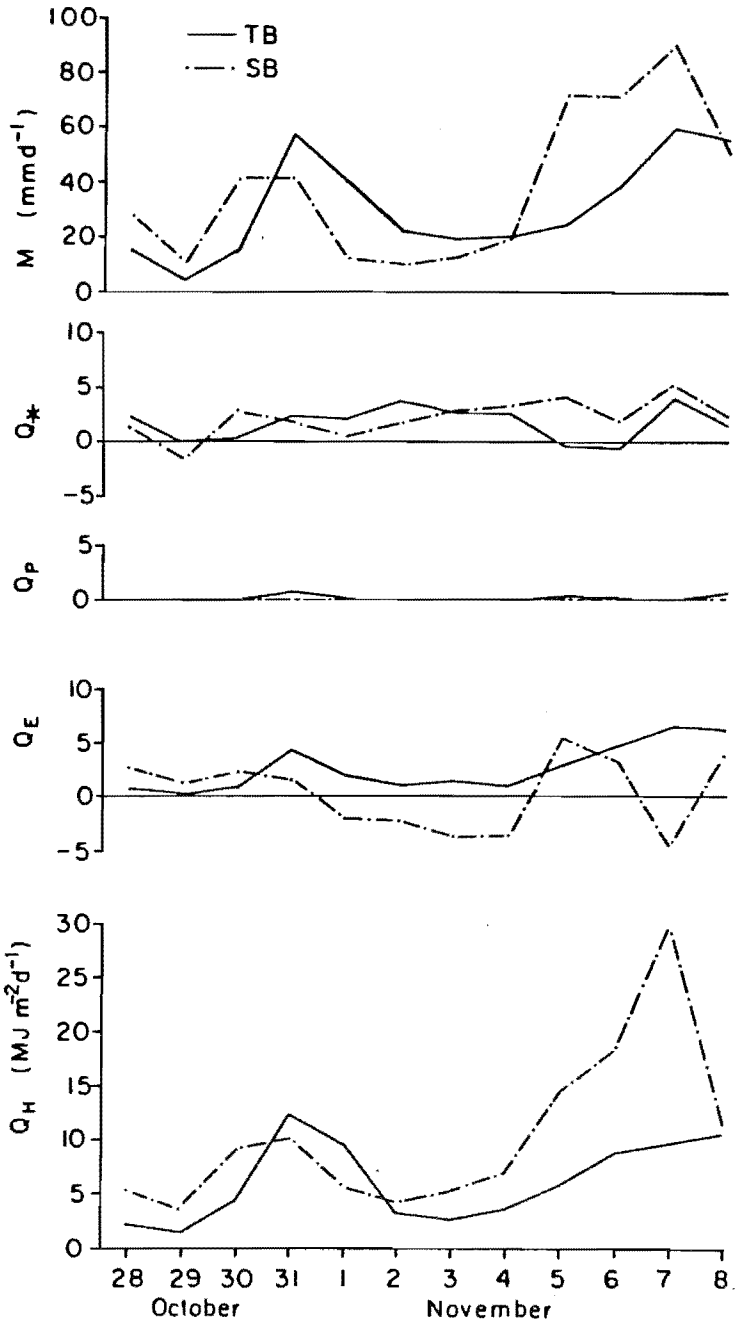

Fig. 3.2. Estimated daily energy budget components (MJ $m^{-2}d^{-1}$) and melt ($mm.d^{-1}$) at TB and SB.

exchanges, which are favoured during periods with warm, humid air and strong winds.

Fig. 3.3 shows three-hourly mean values of the energy fluxes at TB. Generally, Q* displays a strong diurnal pattern. On the evening of 31 October Q* remained positive, probably because of the longwave radiation emitted by warm low cloud. On 5 and 6 November, Q* averaged less than zero. The probable cause is the blocking of solar radiation by cold frontal cloud. In both cases, though, rain on the radiometer domes may have produced erroneous readings. Even in the short term, Q_P was not an important heat source. The greatest three-hourly value was 30 W m^{-2}, corresponding to fourteen percent of Q_M for that period. The sensible and latent heat fluxes are highly correlated because air mass characteristics favouring one also favour the other. The turbulent fluxes show little diurnality because the controls on Q_H and Q_E are independent of or only partially dependent on radiative exchange. MacKay and Thurtell (1978) came to this same conclusion for a continental North American site. The factors controlling the variation in Q_H and Q_E are discussed in the next section.

3.3 CONTROLS ON ADVECTIVE SNOWMELT

The sensible and latent heat fluxes vary both temporally and spatially, and the magnitudes of these variations have significance for snowmelt modelling. In this section, the processes controlling the variations will be discussed separately as to their effects on the temporal and spatial variability of the turbulent exchanges, although

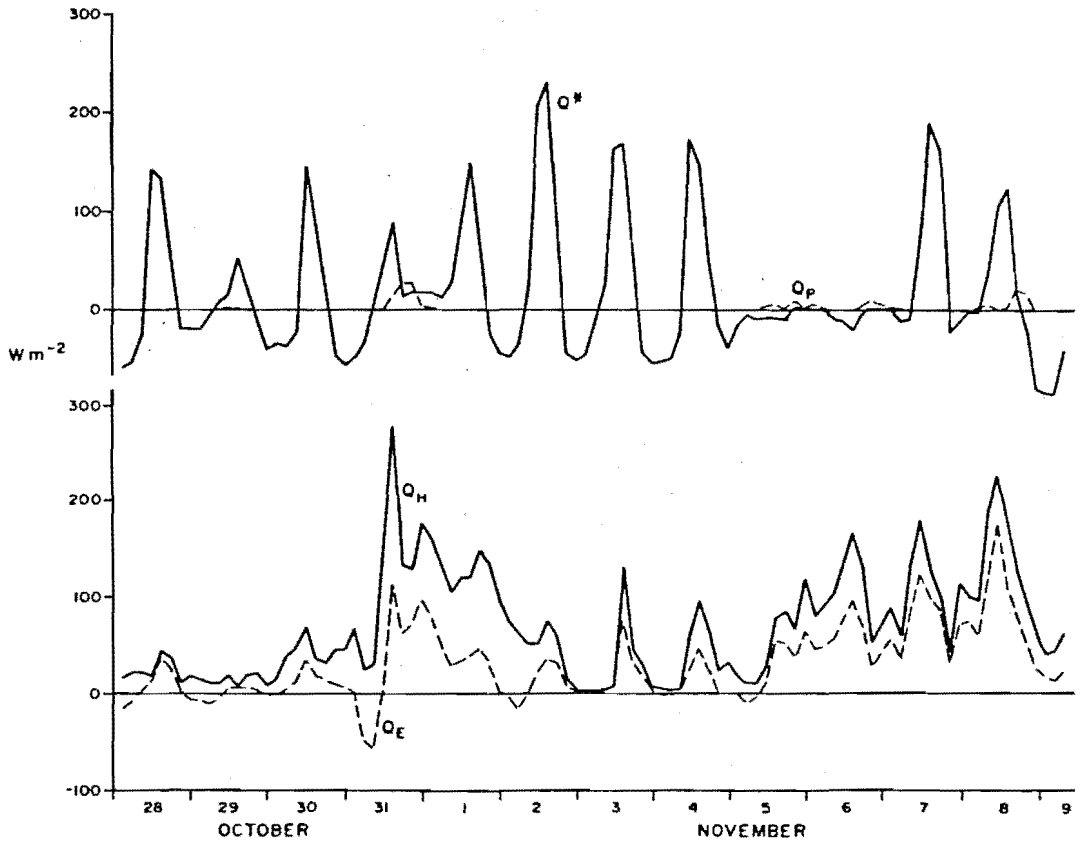

Fig. 3.3. Three-hourly averages of heat input estimates at TB.

the same processes are responsible for both.

3.3.1 Temporal Variability

Examination of Eqs. (3.5) shows that Q_H is a complicated function of air temperature, wind speed and surface roughness. Because the vapour content of maritime air masses is correlated with air temperature, Q_E also depends on these three factors, if the air mass has not undergone much modification. Although air temperature must be above freezing for Q_H to be directed towards a melting snow surface, the higher the air temperature the greater the damping of turbulence due to stable stratification. Increasing wind speed, however, both increases the bulk exchange coefficient and reduces stability. Thus, wind speed can often be more critical than air temperature in controlling turbulent exchange. In the following sections the factors controlling the short term variability of wind speed, temperature and humidity at a site are identified, and the relative magnitudes of their effects assessed.

3.3.1.1 Regional and Local Advection of Heat

The general relationships between the turbulent fluxes and regional wind flow discussed in section 3.2.3 and by Prowse and Owens (1982) are due largely to the advection of warmer, moister air during north-westerly flow than during more southerly flows. However, wind direction over the South Island is not a good index of air mass temperature since a cyclonic wind field over the Tasman Sea can advect

cold air from the south while producing north-westerly airflow over New Zealand (for example, Fig. 3.1, 23 October). The 1000-500 mb thickness in geopotential metres (gpm) was used to index the air mass heat moisture content, since this thickness is proportional to the mean virtual temperature in the layer. The thickness was abstracted from charts prepared every six hours by the New Zealand Meteorological Service and interpolated to provide a value every three hours.

To illustrate the effect of air mass source and to show that the air mass source is not always represented by the wind direction over the South Island, trajectories were plotted by calculating geostrophic wind vectors from the surface pressure field. Three situations were selected, and are shown in Fig. 3.4, along with mean sea surface isotherms for the period 23 to 27 October. Saucier (1955) briefly describes the procedure, which involves much uncertainty, particularly over areas such as the Tasman Sea, where pressure data are sparse.

Airmass A (Fig. 3.4) originated in the south where sea surface temperatures were lowest, but by the time it reached New Zealand the cyclonic wind field produced north-westerly flow over the South Island (Fig. 3.1). At that time, snow was accumulating in TB and SB rather than melting. Airmass B originated over warmer water to the north, but also approached the South Island from the north-west. Airmass C appears to have traversed Australia and travelled over water having intermediate surface temperature, but approached from the south-west. The 1000-500 mb level thicknesses over TB at the times of arrival of air masses A, B and C were 5340

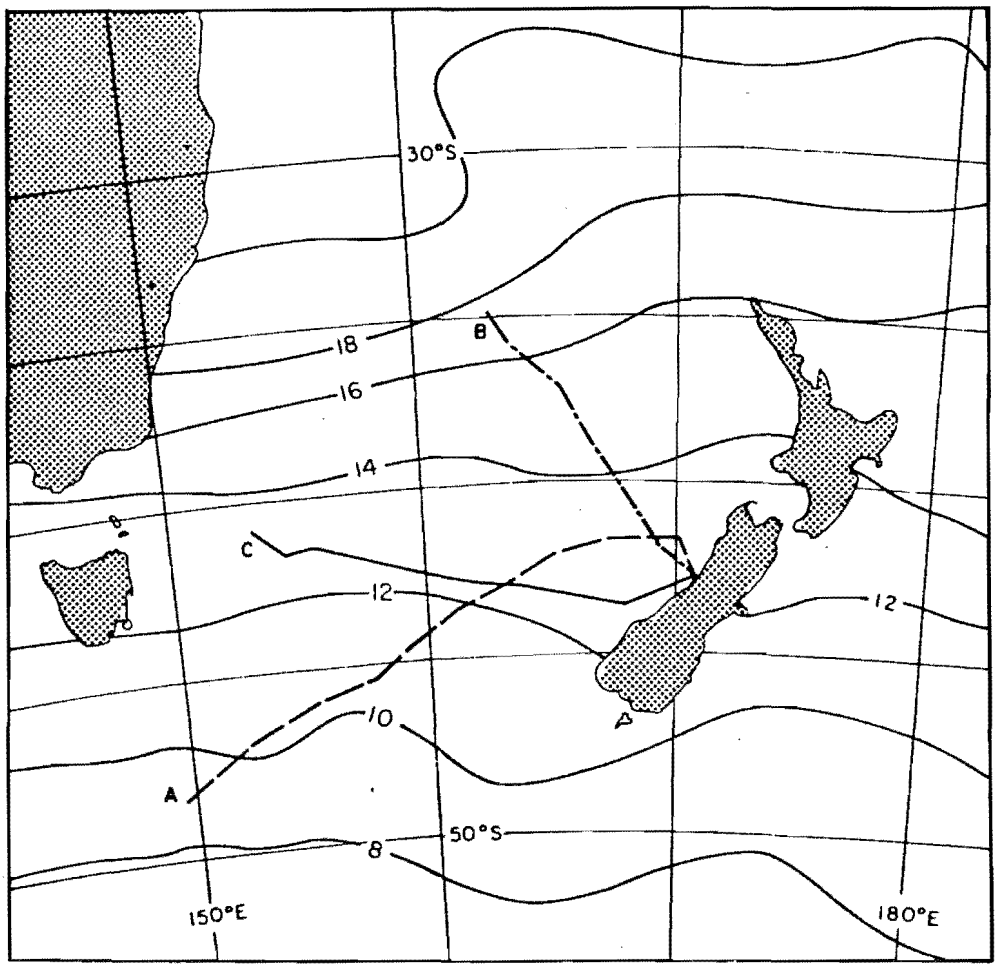

Fig. 3.4. Air mass trajectories and sea surface isotherms (°C), late October and early November 1982.
A - 0600 22 to 1200 23 October
B - 1800 29 to 0600 31 October
C - 0700 3 to 1400 4 November
(all times NZST).

gpm, 5550 gpm and 5520 gpm, respectively, reflecting the relative temperatures and histories of the air masses.

Although regional air mass characteristics exert a strong control on air temperature, local advection can enhance Q_H and Q_E over a snowfield. Local advection occurs when near-surface air layers gain sensible and latent heat from snow-free areas before flowing over snow. This gain of heat and moisture is governed by the net radiation received by the snow-free surfaces. Granger and Male (1978) showed that when local advection occurred, the daily total of sensible heat transfer was more than triple the value predicted by the 850 mb level temperature. Ohmura (1972) inferred from the results of a numerical model that sixty percent of the sensible heat exchanged at the surface of the marginal portions of a glacier was derived from the tundra between the ocean and the glacier.

As mentioned above, the 1000-500 mb thickness (Th) indexes the heat and moisture content of an air mass. Regression analysis shows that Th accounts for fifty-six percent of the variance of the three-hourly mean air temperature and sixty percent of the variance in the three-hourly mean vapour pressure (all values of R^2 are adjusted for degrees of freedom). These correlations suggest that regional air mass characteristics exert a strong control on observed air temperature and vapour pressure over snow. Addition of the concurrent and one lagged value of the three-hourly mean of Q* as indices of local advection increased R^2 to seventy-seven percent for air temperature and seventy-eight percent for vapour pressure. Two possible sources of unexplained variance are

error in measurement of T_a and e_a and air mass stratification, but the most important factor is probably that Q* measured over snow at TB is not a good index of local advection. In addition, the local effect would have increased as the snow-line rose through the study period and the fetch between the local air mass heat sources and the measurement site decreased (Weisman, 1977).

3.3.1.2 Regional and Local Winds

Large-scale air mass movement takes place in response to surface pressure gradients. In the absence of strong pressure gradients, differential heating and cooling in mountainous terrain can induce local scale circulations. Both scales of circulation can be important for turbulent transfer (Obled and Harder, 1979).

The influence of a thermally-induced wind was noted on 3 November, when the regional wind was light. At 1000 h, the observed wind was light (0.31 m s^{-1}), the air temperature was 10°C, and Rb was 5.8. Because of the extreme stability, the estimated Q_H was 0 W m^{-2}. However, at noon, an upslope wind from the west was produced by heating of the snow-free slopes below the basin. The observed wind rose to 3.03 m s^{-1}, the air temperature remained 10°C, and because of the decreased stability, Q_H increased to 109 W m^{-2}. This wind peaked in the afternoon, then died out as insolation decreased and the slope cooled (Fig. 3.5). The sensible and latent heat fluxes varied similarly.

The only relatively calm spell during the melt period

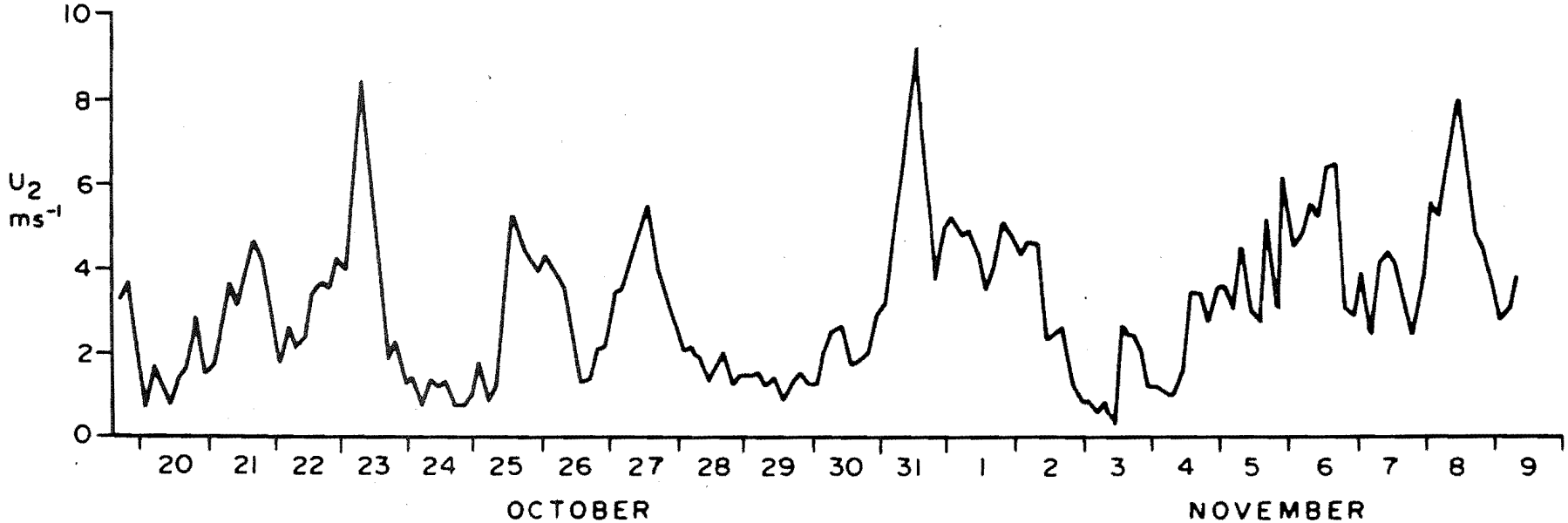

Fig. 3.5. Three-hourly mean wind speed at TB, 19 October to 9 November 1982.

occurred from 2 to 4 November; large-scale air movements dominated the rest of the period. The pressure difference between Auckland and Invercargill (DP) is similar to commonly-used indices of the strength of westerly flows (Trenberth, 1977). A correlation analysis shows that during the melt period the index accounts for sixty-three percent of the variance in the wind speed. The strength of the correlation suggests that DP is a useful short term index of observed wind speed. The unexplained variance is attributable to the presence of local winds, to the effects of wind-terrain interaction, and to details of the pressure field not represented by the index.

3.3.2 Spatial Variability

Spatial variations in Q_H and Q_E are the effects of processes which produce differences in wind speed, temperature and humidity between sites, and exist on different spatial scales. In this section, variability will be discussed with respect to both local variations (that is, within TB) and mesoscale variations (between TB and SB).

3.3.2.1 Local Variability

Sets of ablation stakes were placed at different sites in TB to investigate spatial patterns of melt under different weather conditions. The stake locations are shown in Fig. 2.8. Six stakes were set at each site, but some melted out before 9 November. The stakes were measured on the mornings of 2, 3 and 9 November. Between 2 and 3

November, net radiation accounted for fifty-three percent of the estimated heat input at the instrument site, while between 3 and 9 November, net radiation accounted for only thirteen percent of the estimated heat input. The results of a one way analysis of variance and Duncan's New Multiple Range Test are shown in Table 3.3.

It must be stressed that the measurements are of snow surface lowering, not melt. However, the snow at all sites was thoroughly ripe, and measurements made by Morris and O'Loughlin (1965), O'Loughlin (1969a) and Prowse (1981) indicate that fully ripe snow packs at three different sites in the Craigieburn Range have densities ranging from 400 to 500 kg m^{-3}, with most values between 420 and 450 kg m^{-3}. Thus, snow densities were likely to be reasonably uniform, and the patterns of snow surface lowering during the different weather situations should represent the different patterns of melt.

As shown in Table 3.3, the surface lowering at site 4 between 2 and 3 November was significantly less than at the other three sites, which were not significantly different from each other. Between 3 and 9 November, however, the lowering at site 1 was significantly greater than at the other three sites, which were not significantly different from each other.

The lowering at site 4 between 2 and 3 November was probably less than at the other sites because the site is at a higher elevation than sites 1 and 2, and less exposed to solar radiation (due to terrain shading and its aspect) than site 3, which is at about the same elevation as site 4. Site 4 would thus likely have received less net radiation

Table 3.3 - Statistical comparison of snow surface lowering measurements at Temple Basin. Note: surface lowering is in cm.

a. Clear weather melt, 2-3 November 1982.

(i) Analysis of variance

Source	DF	SS	MS	F	PROB
Between sites	3	21.15	7.05	7.28	0.0021
Within sites	18	17.44	0.97		
Total	21	38.59			

(ii) Multiple Range Test

Homogeneous subsets at 0.05 level

1	Group	4		
	Mean	3.3		
2	Group	1	2	3
	Mean	5.1	5.4	5.9

b. Rain melt, 3-9 November 1982.

(i) Analysis of variance

Source	DF	SS	MS	F	PROB
Between sites	3	340.16	113.39	6.48	0.0087
Within sites	11	192.58	17.51		
Total	14	532.74			

(ii) Multiple Range Test

Homogeneous subsets at 0.05 level

1	Group	4	3	2
	Mean	51.4	53.5	55.3
2	Group	1		
	Mean	63.3		

DF - degrees of freedom
SS - sum of squares
MS - mean square
F - ratio of variances
PROB - probability of greater value of F

and sensible heat than the others. The surface lowering was greatest at site 2, which was at a low elevation and had a sunny aspect. Site 3 had greater surface lowering than site 1 despite its higher elevation, probably because of the sunnier aspect of site 3.

Between 3 and 9 November the pattern is indicative of greater turbulent exchange at site 1 than at the others. One possible explanation is that sites 2, 3 and 4 were located in areas of relatively uniform slope, while site 1 was adjacent to the instruments at the top of a small rise. Jackson and Hunt (1975) developed a theory which predicts the increase in wind shear when air flows over low hills. This theory is supported by the field measurements of Jensen and Peterson (1978) and Bradley (1980). The results of the theory are not quantitatively applicable to the field site because the theory assumes low symmetrical two-dimensional hills. However, the theory qualitatively predicts increased wind shear at the crests of even small terrain features, which would produce increased turbulent exchange, and hence, greater melt during an advective melt situation.

Another possible cause of increased melt could be local advective effects at site 1. However, the snow cover near site 2 was patchier than that near site 1, so local advection does not appear to be an adequate explanation. In addition, an ablation stake was located on a relatively flat site in the predominant upwind direction from site 1. For the period 3 to 9 November the observed surface lowering at that stake was 545 mm, similar to sites 2, 3 and 4 and less than at site 1.

Kojima *et al.* (1973) reported the results of similar

studies carried out over three melt seasons in a small drainage area in Hokkaido. They found that in clear weather, surface lowering showed little decrease with elevation, and that south-facing slopes had 1.6 times as much surface lowering than north-facing slopes. In contrast, the lowering rate on south slopes was only 1.2 times that on north slopes during a melt period characterised by rainy weather, and the surface lowering decreased by one-third from the lowest to the highest site (elevation range 290 m). This decrease in surface lowering with height could be caused by the decrease in temperature, and thus of sensible heat transfer, with height. In the present study, the lack of such a strong surface lowering gradient could be due to the fact that the higher sites, although cooler, could be more exposed to the wind. At any rate, the fact that both studies used surface lowering as a surrogate for melt precludes the drawing of strong conclusions. The results suggest that in any elevation band, melt may be more uniform under cloudy conditions than under clear conditions, but that exposure to the wind is a strong control on the spatial variation of melt.

3.3.2.2 Mesoscale Variability

As mentioned in section 3.3.3, sensible heat was the most important energy source at both TB and SB. Sensible heat flux was greater at SB because conditions there were generally both warmer and windier than at TB (Fig. 3.6). However, on 31 October and 1 November the higher wind speeds at TB produced higher daily inputs of Q_H than at SB, even

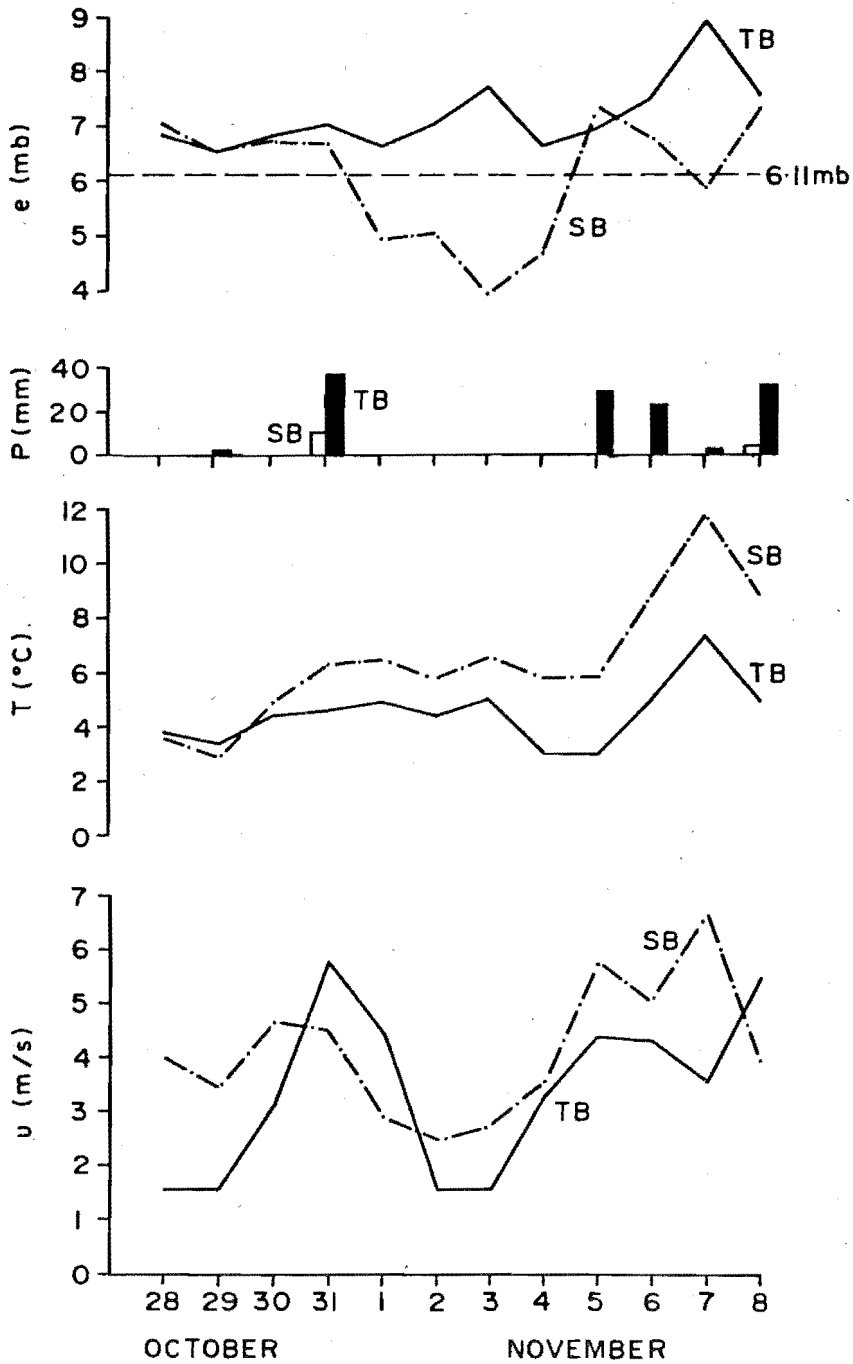

Fig. 3.6. Mean daily values of wind speed, temperature, vapour pressure and precipitation at TB and SB.

though the temperature was greater at SB (Fig. 3.6). Mountain wind fields are complex, so it is difficult from this small sample to make any conclusions regarding the differences in wind speed between the sites. The mean air temperature was lower at SB on 28 and 29 October. This difference in temperature could be due to greater longwave radiative losses at SB and/or the loss of sensible heat to the snow pack as the air mass traversed the mountain ranges. From 30 October on, however, air temperature was greater at SB and the temperature difference displayed a statistically significant (0.01 level) trend with time. This trend coincides with the increase in the area of snow-free ground as the snow-line rose through the melt period. The snow-free areas are sources of sensible and latent heat, and the temperature difference trend probably results from the increasing influence of local advection through time.

The net latent heat input is lower at SB than at TB, even though Q_E was greater at SB on a few days (Fig. 3.2). The low net input results from the low humidities occurring at SB on five of the twelve days; on these days, the snow pack lost energy through evaporation. In contrast, the latent heat flux at TB was toward the snow pack on all days. The vapour pressures are similar at both sites on most days that the regional westerly airflow was strong (Fig. 3.6). The regional airflow was weak from 1 to 4 November, and the vapour pressures reflect the greater maritime exposure of TB. On 7 November, however, the regional airflow was strong from the north-west, and SB vapour pressure was much lower than TB vapour pressure. The wind speeds on 7 November were also out of phase between the two sites. One reasonable

explanation appears to be the presence of an inversion on the west coast, upwind of the mountains, at approximately 1500 m elevation. A New Zealand Meteorological Service meteorologist confirms that such an inversion occurs commonly (Ian Miller, pers. comm.). In such a situation, TB would be affected by the air below the inversion, while SB would experience air from above the inversion, which would have quite different properties, especially after flowing over mountainous terrain. Unfortunately, no upper air data from a west coast site are available to confirm this suggestion.

3.4 IMPLICATIONS FOR MODELLING

Snowmelt models may apply only to a particular point, or they may predict snowmelt averaged over an entire basin. Models can also be classified as being either energy balance models, which explicitly account for all of the energy exchanges, or index models, in which the energy exchange is represented by empirical relationships with one or more variables, commonly air temperature (WMO, 1982). Index models are the most commonly used, because they require less data input than energy balance models. However, several studies have shown that temperature index models are poor predictors of short term melt rates at open sites, particularly when weather systems change rapidly (Anderson, 1976; Price, 1977; Granger and Male, 1978; Braun and Zuidema, 1982). A problem common to both types of models, but especially energy balance computations, is the difficulty of extrapolating the often sparse site

measurements of highly variable quantities such as wind speed and radiation. An additional problem is that of forecasting the input data for flood forecasting applications.

Male and Granger (1981) advocated a somewhat different approach to modelling energy exchange. They suggested that large scale meteorological indices may prove useful for predicting turbulent exchange over snow. Brutsaert and Mawdsley (1976) had some success in employing theoretical relationships between upper-air data and evapotranspiration from a snow-free drainage basin. Kraus (1973) derived similar expressions for use over melting ice, but did not apply them. Granger and Male (1978) developed an empirical relationship between the 850 mb air temperature and sensible heat transfer at the snow surface, which appears to be quite reliable except when local advection or air mass stratification occurs.

The complex wind regimes in mountainous terrain complicate boundary layer processes, precluding presently developed theoretical approaches to relating turbulent exchange to large scale variables. However, the strong control exerted by air mass and circulation characteristics on the factors involved in turbulent exchange suggests that empirical relationships, such as that presented by Granger and Male (1978), may be useful. Local effects would perturb such relationships on hourly time scales, so daily averages were used here to try to minimize local effects. Because Q_H and Q_E are highly correlated at TB, the sum $Q_H + Q_E$ was regressed against Th and DP. The correlation of $Q_H + Q_E$ with Th is 0.84 and with DP is 0.81, while the correlation

between Th and DP is 0.70. Fig. 3.7 shows plots of $Q_H + Q_E$ against Th and DP, with least-squares regression lines drawn. The Th-DP relationship results from the association between warm air masses and strong circulations, as typified by the situation shown in Fig. 3.1 (31 October). Together, Th and DP account for seventy-five percent of the variance of $Q_H + Q_E$ (adjusted for degrees of freedom), with a standard error of 3.0 MJ m^{-2} d^{-1}. The addition of daily net radiation as an index of local effects increased the adjusted R^2 to 0.80 and decreased the standard error to 2.7 MJ m^{-2} d^{-1}, indicating that the use of daily means has not completely filtered out local effects.

A similar regression analysis was performed for the daily totals of Q_H and Q_E at SB. The regressions were performed separately for Q_H and Q_E because the fluxes were not so highly correlated as at TB. Because the air mass would have undergone modification as it traversed the mountain ranges between the two sites, the 850 mb level temperature, vapour pressure and wind speed from the noon Christchurch radiosonde flights were also employed as independent variables. The simple correlation matrix is given in Table 3.4.

The latent heat flux is poorly correlated with all of the variables, and none of the regression relationships is significant. The sensible heat flux is moderately correlated with several of the variables, and the best regression relationship is with Th, with an adjusted R^2 of 0.74 and a standard error of 3.8 MJ m^{-2} d^{-1}. The R^2 value is somewhat misleading because all but one of the values lie below 17.5 MJ m^{-2} d^{-1}, and the other is almost double that

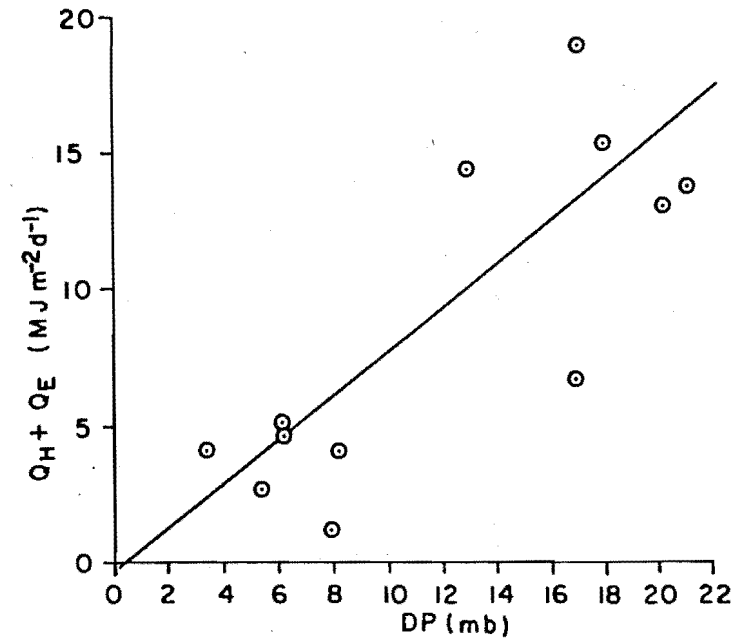

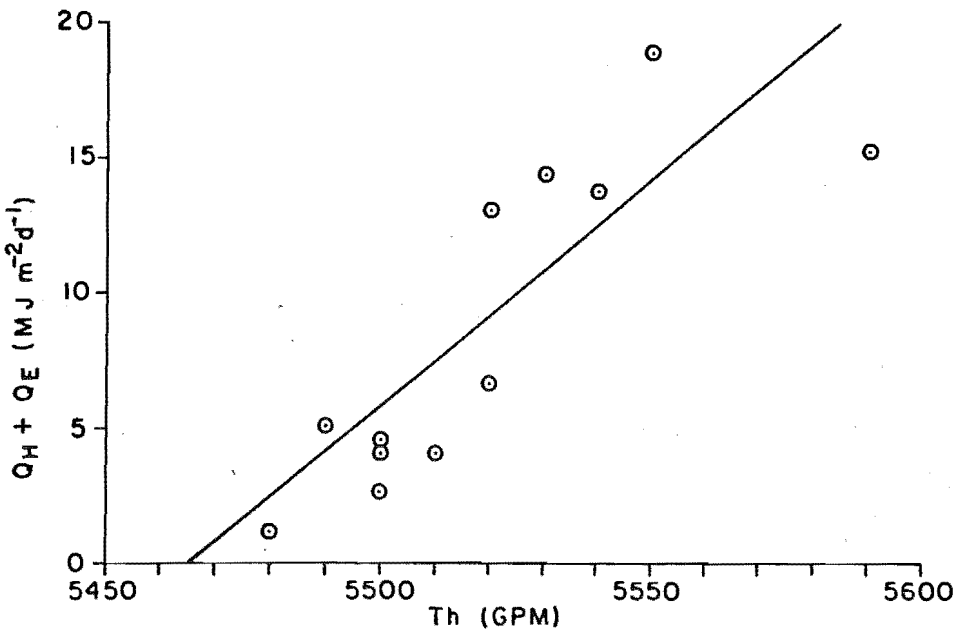

Fig. 3.7. Plots of $Q_H + Q_E$ at TB against Th and DP, with least-squares regression lines drawn.

Table 3.4 - Matrix of simple correlations between heat exchange at Ski Basin and meteorological data.

	u	T	e	DP	Th	Q_H	Q_E
u	1.0	.73	.09	.72	.74	.76	.07
T		1.0	.37	.76	.83	.73	.16
e			1.0	.57	.23	.01	.24
DP				1.0	.70	.70	.36
Th					1.0	.87	.10
Q_H						1.0	.01
Q_E							1.0

u - wind speed at 850 mb

T - air temperature at 850 mb

e - vapour pressure at 850 mb

DP - Auckland-Invercargill pressure difference

Th - 1000-500 mb layer thickness

value at 29.6 MJ m^{-2} d^{-1} (see Fig. 3.8). The R^2 value would decrease if the outlying point was excluded. The correlations between Q_H and the 850 mb level variables would probably be greater if more radiosonde data were available; the values from the noon observations are probably not representative of the daily means in many cases. Another problem is that air mass modification may have occurred between the mountains and Christchurch.

A difficulty in applying a large scale approach in mountainous terrain results from the variation of temperature with elevation; the use of an air mass heat content index is more appropriate for regions having less relief. However, the pressure difference appears to be a good index of the wind speed during snowmelt periods. An advantage of using DP to index wind speed is that DP is readily available for prediction or real-time forecasting, and is probably more representative of wind speed over an area than site measurements, which are not available in many of New Zealand's mountain regions.

3.5 SUMMARY

Analysis of the time series of temperature and wind speed at TB indicates that regional air mass characteristics and circulation provide the strongest controls on the turbulent exchanges of sensible and latent heat. Local advection of heat and locally generated winds enhance Q_H and Q_E during periods of strong insolation, but are not so important during rapid melt situations. Regression analysis shows that the indices of regional air mass characteristics

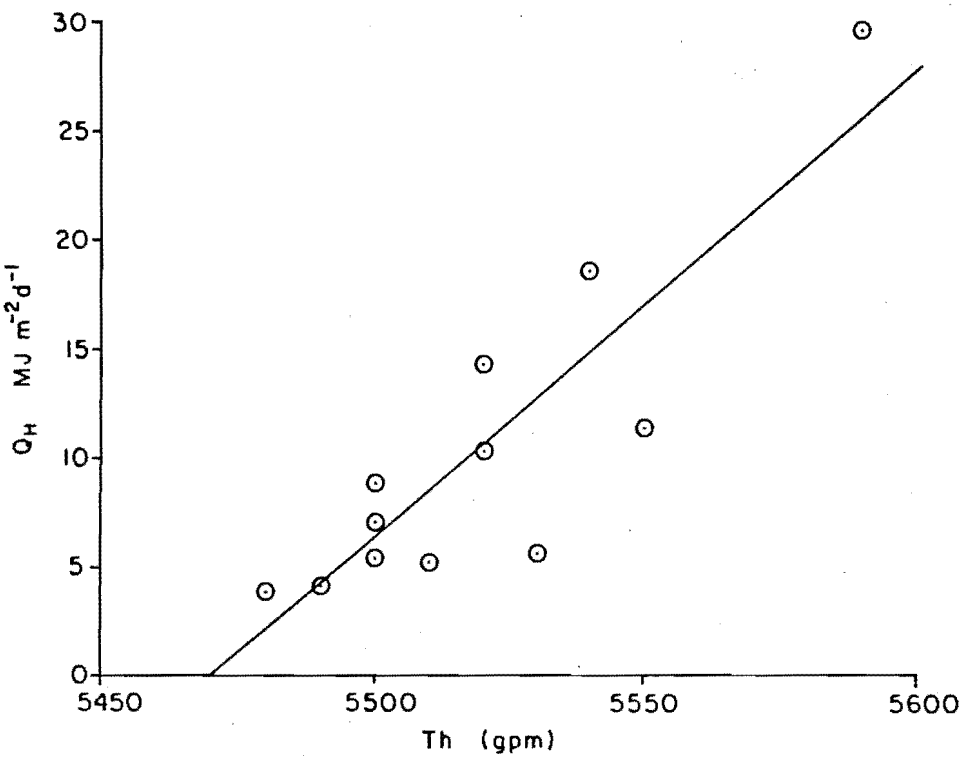

Fig. 3.8. Plot of Q_H at SB against Th, with least-squares regression line drawn.

and circulation explain seventy-five percent of the variance of $Q_H + Q_E$, and are thus useful predictors of snowmelt at TB. These large scale indices are particularly attractive because they are given in forecasts with up to thirty-six hours lead time, and are representative of conditions over a larger area than site measurements.

Measurements of snow surface lowering at four different sites in TB suggest that slope aspect is the major control on the local spatial variability of melt during calm, clear weather melt periods. However, during advective melt situations, exposure to the wind and elevation are the major controls. The theory of Jackson and Hunt (1975) shows that the increase in wind shear can be significant over even low hills, and would produce enhanced advective melt on hill crests. The results of the surface lowering measurements, although not conclusive, accord with Jackson and Hunt's theory, and have significant implications for the choice of representative sites for snowmelt research, even in relatively homogeneous basins.

Comparison of the meteorological variables between TB and SB indicates that under anticyclonic conditions, TB is influenced by moist, maritime air while SB can be influenced by relatively warm, dry air. Under strong regional advective conditions considerable air mass modification can occur as the air mass traverses the mountain ranges. The effects of different air masses and air mass modification produce differences in the snowmelt energy budgets between TB and SB, and imply that energy balance information cannot safely be extrapolated.

The results from this chapter will be discussed further

in the context of runoff modelling in chapter five and in the analysis of snowmelt characteristics in chapter six.

CHAPTER FOUR

RUNOFF PROCESSES

Streamflow generation in snow-covered basins involves two sets of processes. The first are those which generate the water input at or near the snow pack interfaces. The second set are the processes involved in routing the water inputs from their point of origin to the basin outlet; these processes are dealt with in this chapter.

Studies of streamflow generation in New Zealand have so far neglected snow-covered basins, despite the recommendations of O'Loughlin (1969a) and Fitzharris (1979). Fundamental field research into runoff routing processes was beyond the scope of this investigation. However, an attempt is made to gain insight into snow influences on runoff in a New Zealand environment. This attempt is made by relating field observations and climatic considerations to theoretical and empirical findings given in the literature. The first section summarizes some aspects of snow-water phenomena as discussed by other authors. The next two sections discuss field observations of snow-water relationships and runoff generation. The final section summarizes the findings.

4.1 WATER MOVEMENT IN SNOW - A REVIEW

The presence of a snow cover changes the pathways by which water inputs (rain and meltwater) reach a stream (Price et al., 1979). The usual result appears to be an increase in the response time of a catchment (Colbeck, 1978a; Wankiewicz, 1979; Jordan, 1983), although the possibility of flow concentration by snow cover and more rapid delivery to a stream channel may be possible in areas with thick permeable soils. Runoff delay is caused by initial losses through freezing, transient storage and the retention of water against gravity. A discussion of these effects follows.

4.1.1 Initial Losses

When rain or meltwater moves into sub-freezing snow, some or all of the percolating water freezes into the ice matrix, releasing its latent heat of fusion into and warming the snow cover. All of the ice in the flow path must be warmed to 0°C before runoff will occur. The maximum loss due to freezing is equal to $-\Theta/\rho_w L_f$, where Θ, the heat content of the ice matrix, is defined by

$$\Theta = \int_0^h \rho_s(z)\, c_{pi}\, T_s(z)\, dz \qquad (4.1)$$

where z is the vertical coordinate, h is the snow depth, c_{pi} is the specific heat of ice (J kg^{-1} $°C^{-1}$), and $\rho_s(z)$ and $T_s(z)$ are the snow density (kg m^{-3}) and temperature (°C) at position z. A snow pack can again become anisothermal even after active melt and runoff have occurred, for example by radiative cooling at night. Eq. (4.1) gives the maximum

amount of water that can be lost by freezing into a cold pack because of the pack's "cold content". However, many studies have shown that water moving into cold snow concentrates in fingers, and pockets of sub-freezing snow may remain in the pack even after significant water input has occurred (USACE, 1956; Sulahria, 1972; Granberg, 1979 ; McGurk, 1983).

4.1.2 Water Retention Capacity

After the heat deficit of snow pack is satisfied, its water retention capacity must be filled before water can percolate further. Liquid water content and retention capacity can be defined quantitatively in several ways. One is to define them gravimetrically, for example

$$WRG = (\rho_{sw} - \rho_{sd})/\rho_{sd} \qquad (4.2a)$$

where WRG is the gravimetric retention capacity, and ρ_{sw} and ρ_{sd} are the respective densities in kg m^{-3} of the snow with and without the retained water. Water retention can also be defined volumetrically:

$$WRV = WRG\ \rho_{sd}/\rho_{sw} \qquad (4.2b)$$

where WRV is the volumetric water retention capacity.

Snow packs can retain liquid water against gravity through two mechanisms. The first is the capillary force exerted on water by the snow grains. Water held in this manner can be regarded as the irreducible water content (Wankiewicz, 1979), which is here considered to be synonymous with the water retention capacity. The second mechanism is the inhibition of drainage at a discontinuity, for example, at an ice layer. Water retention at a

discontinuity is fundamentally transient, since metamorphism in the presence of liquid water would act to obliterate the discontinuity, allowing drainage (Gerdel, 1954). However, if the snow cover cools sufficiently before the water held at a discontinuity can drain, or if the heat deficit is great enough, the water will freeze into the pack, producing positive feedback, and can produce thick, persistent ice bands such as those observed by Marcus and Moore (1983) on Mount Egmont.

The concept of water retention capacity of snow is analogous to the field capacity of soil (Wankiewicz, 1979). As Wankiewicz noted, it is not clear whether such a concept should apply to fine textured snow. A major obstacle to applying the water retention capacity concept to snow is the difficulty of measuring the liquid content of snow (Colbeck, 1978b). A further problem is that immature snow experiences rapid metamorphism when liquid water is introduced (Colbeck, 1973), such that the water holding properties of the snow may change with time. Mature snow is considered here to be snow which has been in contact with liquid water for a sufficient length of time such that wet snow metamorphism proceeds slowly enough for the snow to approximate a rigid porous medium over a period of days.

There exists no consensus as to the magnitude of water retention capacity, despite the many measurements which have been made. Linsley et al. (1949) and Smith and Halverson (1969) stated that dry snow can retain large amounts of water. Linsley et al. proposed that this retained water could be released suddenly following snow pack ripening, and invoked this mechanism to explain an apparent fifty-eight

hour runoff delay during a rain-on-snow event in California. Bergman (1983), on the other hand, analysed short term changes in snow density profiles during seven natural rain-on-snow events, and found no evidence for the high retention capacities cited by Smith and Halverson (1969). One of the most comprehensive experiments is that of Sulahria (1972). However, he appears to have included layers with both free and impeded drainage in his analysis, making his results somewhat difficult to interpret.

The water retention capacity of freely draining snow depends upon the surface curvature and the surface area within the pores. Therefore, the water retention capacity should possibly increase with density and decrease with grain size, although the grain size distribution may have an effect. Wankiewicz (1979) summarized the results given by several workers in a plot of WRV against wet snow density. Fig. 4.1 is a plot of WRV against dry snow density, incorporating all the points shown by Wankiewicz for which the original references were available, plus three points derived from Smith and Halverson (1969). The volumetric retention capacity is used because WRG is inversely proportional to density, which could produce a spurious negative relationship. Wankiewicz noted that there appears to be no general relationship between WRV and snow density, although the results of USACE (1956) and Ebaugh and DeWalle (1977) suggest that a positive relationship exists for snow samples with similar histories. Ebaugh and DeWalle found that density explained forty-seven percent of the variance of the retention capacity of fresh snow. Wankiewicz attributed the scatter in his plot both to measurement

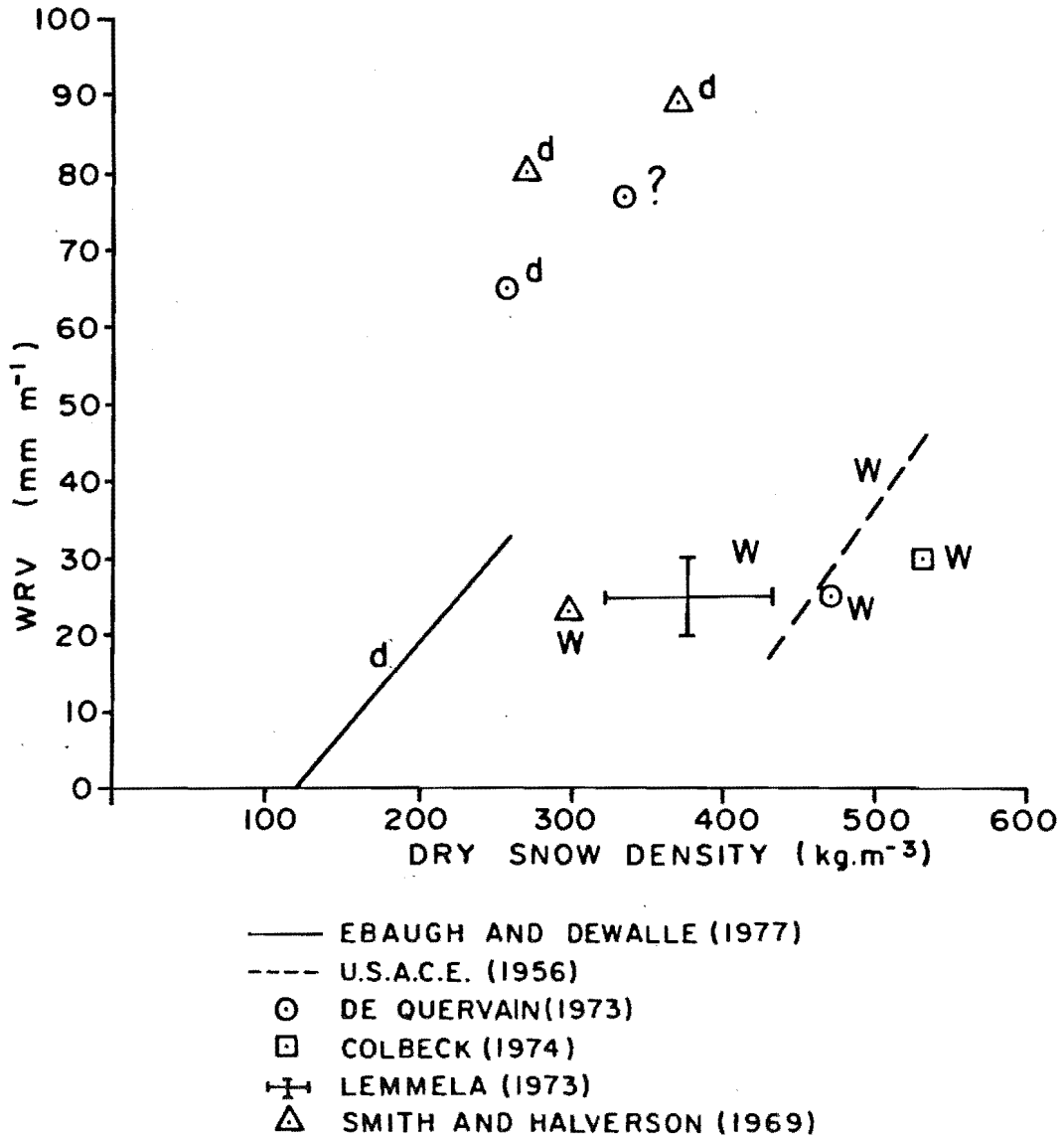

Fig. 4.1. Volumetric water capacities reported in the literature plotted against dry snow density.
"w" = previously wetted snow
"d" = previously dry snow
"?" = wetting history not specified

difficulties and to dependence upon factors other than density, such as grain size distribution and the presence of impeding layers.

An effort was made to extract more information, such as grain size, from the original sources. The amount of extra information was variable, but it was possible to determine whether or not the snow had been in contact with liquid water in all cases but one (see Fig. 4.1). It appears that coarse, mature snow has a generally low water retention capacity which does not range greatly. Finer grained snow or snow which has not had contact with liquid water displays a greater range of water retention capacities, and a degree of dependence on density is suggested. These conclusions are virtually the same as those arrived at by Smith (1974). However, these observations are based upon a limited sample which is variable with respect to measurement technique.

4.1.3 Transient Storage

Transient storage effects result from the dynamics of water movement through snow. Travel times of water through mature snow have been treated both empirically and theoretically. Anderson (1976) developed empirical routing relationships for mature snow covers from lysimeter studies. Colbeck (1972) derived a theory based upon kinematic waves for one-dimensional flow through snow. This theory has been successfully extended to predict slope runoff by coupling unsaturated vertical percolation and saturated downslope flow over an impermeable layer (Dunne et al., 1976). Further extensions treat flow through layered snow (Colbeck,

1975), flow through homogeneous dry snow and heterogeneous flow through ripe snow (Colbeck, 1979a).

In homogeneous ripe snow the force of gravity usually dominates over capillary forces (Colbeck, 1974), and Darcy's law for vertical unsaturated flow in snow can be expressed as (Colbeck, 1978a)

$$v = a \cdot K \cdot S^{*3} \tag{4.3}$$

where v is the flux of water ($m\ s^{-1}$), a is a constant ($m^{-1}\ s^{-1}$) equal to the gravitational acceleration divided by the kinematic viscosity of water, K is the intrinsic permeability (m^2), and S* is the effective saturation of the snow, defined by

$$S^* = (S_w - S_{wi})/(1 - S_{wi})$$

where S_w is the fraction of pore volume occupied by water and S_{wi} is the irreducible water content, expressed as a fraction of pore volume. Colbeck (1972) combined Eq. (4.3) with the equation of continuity to show that the celerity, C, of a flux v is given by

$$C = (dz/dt)|_v = 3 \cdot (a \cdot K)^{1/3} \phi_e^{-1} v^{2/3} \tag{4.4}$$

where ϕ_e is the effective porosity, defined by

$$\phi_e = \phi \cdot (1 - S_{wi}),$$
$$\phi = 1 - (\rho_{sd}/917)$$

Eq. (4.4) shows that the propagation of a flux depends upon the flux, and is valid for steady or decreasing flux. When the flux rate increases with time, as when the surface melt rate increases through the morning, a shock front forms. Colbeck (1978a) showed that the celerity of the shock front (C_s) can solved for by combining Eq. (4.4) with the continuity constraint. The shock front celerity is given by

$$C_s = (a \cdot K)^{1/3} \phi_e^{-1} (v_+^{2/3} + v_+^{1/3} v_-^{1/3} + v_-^{2/3}) \qquad (4.5)$$

where v_+ and v_- are the faster and slower fluxes which bound the shock front.

Inhomogeneities such as ice layers produce heterogeneous flow patterns and temporary storage through ponding. Wankiewicz (1979) introduced the FINA (flow impeding, neutral or accelerating) model to describe the behaviour of liquid water at snow layer interfaces, particularly the generation of multiple flow paths. Gerdel (1954) observed that ice layers break down in the presence of free water and become permeable. Colbeck (1979a) indicated that ponding on ice layers in mature snow can safely be considered negligible in some cases, particularly if the snow is sloping. In such cases the main effect of ice layers and similar heterogeneities is to increase the mean path length of flow by diversion from the vertical, and to generate multiple concentrated flow paths. Colbeck (1975) suggested that flow diversion in sloping snow packs could be accounted for by representing the snow cover as an equivalent anisotropic medium. Colbeck and Anderson (1982) treated snow covers as equivalent homogeneous media, and used Eq. (4.4) to calculate the parameter $K^{1/3}\phi_e^{-1}$ from surface energy exchange and lysimeter runoff data. They found that $K^{1/3}\phi_e^{-1}$ was smaller for a more heterogeneous Vermont snow pack than for a California snow pack, in which ice layer breakdown was probably more advanced. Colbeck (1979a) showed how lysimeter runoff prediction could be improved by using a multiple flow path model based upon Eqs. (4.4) and (4.5). In summary, the principles underlying water movement in mature snow are reasonably well

understood. The main drawback is lack of knowledge of the hydraulic and spatio-temporal characteristics of snow cover heterogeneities.

Water flow in immature snow is complicated by the metamorphism of wet snow, which can feed back to the flow processes by producing preferential flow paths. Wankiewicz (1979) reviewed the thermodynamic phenomena associated with water flow in immature snow. These phenomena include wet snow metamorphism, growth and decay of ice layers and vertical flow path metamorphism.

Colbeck (1976) derived an expression for the celerity of a wetting front in homogeneous cold dry snow by considering continuity requirements at the front. The expression is

$$C_d = v/[\phi \cdot S_w + (\phi - 1) \cdot (.917 \cdot T_s/160)] \qquad (4.6)$$

where C_d is the wetting front celerity (m s^{-1}). Eq. (4.6) accounts for the initial losses to the irreducible water content and the cold content, but ignores changes in snow structure and inhomogeneities. As stated by Colbeck (1976), neglecting metamorphism should not invalidate his analysis for short duration water inputs to snow which has undergone some settling. However, Eq. (4.6) may not be valid for fresh snow. Ebaugh and DeWalle (1977) measured the travel time of artificial rain in columns of refrigerator-stored fresh snow. They noted that marked changes in snow properties occurred during the course of their trials, which lasted several hours. Snow samples prior to wetting contained loosely-packed rod- and plate-shaped crystals with sizes ranging from .1 to .3 mm. After wetting and draining, snow grains were rounded, more tightly packed, and ranged in

size from .2 to .8 mm. Initial sample densities averaged 165 kg m^{-3}, increasing to 241 kg m^{-3} over the course of the experiment. Unfortunately, Ebaugh and DeWalle (1977) did not present their results in a form for which a comparison could be made with Eq. (4.6).

Colbeck's (1976) model for water flow in dry snow appears not to have been tested against field observations. A well-documented natural rain-on-snow event occurred in January 1953 at the Central Sierra Snow Laboratory (CSSL) in California (USACE, 1956). A detailed reconstruction of the event is given by USACE (1954). An attempt was made to simulate the event using Tucker and Colbeck's (1977) kinematic wave routing program. This program was modified by the present author to use Eq. (4.6) to calculate the celerity of the wetting front. However, the execution failed because the storage space for interpolation between shocks was exceeded; the wetting front was apparently penetrating too slowly. Table 4.1 shows some approximate calculations of lag time using the mean surface flux for the first 10 h period, which was the time from the onset of rain to the appearance of lysimeter runoff (USACE, 1956). Although this approach is not rigorous because of the non-linearity of Eq. (4.6), it should provide a reasonable estimate of the order of magnitude. Lag times computed from the minimum and maximum hourly inputs are also shown. Eq. (4.6) clearly overestimates the lag time. However, the computation of these lag times assumed uniform flow; flow concentration in vertical flow paths increases C_d, because of the non-linearity of Eqs. (4.6). Colbeck (1978a) and Wankiewicz (1979) have shown that the celerity of

Table 4.1 - Estimation of lag time during the January 1953 Central Sierra Snow Laboratory rain-on-snow event.

Initial Conditions (USACE, 1956: Plate 8-9)

ρ_s = 320 kg m^{-3}
h = 2130 mm
T_s = -3°C
ϕ = .651

Estimated Permeability

$K = .077 \cdot d^2 \cdot \exp(-7.8 \rho_s/\rho_w)$
(Shimizu, 1970, cited by Colbeck, 1978a)
$= 6.35 \times 10^{-3}$ mm^2 if d = 1 mm
or 25.4×10^{-3} mm^2 if d = 2 mm

Lag Times

	surface flux (mm s^{-1} x10^4)	C_d (mm s^{-1} x10^3)	lag time (h)
mean	5.6	8.3 (9.2)	71 (64)
maximum	2.1	3.4	176
minimum	10.6	15.0	39

Note: Values for C_d and lag time in parentheses are for d = 2 mm; others are for d = 1 mm.

concentrated flow (C_c) relative to the celerity of uniform flow (C_u) for the same surface flux is

$$C_c/C_u = f^{(n-1)/n}$$

where f is a unit surface area of snow divided by by the plan area of vertical flow paths within it, and n = 3 (Colbeck, 1978a). Taking f = 25 (after Wankiewicz, 1979), C_c/C_u would be 8.5. This concentration would reduce the calculated lag from 71 h to 8.4 h, which is much closer to the observed lag. Further evidence for concentrated flow is the recorded presence of cold cells in the upper snow layers, nine hours after the onset of rain (USACE, 1954).

Bergman (1983) analyzed seven natural rain-on-snow events at CSSL. He noted that ice lenses and high density layers produce concentrated flow, and that lag times were typically five to twelve hours for snow packs of approximately 2 m depth. These results concur with the analysis presented above. Bergman also noted that during one intense storm water flowed in channels at the snow surface, presumably because the rainfall intensity exceeded the infiltration capacity of an ice layer just below the surface. Thus, it appears that in the relatively warm snow covers in the Sierras, snow pack inhomogeneities concentrate water flow, particularly during rain-on-snow events, and reduce the time lag to runoff in comparison to homogeneous snow cover.

4.2 FIELD OBSERVATIONS OF SNOW-WATER PHENOMENA

The hydrological properties of snow depend upon the thermal and structural characteristics of the snow cover. These characteristics are intimately related to the climatic conditions under which the snow pack has developed. Consequently, the snow covers at Temple Basin (TB) and the Craigieburn Range should represent the range of properties found in the Waimakariri catchment, based upon the synthesis presented by Owens et al. (1983). In this section, snow cover properties at TB and in the Craigieburn Range are described, and observations of snow-water movement are presented.

4.2.1 Snow Cover Characteristics

Descriptions of snow cover properties which are relevant to the Waimakariri catchment are given by Morris and O'Loughlin (1965), O'Loughlin (1969a), McNulty and Fitzharris (1980), Prowse (1981), Owens et al. (1983) and Prowse and Owens (1984). The following discussion is based upon these works and personal observations.

Snow pack structure is strongly influenced by the characteristics of the storms which deposit the snow. McGregor (in prep.), following Neale and Thompson (1977), classified snow storms in the eastern South Island as being warm advection or cyclonic vorticity. Warm advection storms are typified by strong winds from the westerly quarter, while cyclonic vorticity storms often result from the proximity of a centre of low pressure. A detailed general

analysis of the differences in characteristics between the storm types has not been performed, but McGregor (in prep.) has analysed avalanche-producing storms using Ski Basin (SB) data, and found significant differences between westerly storms and those associated with southerly to easterly air flow. The westerly storms had a mean air temperature of -1.5°C and a mean maximum six-hour precipitation total of 17.6 mm, compared to -3.6°C and 7.1 mm for the other storms.

The importance of the different storm types in depositing snow varies spatially. Southerly storms deposit more snow on the southern end of the Craigieburn Range than on the northern end, while the opposite holds for westerly to north-westerly storms. Almost all of the snow received near the Main Divide is from westerly storms. Only the stronger southerly storms appear to deposit large amounts of snow at TB. The consensus from regular skiers at TB is that significant falls of southerly snow, which is cold, dry and powdery, occur only once or twice per year. Most large falls at TB are from the west, and consist of heavy wet snow which is often unskiable until it settles.

The snow cover in the Craigieburn Range develops from a series of usually low-magnitude snowfalls which can differ greatly in characteristics; hence, the resulting structure is stratigraphically complex. The deposited snow undergoes metamorphism, which can act to increase or decrease the heterogeneity. Colbeck (1982) reviewed snow metamorphism and proposed new terminology for the snow grain forms. The terminology used by Sommerfeld and LaChapelle (1970) is used here, although it is acknowledged that the term melt-freeze (MF) is often applied to grains which have undergone wet

snow metamorphism, and which develop for reasons other than melt-freeze cycles.

It can be seen from Fig. 2.3 that temperatures are generally warm at SB. In addition, Prowse (1981) estimated that, on average, over fifteen percent of the precipitation in all months except August falls as rain. From these observations and other indirect climatic evidence (Prowse, 1981), it appears that equi-temperature (ET), wet snow and MF metamorphism should dominate. However, the coincidence of occasional prolonged cold spells and thin snow cover can result in temperature gradient (TG) metamorphism at the base of the pack. TG crystals can also develop near inhomogeneities such as ice layers, possibly because of the local influence on heat and vapour transfer of such layers (Colbeck, 1982; Prowse and Owens, 1984). The effects of wind also play a strong role in snow cover formation in the Craigieburn Range, particularly with respect to forming wind slab and increasing new snow density.

Snow density is an important snow pack characteristic. Prowse (1981) showed that mean snow pack density at SB fluctuated greatly from day to day, decreasing with the addition of new snow, and increasing between falls, particularly when melt or rain-on-snow occurred. The mean density exceeded 350 kg m^{-3} in every month of the snow season of 1980, but monthly averages increased from 265 kg m^{-3} in June to 419 kg m^{-3} in October. Prowse and Owens (1984) showed that density characteristics in the Craigieburn Range lie between those of maritime and continental climates.

Snow pack temperature regime is another hydrologically

important snow characteristic. The relatively warm climate of the Craigieburn Range and the frequency of mid-winter rain-on-snow events suggest that snow cover in the Craigieburn Range is warm. Prowse (1981) confirmed this suggestion by systematic measurement of temperature and density profiles on sunny and shaded aspects at about 1800 m elevation. Prowse found that temperatures at 300 mm depth usually ranged between -2°C and -5°C, indicating that the snow is relatively warm according to Smith's (1974) criterion. Furthermore, the total heat deficit (defined in Eq. (4.1)) rarely exceeded 2 MJ m^{-2}, with a maximum observed value of 4.1 MJ m^{-2} on the shaded slope. These values of 2 and 4.1 MJ m^{-2} are equivalent to the energy required to melt approximately 6 and 12 mm of water equivalent, respectively.

In contrast to the Craigieburn Range, very little work has been carried out on snow cover near and west of the Main Divide. The Ministry of Works and Development carried out snow surveys on the Ivory and Tasman Glaciers, but they did not investigate structure or temperatures. Ho (1982) investigated snow structure in the Mount Cook region. Based upon the available information, Owens et al. (1983) constructed synthetic snow pit profiles. They separated the western mountain regions into two groups, one for elevations above 2200 m, the other for elevations between 1500 and 2200 m. The western high snow cover experiences less mid-winter melt and rain-on-snow than at lower elevations, and reaches depths of up to 10 m, especially at favourable depositional sites such as the Tasman Glacier. The synthetic western low snow cover corresponds to most of the snow zones in the

western Waimakariri catchment. The typical western low pack proposed by Owens et al. achieves a maximum depth of about 3 m, and is dominated by ET and MF grains and ice layers. The western low pack is warmer, denser and more homogeneous than the eastern and interior packs typified by those in the Craigieburn Range.

Regular systematic snow pit investigations were not carried out at TB. However, pits were dug periodically in which some or all of density, temperature and grain type were examined. These examinations confirm the major features of the synthetic western low snow pack mentioned above. For example, snow depths were measured on four transects in TB roughly at the time of peak snow accumulation in 1982. The maximum depths in flat areas were between 3 and 4 m, but were much less on sunny, windward slopes. Snow pack structure at TB was composed of ET and MF grains and ice layers. Faceted crystals, which result from TG metamorphism, were observed only in 1982, when the establishment of a thin snow cover was followed by prolonged cold, clear weather. However, subsequent rain-on-snow and melt obliterated the faceted crystals. Most of these differences between the western and eastern snow characteristics are probably due to the warmer, more maritime climate near the Main Divide and the greater amounts of rain and melt water which run through the pack.

4.2.2 Snow-Water Movement

Dye experiments and a trial experiment using tensiometers and funnel lysimeters were carried out at TB to investigate snow-water phenomena. The trial experiment involving tensiometers and lysimeters took place from 2 to 3 November 1982. The tensiometers were made by attaching the porous glass end of a gas distribution tube to glass tubing of the same diameter. These tubes were connected to a manometer filled with water, and the application was similar to the description given by Jordan (1983). This trial was only partially successful. The interiors of the funnels did not remain in contact with the snow within them, and it is believed that this lack of contact affected the funnel outflow. The tensiometers appeared to perform reasonably well. Unfortunately, the author had to leave the field on 3 November, and a suitable opportunity to use the tensiometers did not arise again.

Four tensiometers were set up approximately 100 mm apart in each of two rows, at 450 mm and 850 mm below the surface. The surface melt rate estimated from the energy budget computations (see chapter three) and the mean capillary pressure in each layer are shown in Fig. 4.2. The variations in capillary pressure are similar to those reported by Wankiewicz (1978) and Jordan (1983) for similar surface flux rates in two different environments in British Columbia. This supports Jordan's (1983) statement that the texture of mature snow is remarkably similar between environments.

Dye experiments consisted of spreading methylene blue

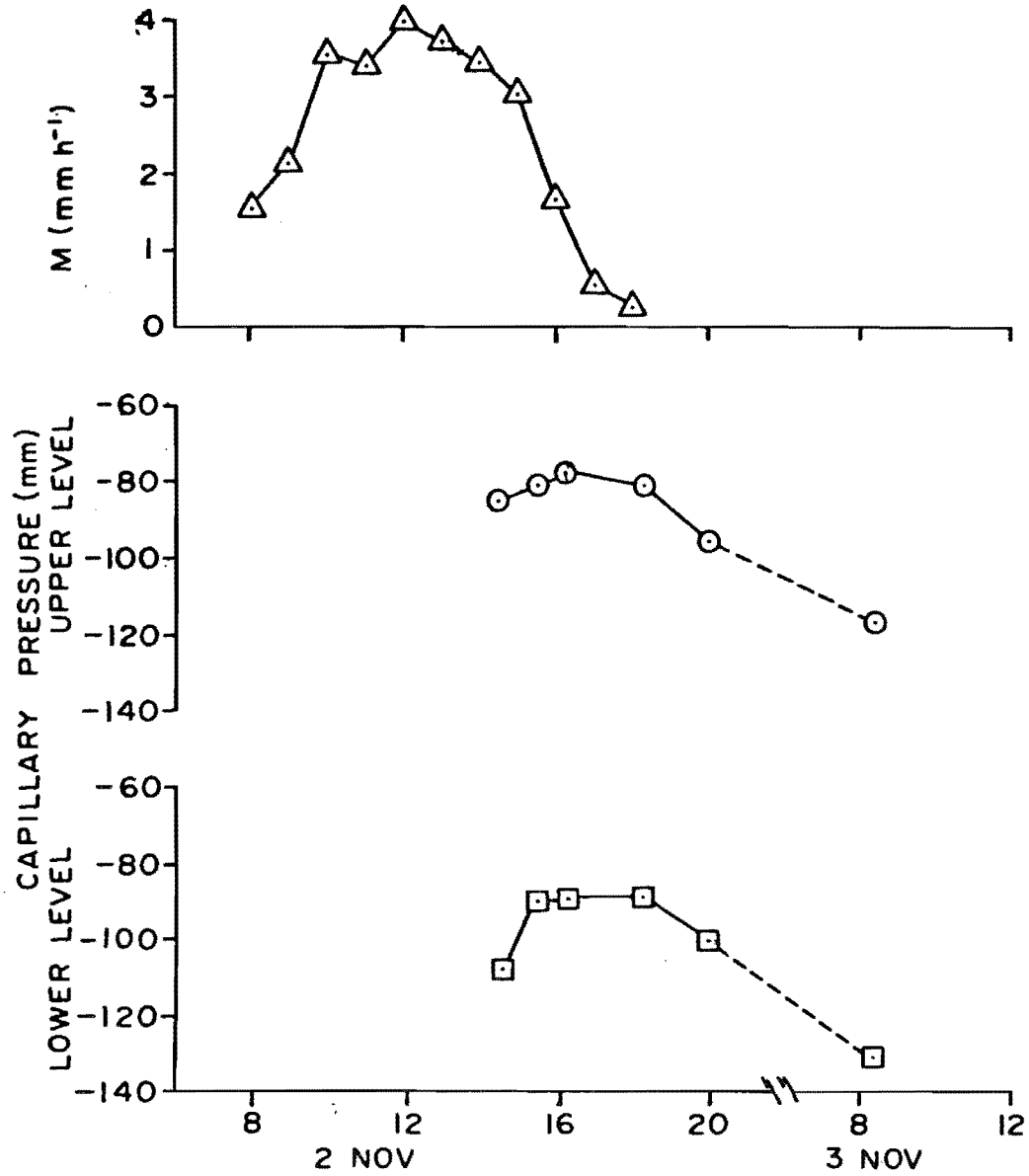

Fig. 4.2. Estimated melt rates and capillary pressure at TB meteorological site, November 1982.

dye over an approximately 1 m square area of snow surface adjacent to a snow pit, and periodically digging the face of the pit back to reveal the movement of the dye through the snow. These experiments were carried out in a variety of melt and rain-on-snow situations throughout the field seasons of 1982 and 1983. The movement of the dye was generally similar to the patterns illustrated by other authors, for example Gerdel (1954) and Jordan (1978).

Water percolation on sloping ground followed a zig-zag path, flowing vertically between impeding layers and downslope along the layers until breaking through into the underlying snow. Flow was usually diverted 2 to 3 m or less along an impeding layer before flowing vertically into the underlying snow. Mean vertical percolation rates were usually on the order of 1 m h^{-1}, even including the diversions along the ice layers.

In level areas, the dye moved in a fingering path. Textural contrasts and ice layers impeded the downward movement of these fingers; dye would then spread horizontally above the impeding layer before flowing as fingers into the lower layer. One experiment was carried out on 20 October 1982. The dye was applied at 1440, under clear skies with wind speeds between 1 and 2 m s^{-1} and an air temperature of 5°C. Surface melt would thus have been primarily radiative, with a melt rate on the order of 4 to 5 mm h^{-1}, based upon the net radiation values shown in Fig. 3.3 and an estimated correction for the decreased albedo of the dyed snow. After 2 h, the fingers had penetrated approximately 2.5 m while the background flow had penetrated about 2 m. Substituting a celerity of 1 m h^{-1} (.00028

m s^{-1}) and a flux of 5 mm h^{-1} (1.4×10^{-6} m s^{-1}) into Eq. (4.4), the parameter $K^{1/3}/\phi_e$ can be calculated to be approximately 4×10^{-3} $m^{2/3}$. This value is higher than the values found by Colbeck and Anderson (1982) in Vermont and California, which range from 2.5 to 3×10^{-3} $m^{2/3}$. Assuming a density of 400 kg m^{-3}, a value of $K = 110 \times 10^{-10}$ m^2 can be calculated. This permeability is three to four times greater than those calculated by Colbeck and Anderson.

Much of the difference between the estimate of K derived above and those calculated by Colbeck and Anderson can probably be attributed to the crudeness of the estimates of surface flux and celerity used here, particularly because any errors would be magnified by cubing. However, some of the difference may be real. The TB snow pack frequently had water run through it. After the snow cover had become established, the longest period in which a marked rise in the water level did not occur in the stream draining TB was two weeks. Between 1 September and 20 October 1982 six rain-on-snow events occurred which produced water level rises. The effect of all of this water would be to cause ice layers to become more permeable (Gerdel, 1954). As suggested by Colbeck and Anderson (1982) and Jordan (1983), the condition of snow pack heterogeneities may cause the major differences in snow-water movement between environments.

As discussed in chapter two, the winter of 1982 was fairly typical in terms of the snow accumulation and the occurrence of rain-on-snow. Therefore, it can be concluded from the field observations presented that the snow cover in the western portions of the Southern Alps below 2200 m

elevation normally matures throughout the winter, and should yield runoff fairly rapidly in a rain-on-snow situation. For example, consider a 2 m deep snow pack with density of 350 kg m^{-3} and a grain diameter of .5 mm, which is typical of ET grains and somewhat smaller than mature grains. Shimizu's (1970; see Table 4.1) formula yields a permeability of 12.6×10^{-10} m^2. For a rain intensity of 10 mm h^{-1}, which occurred many times throughout the field seasons, the travel time computed from Eq. (4.4) is under three hours. However, flow concentration would act to reduce the travel time through the snow (Wankiewicz, 1979). Rainfall intensities can be much greater than 10 mm h^{-1} near the Main Divide. The two-year return period twenty-four hour rainfall intensity at Arthur's Pass is equivalent to an intensity of over 10 mm h^{-1} (Tomlinson, 1980). Thus, snow cover should have little impact on water routing during flood-producing events west of and near the Main Divide, except in areas with exceptionally deep snow.

O'Loughlin (1969a) and Prowse (1981) made observations of the behaviour of free water in the snow cover in the Craigieburn Range. O'Loughlin reported measurements of thermal quality at SB made in September and October 1968. The snow pack was almost always isothermal at 0°C and thermal qualities were as low as ninety-one percent, equivalent to a water content of ten percent by weight of dry snow. O'Loughlin also used dye to estimate percolation rates in mature snow. He did not report surface flux conditions, but the percolation rates, which ranged from 10 to 300 mm per minute, are comparable to those measured by Gerdel (1954), also in mature snow.

Prowse (1981) recorded snow pit observations of temperature, density, hardness and a qualitative assessment of free water content at various sites over three winters. Prowse noted the impact of melt-freeze cycles on snow pack structure. Surface melting which produced persistent crusts was caused by warm winds and the associated turbulent heat transfer; sun crusts tended to be thin and were believed to break down rapidly (Prowse, 1981). Melt-freeze cycles were associated with the alternating passage of warm northwesterly and colder southerly weather systems, rather than diurnal variations in net radiation. Contrary to observations by Gerdel (1954) and at TB, water occasionally tended to pond above ice layers within the pack, and to freeze into the matrix before ice layer disintegration and drainage could occur. This freezing of ponded water one season produced an ice layer 80 mm thick, which was composed in some parts of clear ice (Prowse and Owens, 1984).

One reason for the apparent differences in the nature of water movement at ice layers between TB and the Craigieburn Range may be related to the magnitude of the water inputs. Much more rain falls near the Main Divide during westerlies than in the Craigieburn Range. In fact, rain often falls near the Divide but not further east (see for example Fig. 3.6). Wankiewicz (1979) discussed the time required for an ice layer to break down. If a small amount of water became ponded on an ice layer, and if the ice layer was close enough to the surface such that heat conduction through the snow did not limit heat loss from the ponded water, it is conceivable that all of the water could freeze before ice layer bonds broke down, particularly if

the snow below the ice layer was cold. Repeated melt-freeze cycles would have a feedback effect. Densification associated with MF and wet snow metamorphism would increase the conductivity of the snow, promoting heat loss from ponded water below the surface; and ice layer thickening would insulate the base of the ice layer from the generation of the latent heat of fusion at the top of the layer, delaying ice layer disintegration.

The preceding discussion has indicated that ponding of water on ice layers and refreezing can have an important influence on water movement in snow in the Craigieburn Range. However, the frequency of occurrence of ice layer development and its general hydrological significance cannot be assessed from the available information. More specific studies and observations over a longer time span would be required. Such studies would also have important applications for understanding avalanche formation in this and similar environments (Prowse and Owens, 1984).

4.3 SNOW-SOIL-WATER INTERACTIONS

Snow cover not only influences the time required for rain and snowmelt to reach the base of the snow pack, but also can affect the pathways by which the water travels from the base of a pack to a stream channel. In fact, Price et al.(1979) stated that, in the mid-latitudes, the interactions at the snow-soil interface exercise a far more important control on basin outflows than the water movement within the snow pack. An attempt is made here to assess probable snow influences in the Waimakariri catchment.

The main surface cover types found in the seasonal snow zone in the Waimakariri catchment are bare rock, scree, tussock grassland and beech forest (see section 2.5). Runoff production from bare rock outcrops occurs as overland flow. Rock outcrops rapidly concentrate runoff, and waterfalls were observed to develop on rock outcrops in TB shortly after the onset of heavy rain. Most rock outcrops had little if any snow cover because of wind scour, so the influence of snow on runoff from outcrops should be minimal.

Screes exhibit a variety of forms and hydrological characteristics (O'Loughlin, 1965; Pierson, 1982). Some scree surfaces are underlain by a layer of fine material, which often has a crust. This layer may have a low infiltration capacity, forcing water to move through and over the surficial scree gravels (Pierson, 1982). Where infiltration is not impeded, water flows mainly through the subsurface scree deposits, and the mode and rate of movement depend upon the characteristics of the deposits. For example, where subsurface deposits comprise coarse gravels, water movement occurs as turbulent flow amongst the gravels and boulders, probably at the bedrock surface. The gurgling of channelized flow below the scree surface could be heard at several sites in TB. On other screes, subsurface movement may occur as saturated or unsaturated flow, either vertically or downslope, depending upon the texture and layering of the materials.

Snow cover should not affect runoff routing on scree deposits for which subsurface flow dominates. However, snow cover should influence runoff routing in situations where overland flow is important, by changing non-linear overland

flow over a bare surface to linear Darcy flow at the base of a snow pack (Wankiewicz, 1979). Situations in which overland flow would be important over screes include the cases of limiting infiltration capacity of underlying deposits, saturation of thin scree deposits and the existence of concrete frost and/or superimposed ice at or near the snow-scree interface. An exceptional case may occur where concentrated flow from upslope rock outcrops erodes a channel at the base of the snow pack. From some observations made at TB, it appears that subsurface movement through screes and concentrated channel flow in areas with extensive bedrock outcrops are the major modes of water movement there.

Runoff production in tussock grassland areas appears from observations made at TB and by Griffiths and McSaveney (1983b) in an alpine basin west of the Main Divide to be dominated by concentrated flow in shallow runnels or micro-channels. However, Mosley (1982) observed that most of the water he applied artificially at tussock sites near CF moved into the subsurface, either through the matrix or through macro-pores. This difference in runoff mechanism could be caused by differences in soil moisture conditions during the observation periods at the three areas. In any case, snow cover may have little effect on runoff routing in tussock areas, because the tussock supports the snow at least partially clear of the ground surface (Chinn, 1969; Weir, 1979), and would permit concentrated flow to occur in the gap between the base of the snow and the ground surface. Such flow was observed at TB while excavating pits during rain-on-snow events. The effects of concrete frost on water

movement would thus be reasonably independent of snow cover.

Mosley (1979; 1982) found that water movement under beech forests moved primarily into the subsurface, although overland flow over the forest litter occurred at some sites. In the absence of concrete frost or superimposed ice, the presence of snow cover should have little effect on water movement from the base of the pack to the stream channel.

It is apparent from the preceding discussion that concrete frost or superimposed ice may have an important effect on runoff generation in New Zealand mountain catchments, and this effect may depend upon the presence or absence of snow cover. O'Loughlin (1964) described the occurrence of both forms of ground ice on both the eastern and western sides of the Craigieburn Range in 1963. However, the conditions governing the development, persistence, thaw and hydrological impact of ground ice in New Zealand appear to have been largely ignored (Watt, 1979).

4.4 SUMMARY

Water movement in mature snow is reasonably well understood, and quantitative models have been applied successfully to predict runoff. Water movement in immature snow is less well understood. The water retention capacity of dry snow is controversial, and the magnitude of this retention can have an overriding influence on runoff production.

Snow pack characteristics and hydrological behaviour vary with elevation and distance from the Main Divide. The

snow zones of the Waimakariri catchment are well represented by the eastern/interior and western low elevation snow cover types described by Owens et al. (1983), although the boundary between the two has not been defined. Climatic conditions in the seasonal snow zone of the Central Sierra Nevada share many common features with those of the Waimakariri catchment. Although the Waimakariri catchment has a higher latitude, the higher elevation of the Sierra Nevada would tend to compensate for this. Both regions have relatively warm climates, with occasional mid-winter rain-on-snow episodes (USACE, 1956; Prowse, 1981), although the frequency and magnitude of rain-on-snow in California may be more similar to conditions at TB than in the Craigieburn Range. The magnitude, frequency and duration of cold, anisothermal snow episodes as observed in the Craigieburn Range (Prowse, 1981; McGregor, in prep.; Weir, 1983) are similar to those reported by McGurk (1983) in the Central Sierra Nevada. Observations by USACE (1956) and Bergman (1983) in the Sierra Nevada indicate that flow concentration due to ice and other layers produces more rapid water movement than would be predicted by homogeneous flow models.

Consideration of structural and thermal characteristics, water transmission properties and the frequency and magnitude of water inputs indicates that the western low elevation snow pack, as typified by those at TB, should have a small effect on water routing, which should be negligible on a daily basis. The eastern snow pack, although relatively warm, appears occasionally to be able to impound water on ice layers, and subsequently lose

sufficient heat for this water to freeze before ice layer disintegration and drainage can occur. These thick ice layers may have a profound influence on runoff lag times, and deserve further attention.

The effect of snow cover on the movement of water from the base of the snow pack to the stream channel is difficult to predict, because of the great variability of runoff mechanisms and lack of knowledge about ground ice characteristics. Snow cover effects are particularly uncertain for scree surfaces and under beech forests. However, snow cover should not have so great an effect on runoff generation from alpine tussock grassland, because the vegetation cover provides a porous zone between the ground surface and the snow, in which turbulent overland flow could occur.

CHAPTER FIVE

HYDROLOGICAL MODELLING

In this chapter, attempts to develop and test models of snow accumulation, ablation and runoff which are suitable to the conditions found in the Waimakariri catchment are described. The first section reviews modelling approaches and outlines the approaches used here. Processes which are relevant to modelling and the process representations employed in this study are discussed in the following three sections. The pre-processing of data and the application of models to both snow course and streamflow data are described in sections 5.5 to 5.7. The final section summarizes the findings from this chapter.

5.1 MODELLING APPROACHES

Many varieties of hydrological models exist. Sorooshian (1983) distinguished between "conceptual" models, which explicitly represent many of a system's unit processes, and "systems-theoretic" models, which treat hydrological systems as black boxes. Systems-theoretic models often perform better than conceptual models for rainfall runoff (Sorooshian, 1983), but conceptual models are superior for modelling snowmelt runoff (Anderson, 1979; Saelthun, 1979). Therefore, this study focuses on the development and application of conceptual models.

Conceptual models of runoff from basins influenced by

seasonal snow cover comprise two components. The first is a snow routine, which uses meteorological input to determine the phase of precipitation and to calculate snowmelt. The second is the transformation of rain and snowmelt inputs at the ground surface into streamflow at a gauging site.

Computations of basin snowmelt inputs require both the energy available for melting and the area covered by snow. Two methods and combinations of the two have been used to assess the snow covered area within a basin. One is to use estimates derived externally, for example by remote sensing (Rango and Martinec, 1979; Bagchi, 1982). The other is to divide the catchment into elevation zones and to model snow accumulation and ablation in each (Anderson, 1973). The snow covered area can then be determined using the basin's hypsograph and knowledge of which elevation zones have snow cover. A hybrid approach is to use external snow cover data to update the simulated snow pack water equivalent (Carroll, 1979). Fitzharris (1979) reviewed the possibilities for modelling and monitoring snow cover in New Zealand. He concluded that, given the dynamic nature of New Zealand's snow environment and the current state of the art in remote sensing with respect to the tradeoffs between temporal and spatial resolution, modelling snow accumulation and ablation on a daily basis may be the most promising approach. Approaches to calculation of the available energy have been discussed in chapter three and will receive further attention later in this chapter.

Transforming surface water inputs into streamflow can be accomplished in several ways. Models like the HEC-1 (described by Viessman et al., 1977) route water inputs

directly to a gauging point via a unit hydrograph. Martinec's (1975) model similarly routes inputs directly to the basin outlet. The response function in Martinec's model is essentially an exponential decay function, with the recession constant depending upon the current discharge. A major problem with Martinec's transformation model is that evaporative and soil moisture losses are accounted for by one parameter which is difficult to specify for forecasting applications. Other models, like the Stanford Watershed Model (described by Viessman et al., 1977), attempt to represent the most important runoff processes by parameterized relationships. As noted by Sorooshian (1983) and many others, the large number of free parameters which must be calibrated in these models and the interdependency of many of the parameters complicate the calibration procedure. The model user can never know whether a global or just a local optimum has been reached. Therefore, if a user is interested in forecasting flows in a basin and not in simulating the effects of land use changes, a reasonable approach is to employ a simple conceptual model with a minimal number of parameters.

The Swedish Meteorological and Hydrological Institute (SMHI) developed a conceptual runoff model called HBV. The main development criteria were to minimize input data requirements and to maintain as simple a model structure as possible. The model is presently widely used in Norway and Sweden in catchments with a range of climatic and physiographic characteristics (Bergström, 1979; Saelthun, 1979). Modified versions of the model have also been applied to a large drainage basin in India (Bhatia et al.

1984) and to groundwater simulation (Bergström and Sandberg, 1983). The HBV model has been adopted in this study for its demonstrated versatility and simple model structure, which is described in section 5.5.

The temporal resolution of models depends upon the intended use and data availability. Climate stations are particularly sparse in New Zealand's mountain regions (Prowse, 1981), and daily climate observations including maximum, minimum, wet bulb and dry bulb temperatures and daily precipitation are the most commonly available. Most climate stations are at low elevations; only three full-time stations in the South Island lie above 900 m. Therefore, this study concentrates on developing and evaluating models which operate on readily-available daily climate data. Some attention is paid to the problems involved with using low elevation data for modelling alpine snow cover.

5.2 PRECIPITATION AND SNOW ACCUMULATION

The main factors involved in the disposition of precipitation are the phase of precipitation, vegetation effects, redistribution of snow and the dynamics of snow-water systems. The first three factors are discussed in this section, while snow-water relationships are discussed in section 5.3.

5.2.1 Form of Precipitation

Determination of the form of precipitation reaching the ground is a critical procedure in hydrological modelling because rain generally runs off quickly while snow may be stored for months before it is released as meltwater. Near-surface air temperature is the most commonly used variable for discriminating rain from snow events. The transition temperature depends upon the temperature structure between the surface and the freezing level, which varies from event to event. Observations made in the field by Prowse (1981) and the present author indicate that rain rarely occurs at air temperatures below 0°C and snow rarely occurs at temperatures greater than 2 to 3°C in the Waimakariri catchment. Between 0°C and 3°C, precipitation is often in the form of mixed rain and snow or sleet, but both pure rain and pure snow can occur.

A complication can occur when daily mean temperatures and rainfall totals are used, and weather systems change rapidly. For example, rain can fall during the early part of the day, followed by a cold southerly wind and no precipitation. In this situation, the mean daily temperature may be below the transition temperature, so the model will incorrectly determine the precipitation to be snow.

Some workers have used discrimination criteria based upon the maximum and/or minimum temperatures (for example, Bagchi, 1982; Ffolliott and Brooks, 1983). However, it is not known whether these criteria perform better than those based upon mean daily temperature, and the extrapolation of

the maximum and minimum temperatures may involve greater uncertainty. In this study the mean temperature is used as the discriminating variable.

5.2.2 Interception by Vegetation

Although the processes governing interception losses are complex, Pearce and McKerchar (1979) stated that the representation of these losses as constant percentages of rainfall should be reasonable for most vegetative types in New Zealand, especially considering the inherent inaccuracy of precipitation measurements. Studies by Rowe (1975; 1983) indicate that rainfall interception losses from beech forest average thirty to thirty-five percent of gross rainfall. Pearce and McKerchar (1979) assumed rainfall interception losses of twenty percent for tussock and scrub. O'Loughlin (1969a) reported measurements of snow water equivalent in open areas and under adjacent mountain beech forest. He found that water content in the forest ranged from nine to fifty-five percent less than that in the open, with an average difference of thirty percent.

In this study, forest precipitation is reduced by thirty percent, whether rain or snow. When the non-forested portions of the basin are free of snow, rain falling on tussock is decreased by twenty percent.

5.2.3 Redistribution of Snow

Wind influences on snow accumulation are complex and usually not explicitly included in snow accumulation and ablation models. The spatially lumped nature of operational models implies that the net effect on a basin scale can be accounted for implicitly by parameters which control snowmelt runoff volumes, such as the snowfall correction factor in the Swedish HBV model (Bergström, 1975).

Avalanches are another mechanism which can redistribute hydrologically significant quantities of snow in alpine environments (Obled and Harder, 1979; Martinec and de Quervain, 1975). However, the importance of avalanche redistribution in New Zealand is unknown, and no operational models have been developed for general use in snowmelt runoff models.

5.2.4 Correction of Precipitation Data

Raingauge catch deficiency, particularly for solid precipitation, is well-recognised and is discussed by many authors. In addition, precipitation measurements can rarely be regarded as random samples because gauge locations are generally biased toward low elevation, accessible sites. Hence, some correction must be made to measured precipitation to produce basin precipitation values. As mentioned in section 5.2.3, precipitation correction factors also absorb the effects of evaporation, sublimation and interception losses. Bergström and Jönsson (1976) stressed the importance of correction factors in Scandinavian

catchments. Most models employ different correction factors for rain and snow, both of which can be set a priori or determined through calibration. In this study, the rainfall correction has been set to 1.0 because the gauge is located at a relatively sheltered site. The snowfall correction factor and the precipitation gradient with respect to elevation will be treated as free parameters.

5.3 ABLATION

Ablation is defined as the net loss of water in any phase from a snow pack. This loss can occur through wind erosion, evaporation, sublimation and the runoff of melt water. Wind erosion has been mentioned in the last section, snowmelt is discussed in chapter three and runoff processes are discussed in chapter four. In this section, modelling considerations associated with snow pack ablation are discussed.

5.3.1 Evaporation and Sublimation

Bengtsson (1980) and Lang (1981) reviewed the importance of evaporation to the mass and energy balances of snow covers. Both authors concluded that, due to the general lack of available energy when the atmospheric vapour pressure gradient is large and vice versa, evaporation and sublimation losses from a stable snow pack are negligible, although the energy exchange associated with the vapour transfer can influence snowmelt rates. However, as mentioned in section 5.1, losses from blowing snow can be

significant. Prowse (1981) estimated evaporation rates from snow at Ski Basin (SB) using aerodynamic formulae. His estimates show that short-term evaporation rates can be greater than 5 mm d^{-1}, but condensation more than compensates in the long term.

Mass gains through condensation are generally small compared to snowmelt and rainfall quantities. For example, the greatest estimated daily condensation melt component at Temple Basin during the 1982 melt period was 22 mm (see Fig. 3.2); the associated quantity of condensate would be 3 mm, or five percent of the daily melt. On most days the condensation was less, and over the whole melt period condensate would have averaged three percent of the snowmelt. Because of the generally small magnitude of evaporation/condensation and the uncertainties involved with calculating areally-representative values, many models, including those developed in this study, do not explicitly account for vapour transfer, but allow effects to be absorbed by other parameters.

5.3.2 Internal Processes

It was considered from the results of chapter four that initial losses due to freezing and transient storage could be safely neglected in the Waimakariri catchment, at least for a daily time step. However, in line with the results of chapter four and the HBV snow routine (Bergström, pers. comm.), the effects of water retention and freezing are included. Following the representation used in the HBV model, a gravimetric liquid water holding capacity must be

exceeded before snow pack drainage occurs. The water holding capacity, WRG, is determined empirically. If the air temperature drops below 0°C, freezing of the liquid water content is computed as

$$RFR = CRF \cdot (0 - T_a)$$

where RFR is the quantity of water (mm d^{-1}) which is frozen and added to the snow pack and CRF is a refreezing coefficient (mm d^{-1} $°C^{-1}$), which also is determined by calibration. Water retention and refreezing were not computed in the forested areas.

5.3.3 Snowmelt

Snowmelt is often computed from index models. The most basic temperature index is the degree-day model, which can be expressed as

$$M = DDF \cdot (T_a - T_e) \qquad (5.1)$$

where DDF is the degree-day factor (mm d^{-1} $°C^{-1}$) and T_e is a base temperature (°C), often set to 0°C (Anderson, 1973). As discussed in chapter three, simple temperature indices are inadequate for calculating short term melt rates in environments such as the Waimakariri catchment. Two methods have so far been proposed to overcome the failure of Eq. (5.1) in changing meteorological situations. One is to incorporate more variables into the snowmelt index (for example, Zuzel and Cox, 1975). However, adding more variables which are measured at a site involves the same problems as energy balance computations. The other approach, due to Anderson (1973), is to calculate melt differently according to whether or not rain is falling.

Huber (1983) found that Anderson's (1973) scheme performed better than four other accumulation and ablation algorithms which were all variations on the basic degree-day approach.

The advantage of Anderson's model is that it requires no more data than the others, but can still account somewhat for the role of the latent heat flux in producing high melt rates during rain-on-snow events (Light, 1941; Zuzel et al., 1983). However, the variation of wind speed is ignored, and Anderson (1973; 1976) acknowledged that the model would fail in some cases when the turbulent transfer coefficients deviated from the assumed values.

The influence of forest cover on snowmelt has been discussed by several workers (for example, USACE, 1956; Fitzgibbon and Dunne, 1983). Forest cover decreases insolation, increases net longwave radiation and decreases wind speed, inhibiting turbulent exchange. Thus, snowmelt rates in forested areas are largely insensitive to changing weather situations, and temperature index models perform well (Male and Gray, 1981; Fitzgibbon and Dunne, 1983). Reported values of the degree-day factor for use with mean temperature in heavily forested areas range from around 1 mm d^{-1} $°C^{-1}$ (USACE, 1956; Anderson, 1973) to 2 mm d^{-1} $°C^{-1}$ (Bengtsson, 1982).

Daily observations of temperature and precipitation are the most commonly available meteorological information in New Zealand. Therefore, considering the results from chapter three, a model similar to Anderson's scheme should be the most appropriate for New Zealand conditions. The details of an index energy budget model (IEB) for use in the Craigieburn Range follow.

Sensible heat is the most important source of energy for snowmelt in the Craigieburn Range under all conditions, with net radiation being the next most important in clear weather and latent heat in rainy situations (Prowse and Owens, 1982). Accordingly, when daily precipitation is less than 10 mm, the threshold value used by Anderson (1973), the energy used for snowmelt is assumed to be from net radiation and sensible heat; when precipitation exceeds 10 mm, all surface exchanges are assumed to contribute. Net radiation on clear days is represented by a function which is similar to Anderson's (1973) clear weather melt index:

$$Q^* = RMF \cdot [0.5 + 0.5 \cdot \cos(2\pi JD/365)] \cdot T_a/.259$$

where RMF is a radiation melt factor ($mm \cdot d^{-1} {}^{\circ}C^{-1}$) and JD is the Julian day number referenced to the summer solstice. On rainy days, shortwave radiation is assumed negligible, and the atmosphere is assumed to radiate as a black body at the air temperature. Anderson (1973) showed that under these assumptions net radiation on rainy days can be expressed in $W\ m^{-2}$ as

$$Q^* = 4.6\ (T_a - T_s)$$

Precipitation heat flux is calculated from Eq. (3.8), assuming that the precipitation is at air temperature. The turbulent fluxes are represented by

$$Q_H = C_p\ (C1 + C2 \cdot DP)(T_a - T_s)$$

$$Q_E = (C1 + C2 \cdot DP)(e^*(T_a) - 6.11)$$

where C1 and C2 are empirical constants, and DP is the Auckland-Invercargill pressure difference. The inclusion of DP as an index of wind speed is intended to improve the model's performance under strong regional advective conditions. The daily total of energy used in snowmelt is

converted from W m^{-2} to mm d^{-1} by multiplying Q_M by .259.

Snowmelt rates under forest cover have not been investigated in New Zealand. Therefore, forest melt rates are calculated from

$$M_F = 1.5 \cdot T_a + P_F \cdot T_a / 79.7$$

where M_F is in mm d^{-1}, P_F is the net precipitation in the forest in mm d^{-1}, and 1.5 is an intermediate value of the melt factors reported for forested sites. The second term on the right hand side represents the melt due to the precipitation heat flow.

5.4 RUNOFF TRANSFORMATION

The runoff processes can be modelled using either spatially lumped or distributed representations. Experience with the HBV-3 model indicates that the increase in model performance using a distributed model does not compensate for the increased computational costs and difficulty in fitting when the parameter values are allowed to vary spatially (Bergström, 1975; Bhatia et al., 1984). Because the major goal of this study is to evaluate models of snow storage and release and not to test runoff models, a lumped transformation model has been adopted. The structure of the transformation model is shown in Fig. 5.1, and each of following sections describes a component of the model.

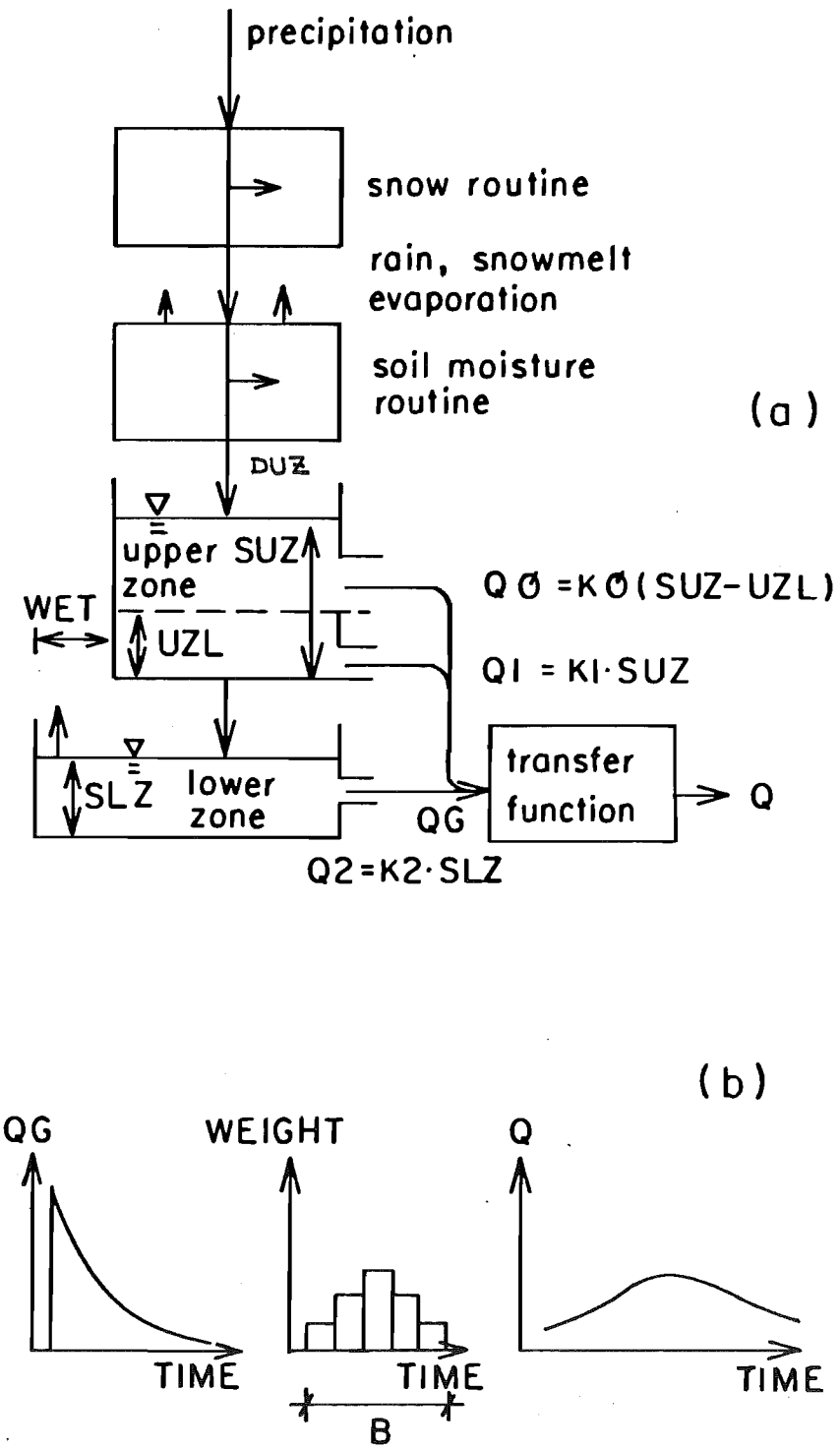

Fig. 5.1. Schematic diagram of the HBV-3 model (after Bergström and Jönsson, 1976).
(a) model structure
(b) transfer function

5.4.1 Soil Moisture Accounting

Rainfall and snowmelt calculated by the snow routine become input to the transformation routine. The water input first enters the soil moisture zone. A portion of the input passes through to the upper subsurface storage zone, while the rest stays in the soil moisture zone where it may be lost through evapotranspiration. The portion which passes through to the upper zone, DUZ (mm), is determined according to

$$DUZ = \begin{cases} WIN \cdot (SM/FC)^{BETA} & SM<FC \\ WIN & SM \geq FC \end{cases}$$

where WIN is the input to the soil moisture zone (mm), SM is the present soil moisture storage (mm), FC is the field capacity (mm) and BETA is a parameter. After a dry spell when soil moisture content is low, the water input will not add as much to runoff as it would after a wet period. Water input is added to the soil moisture routine and partitioned mm by mm, as this is more realistic than allowing the antecedent soil moisture content to govern the disposition of the entire day's input.

Evaporative losses from the soil moisture zone are also governed by soil moisture content, and are calculated from

$$E = \begin{cases} PET\ (SM/CL) & SM<CL \\ PET & SM \geq CL \end{cases}$$

where E is evaporation (mm), PET is potential evapotranspiration (mm) and CL is the soil moisture content below which evaporation is impeded (mm). The values of PET used in the model are intended to be normal monthly values calculated from Penman or Thornthwaite equations or derived

from pan estimates. Monthly evapotranspiration rates were derived by estimating the annual rate and then distributing evaporation through the year according to the distribution of pan estimates at Harper River, which is given by Bowden (1983). The Harper River station lies several kilometres outside the Waimakariri catchment at an elevation of 533 m. Potential evapotranspiration at Craigieburn Forest (CF) is estimated to be 400 mm a^{-1}, based upon corrected pan estimates given in unpublished FRI reports. The derived rates are shown in Fig. 5.2. Evaporation is assumed to occur from forested areas throughout the year, but from non-forested areas only when free of snow.

5.4.2 Upper Zone Storage

Subsurface storage is composed of an upper and a lower zone. The upper zone governs quick runoff while the lower zone governs delayed runoff. After DUZ is added to the upper zone storage, SUZ, water is released from the upper zone at two rates, Q0 and Q1. In physical terms, Q0 is analogous to saturated overland flow from variable source areas and subsurface stormflow, while Q1 represents flow generated by other mechanisms such as interflow. However, these physical interpretations must not be pushed too far, because Q0, Q1 and Q2 (from the lower zone storage) were incorporated into the structure to allow enough degrees of freedom to fit recession curves with three semi-logarithmic linear components (Bergström and Jönsson, 1976), not to simulate physical processes.

When SUZ exceeds a threshold value, UZL, Q0 is given by

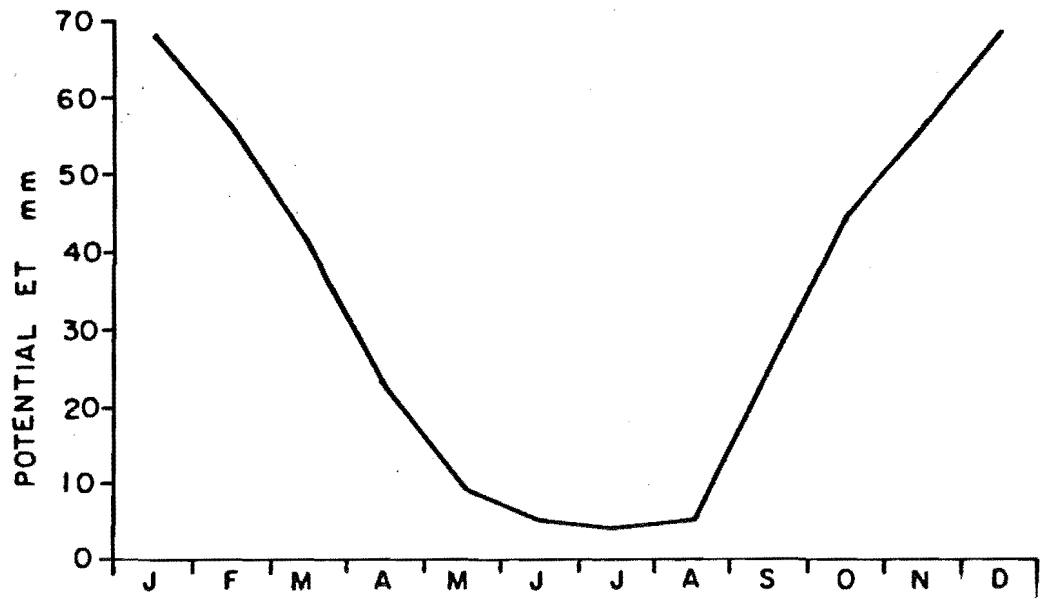

Fig. 5.2. Estimated monthly potential evapotranspiration at CF.

$$Q0 = K0 \cdot (SUZ - UZL)$$

where K0 is a recession constant (d^{-1}). If SUZ is less than UZL, Q0 = 0. When Q0 is not zero, the water released through Q0 is subtracted from SUZ, and Q1 is calculated from

$$Q1 = K1 \cdot SUZ$$

where K1 is another recession constant (d^{-1}). The water lost through Q1 is subtracted from SUZ. Finally, a quantity of water, PERC (mm), is lost from the upper zone to recharge the lower zone. If SUZ is less than PERC, all of SUZ is lost to the lower zone.

5.4.3 Lower Zone Storage

The recharge from the upper zone is added to the lower zone storage, SLZ. Evaporation from lakes and wet areas is assumed to occur at the potential rate and is subtracted from SLZ. These losses are expressed as PW PET, where PW is the decimal fraction of the catchment covered by wet areas. The release of water from the lower zone is analogous to the groundwater component of streamflow and is

$$Q2 = K2 \cdot SLZ$$

where K2 is the lower zone recession constant (d^{-1}).

5.4.4 Channel Routing

The generated runoff from the basin each day is calculated as

$$QG = Q0 + Q1 + Q2$$

This runoff is converted from mm d^{-1} to L s^{-1} and routed to the basin outlet using a triangular function (Fig. 5.1).

In order to reflect the change in flow velocities with discharge, the base of the triangular function, B, is expressed as a function of discharge:

$$B = BMAX - CRT \cdot QG$$

where BMAX is the maximum base (d), corresponding to lowest flows, and CRT ($d \cdot s \cdot L^{-1}$) is the rate of decrease of concentration time with discharge. Both BMAX and CRT are obtained through calibration.

Channel routing may be necessary for large catchments such as the Waimakariri. However, Camp Stream is small enough that channel storage effects can be neglected on a daily time scale.

5.5 PROCESSING OF INPUT DATA

Data are collected at points, and it is often desirable to model conditions at points other than the observation sites or conditions averaged over some area. Hence, observed data generally require some degree of processing before becoming model input. This section considers the types of pre-processing required, with particular attention to the representation of temperature and precipitation fields.

5.5.1 Discretization of Catchment

Processing of input data strongly depends upon the spatial subdivision of the drainage basin or area of interest. This subdivision is ideally made on the basis of homogeneity of the input variables and of the response of

the model unit to the input. Spatial variability in land use, vegetation and geology can also influence hydrological response in a manner which is not adequately represented by lumped representations. Heterogeneity of response can be represented by constructing model units on the basis of vegetation and/or other characteristics and modelling processes differently in each unit, or by modifying the process representations by factors which account for the portions of a model unit having certain characteristics. An example of the former approach is given by Lundquist (1982), who routed water inputs to the basin outlet differently according to where they occurred on a glacier. The USACE (1956) used the second approach in their generalized snowmelt formulae to account for variations in forest cover and exposure.

Some quantities, particularly temperature, vary strongly with elevation. This variation must be accounted for in determining the phase of precipitation in different model units. Accordingly, most models for snow covered basins are subdivided on the basis of elevation, in addition to horizontal subdivisions.

In this study, Camp Stream was subdivided into elevation bands. Within each band, net precipitation, snow accumulation, melt and evaporation are calculated separately for forested and open areas, as discussed in sections 5.2.2, 5.3.3 and 5.4.1.

5.5.2 Distribution of Temperature

Temperature varies mainly with altitude in the free atmosphere. Assuming adiabatic conditions, the lapse rate for unsaturated air is 9.8°C km^{-1}. For air saturated with water vapour the lapse rate depends upon the temperature and atmospheric pressure, and on average is 5 to 6°C km^{-1} for elevations between 1500 and 5000 m (Obled and Harder, 1979). However, near-surface air temperatures depend upon many factors other than elevation, including exposure to the prevailing air mass, incoming all wave radiation, the local wind field, and surface characteristics which determine the energy balance. Snow cover, with its distinctive radiative and thermal properties, can profoundly influence temperature fields. The factors governing the temperature field vary diurnally and seasonally, producing similar variations in observed lapse rates in mountainous terrain (Obled and Harder, 1979).

Where a network of temperature stations exists, temperature can be extrapolated through objective or quasi-objective methods, for example, that described by Anderson (1973). Because the model applications in this study are concerned with a small area having fairly uniform exposure, the assumption that temperature varies mainly with elevation is probably justified. Prowse (1981) found that lapse rates in the Craigieburn Range for storm periods had a mean of 6.2°C km^{-1} with a standard error of 0.2°C km^{-1}. This rate is close to the saturated adiabatic lapse rate for similar temperatures and atmospheric pressure. However, the most commonly available temperature data are the daily

maxima and minima, which may not decrease with elevation according to a uniform lapse rate.

Maximum and minimum temperatures and precipitation are read at 0900 at CF and between 1000 and 1100 at SB. The minimum temperature is assumed to have occurred on the morning of the observation and is entered in the climate record on that day. The maximum temperature and precipitation, on the other hand, are entered on the previous day. To preserve synchronism when using the morning observations of precipitation, the precipitation and maximum temperature on one day and the minimum temperature of the following day are used to calculate daily precipitation and average temperature.

The elevational variation of temperature can be defined reasonably well in the Craigieburn Range due to the existence of the CF and SB stations. In many other mountain areas only lowland data are available. For example, Anderton (1974) in the Pukaki catchment and Fitzharris et al. (1980) and Fitzharris and Grimmond (1982) in the Fraser catchment had to extrapolate temperatures at valley stations to higher elevations using assumed lapse rates. Commonly-used lapse rates in mountainous areas are 6°C km^{-1} (Obled and Harder, 1979; Bergström and Jönsson, 1976) and 6.5°C km^{-1} (Bagchi, 1983; Young, 1982). The lapse rates of the daily maximum, minimum and mean (of the maximum and minimum) temperatures have been calculated from the daily observations at CF and SB for the period 1972 to 1981, inclusive. Fig. 5.3 illustrates for example the variation of the lapse rate of mean temperature with season and precipitation. Two-way analyses of variance using a

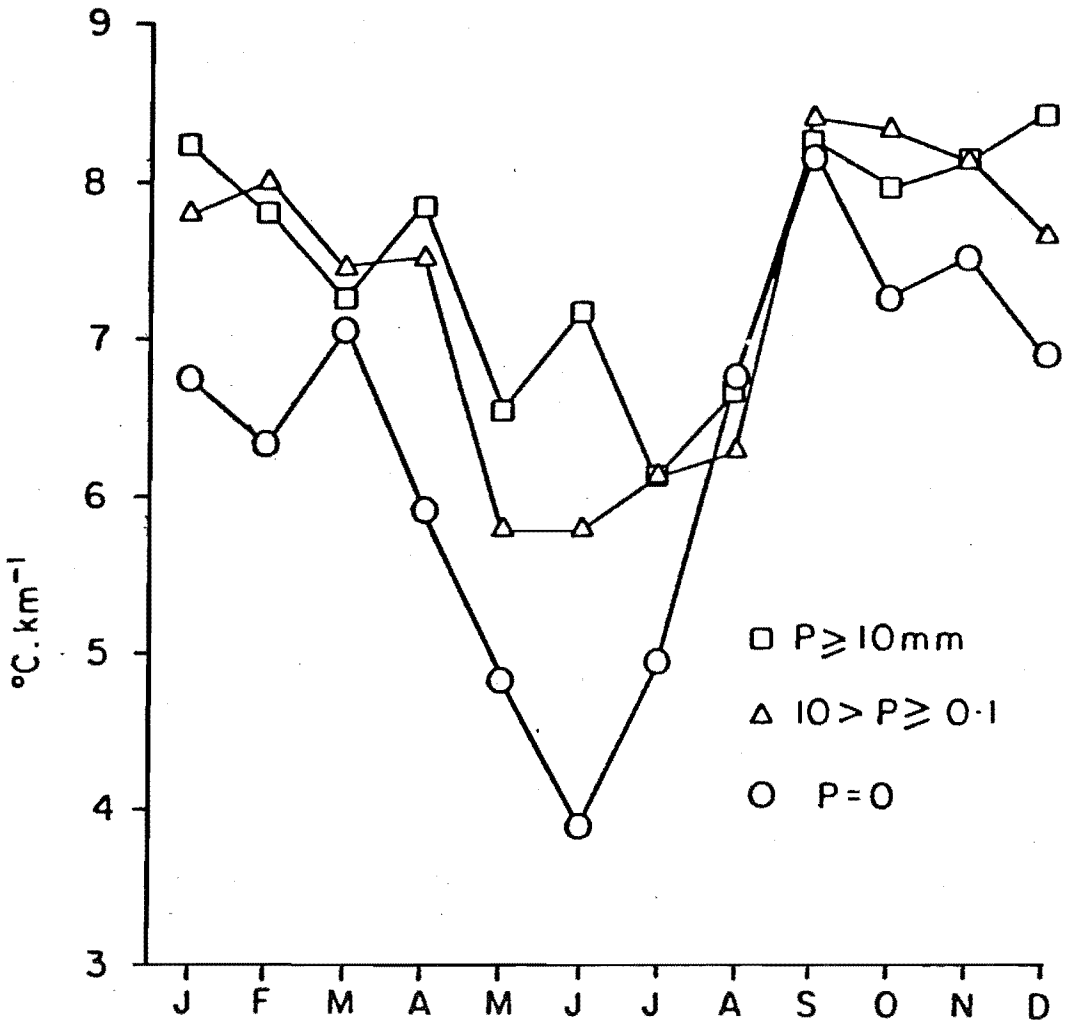

Fig. 5.3. Lapse rates of mean daily temperature between CF and SB for three precipitation classes. Although not shown for reasons of clarity, standard deviations in a given category range from 1.5 to 4.0 °C km⁻¹.

fixed-effects model indicate that the main effects of precipitation and month and the interaction effect are all significant at greater than the .95 level for the lapse rates of maximum, minimum and mean temperatures.

Lapse rates of all three temperatures for all precipitation classes are lowest in mid-winter, when insolation is minimal and inversion effects at CF are greatest. The lapse rates for minimum and mean temperatures increase with precipitation overall, but this trend is not consistent for all months. Lapse rates of maximum temperature are lower overall for days with precipitation than for days without. The grand means of the lapse rates are 10°C km^{-1} for maximum temperatures, 3.6°C km^{-1} for minimum temperatures and 6.8°C km^{-1} for mean temperatures. It is important to note that these lapse rates are average values for the elevation zone between CF and SB, and that lapse rates vary with elevation. This analysis indicates that great errors can be involved with extrapolating measurements from low level stations because radiative and other effects cause lapse rates to deviate markedly and systematically from free air values.

5.5.3 Distribution of Precipitation

Precipitation fields exhibit great spatial and temporal variability. Long term averages of precipitation in mountainous regions are controlled strongly by elevation, exposure to dominant precipitation-bearing air masses and distance from ridge crests (Griffiths and McSaveney, 1983a; see also Fig. 2.4). The control exerted by these factors

varies greatly on shorter time scales due to the variability of mechanisms producing precipitation.

Variability in the precipitation fields in the Craigieburn Range is difficult to specify despite the gauge networks which have been maintained at various times. Problems with varying gauge exposures at different sites and with the effects of cold and snow reduce the homogeneity of data quality. McCracken (1980) suggested on the basis of precipitation and snow course measurements that SB receives 1.24 times more mean annual precipitation than CF. Prowse (1981) analysed thirty-three storms for which reliable records were available at both CF and SB. The ratio of total precipitation received during all storms at SB compared to that at CF is 1.25, which is similar to the long term ratio. However, the ratio for individual storms ranged from approximately 1.0 to 5.0, with much scatter. Hendrick et al. (1979) found in the northeastern United States that the ratios of storm precipitation between high and low elevation stations also varied greatly, and that only a small portion of the variability could be explained by differences in storm characteristics.

The estimation of precipitation in this study is constrained greatly by the quality and availability of data. Daily precipitation totals at CF are used in the application of the snow accumulation model because these data span the period of interest with the least gaps and greatest homogeneity, particularly in winter when many of the higher elevation gauges were adversely affected by wind, cold and snow. The daily totals are adjusted to higher elevation sites using a constant value of precipitation increase with

elevation, which is determined through calibration. This correction factor absorbs the effects of evaporation and wind redistribution. It is recognized that the use of a constant correction factor introduces error into the estimation of event precipitation. Precipitation totals from the Camp Stream gauge are used in the runoff model for Camp Stream basin.

5.6 SNOW ACCUMULATION MODELLING

Many conceptual runoff models incorporate snow accumulation and ablation algorithms which use meteorological input to monitor the snow storage within a basin. The parameters in these algorithms are usually optimized on the basis of providing the best fit to an observed hydrograph. However, this comparison is indirect, and several workers have directly compared modelled snow water equivalent to water equivalent measurements during the accumulation season (for example Anderson, 1976; Speers et al., 1979; Huber, 1983). An advantage of such comparisons is that, if the model performs adequately, it can be used to increase the temporal resolution and extend the record of measurements (Woo, 1972), which can be difficult and costly to make, particularly in New Zealand (Gillies, 1964). Another advantage is that parameter values in the snow routine can at least be assigned good initial values independently of calibration with streamflow data. In this section, modelled snow accumulation is compared to snow course data in the Craigieburn Range, and the utility and limitations of this approach are assessed for New Zealand

conditions and data availability.

5.6.1 Snow Course Data

The snow course data used in this study were collected by the Forest Research Institute in Allan's Basin (AB) at an elevation of 1750 m (see Fig. 2.8). Drifting of snow is uncommon on the snow course, which lies on a smooth lee slope of approximately 28 (Morris and O'Loughlin, 1965). Snow depth and density were sampled at points 20 m apart on a transect which followed the local contour. Density was measured with an Italian CN-1 sampler for the first years, but from 1968 onwards a Mount Rose sampler was used (C.L. O'Loughlin, pers. comm.).

The original data, with the exception of two surveys in 1969 and five in 1970, are not readily available, although most of the dates of the 1967 and 1968 surveys were recovered from field notes made by C.L. O'Loughlin (pers. comm.). Water equivalents and dates of survey for other years were reconstructed by electronically digitizing Fig. 2.6. It appears from the 1969 and 1970 field notes that one density measurement and four depth measurements were usually made at each of thirteen points on the transect. Water equivalent was then calculated as the product of the mean density and mean depth based on all samples, rather than calculating a water equivalent at each sampling point and then averaging the point values.

Snow course data are subject to both measurement and sampling errors, each of which can have random and systematic components. Snow sampler bias is mentioned in

chapter three. The densities used for calculating water equivalent were not corrected for sampler bias by the Forest Research Institute; therefore, the water equivalents from Fig. 2.6 have been reduced by eight percent for use in this study. The variabilities of both snow depth and density are probably much larger than the measurement imprecision, so errors in water equivalent should be caused mainly by sampling errors. Table 5.1 shows estimates of the sampling errors for the 1970 snow course water equivalents (densities not adjusted). The errors were calculated from the following formula, which applies when X and Y are independent variables (M.H. Smith, pers. comm.):

$$C_v^2(XY) = C_v^2(X) + C_v^2(Y) + C_v^2(X)C_v^2(Y) \qquad (5.2)$$

where $C_v(X)$ is the coefficient of variation of X, which is defined as the standard deviation of X divided by the mean. Eq. (5.2) was applied by substituting the mean density for X and the mean depth for Y. The coefficients of variation then correspond to the standard errors of the means divided by the means. The results in Table 5.1 show that the water equivalent values are precise to within 70 mm or so, but some bias will still exist whenever the sampler bias was not equal to eight percent.

5.6.2 Procedure

The data used in these simulations were the maximum and minimum temperatures at SB and CF, daily precipitation at CF and values of the Auckland-Invercargill pressure difference at 1200 local time. Because the time frame of the temperature and precipitation data is from one morning

Table 5.1 - Sampling error estimates for Allan's Basin snow course measurements.

Date 1970	7-29	8-11	8-25	9-15	10-5
$\bar{h}$	702	865	793	633	637
n(h)	12	52	55	46	52
s($\bar{h}$)	81	63	42	66	61
$C_v(\bar{h})$	.116	.073	.054	.104	.096
$\bar{\rho}_s$	274	330	298	414	401
n(ρ_s)	9	7	5	5	7
s($\bar{\rho}_s$)	11	21	34	11	16
$C_v(\bar{\rho}_s)$	.039	.064	.113	.027	.040
WE	192	285	236	262	255
C_v(WE)	.140	.119	.148	.121	.121
s(WE)	27	34	35	32	31

h - snow depth (mm)

ρ_s - snow density (kg m^{-3})

WE - water equivalent of snow pack (mm)

n - number of samples

$\bar{x}$ - mean value of variable x

s(x) - standard deviation of x

$C_v(x)$ - coefficient of variation = $s(x)/\bar{x}$

observation to the next, the corresponding pressure difference was calculated as a weighted sum of the values at 1200 on the days spanned by the 0900 to 0900 time frame. The weights used were 15/24 and 9/24.

Two models, the IEB and the DDF, were applied using CF precipitation and SB mean temperatures as input. In addition, the DDF model was applied using CF temperature to investigate the inaccuracies involved with using low elevation climate data to model alpine snow cover. In all applications, temperatures were extrapolated to the snow course elevation using a lapse rate of 6.5°C km^{-1}.

Accumulation is calculated in the same way in both models. Precipitation at CF is multiplied by a correction factor, RCF, and is considered to be snow if the temperature is less than a base temperature, TB, and rain otherwise. No melt is assumed to occur on snow days, even if T_a is greater than 0°C. If no precipitation falls on a day with T_a greater than 0°C, melt is assumed to occur. The DDF model has five free parameters, WRG, CRF,TB, RCF and DDF, while the IEB model has seven: WRG, CRF, TB, RCF, RMF, C1 and C2.

The models were calibrated by mapping the response surface of an objective goodness-of-fit criterion. The advantage of this procedure over automatic optimization methods is that local optima are more easily recognized and avoided. Fixed intervals of 0.1 for TB and RCF, 0.5 for DDF and RMF, 0.25 for C1 and 8.0 for C2 were used as a compromise between maximizing the extent of the parameter space examined and the resolution while minizing computational time. The parameter values found may not be true optimal values, being constrained by the intervals

used. The criterion employed is Nash and Sutcliffe's (1970) model efficiency, given by

$$E = (F_o^2 - F^2)/F_o^2$$

where

$$F_o^2 = \Sigma (X_i - \bar{X})^2$$

$$F^2 = \Sigma (Y_i - X_i)^2$$

Here, X_i is the observed series, Y_i is the modelled series and $\bar{X}$ is the mean of X_i. Possible values of E range from unity, indicating a perfect fit, to negative infinity for poor fits. A value of E equal to zero implies that $\bar{X}$ is as efficient a predictor as Y_i. This criterion is equivalent to minimizing the squared error between observed and modelled values. It should be noted that model fitting on the basis of least squares criteria can result in biased parameters because of the statistical properties of input data and model output (Sorooshian, 1983). The procedure is used here to provide an objective comparison of model performance during different simulations.

To investigate the sensitivity of the different modelling approaches to the sampling period used, each was first calibrated using the 1967-68 data and then run on the 1969-73 data using the 1967-68 optimal parameters. The three approaches were then calibrated using the entire data sequence to investigate the overall ability of the models to fit the snow course data.

5.6.3 Results

Table 5.2 summarizes the optimal parameters found by the mapping procedure. The parameters WRG and CRF were included for the calibration of the DDF model with SB temperatures. However, model performance decreased whenever they were not set to zero, so they were set to zero for all other runs. It should be noted that TB and RCF for the IEB model were set to the values found for the DDF model using SB temperatures, to reduce the number of free parameters in the IEB model. These values for TB and RCF are stable with respect to the calibration period used, relate closely to observations and precipitation measurements (see sections 5.2.1 and 5.5.3) and thus are physically reasonable. The optimal values for TB and RCF found using CF temperatures are less realistic and are unstable.

Fig. 5.4 shows portions of the model efficiency topography surrounding the optimal values for the DDF model. The same intervals for mapping have been used so that model sensitivity can be compared. Interaction between each pair of variables is apparent when either CF or SB temperatures were used, but the sensitivity is greater when CF data were used. This interaction implies that an incorrect setting of one parameter can to some extent be compensated for during calibration by distortion of other parameter values. However, the optima in both cases are reasonably well defined. Fig. 5.4 illustrates the response surfaces for the parameters controlling melt in the IEB model. Again, all variables interact, and the optimum lies on a broad peak. This broad peak probably results from the temporal

Table 5.2 - Optimal parameters from snow accumulation simulations.

		1967-68	1967-73
1	DDF	4.0	4.0
	TB	2.1	2.2
	RCF	1.2	1.1
2	DDF	8.0	6.0
	TB	1.2	1.2
	RCF	1.3	1.3
3	RMF	0.0	1.0
	TB	1.2	1.2
	RCF	1.3	1.3
	C1	40.0	32.0
	C2	1.0	0.75

1 - Degree-day model using CF temperatures.
2 - Degree-day model using SB temperatures.
3 - Index energy budget model using SB temperatures.

Note: WRG and CRF set to zero for all simulations.

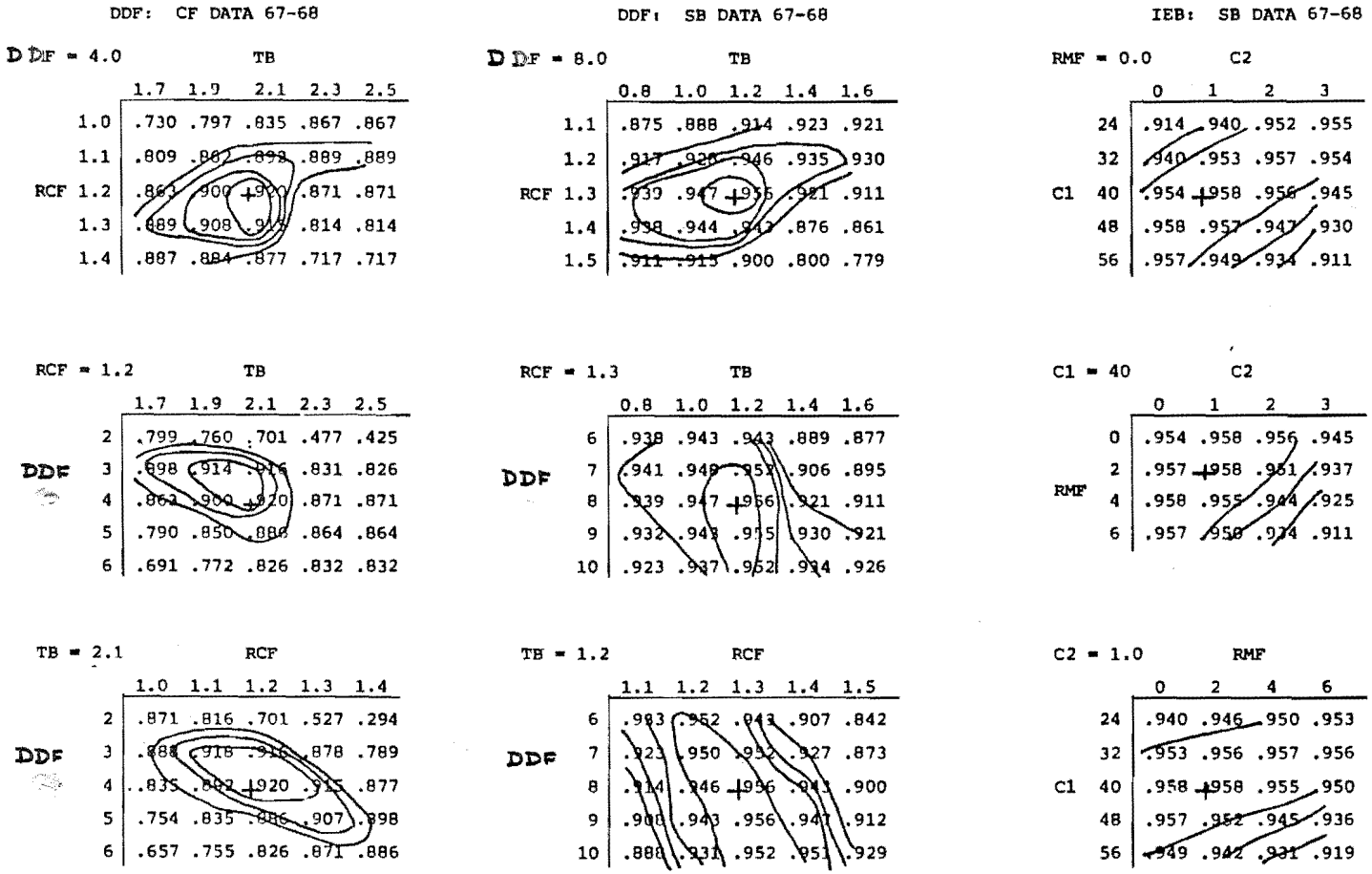

Fig. 5.4. Response surfaces for 1967, 1968-69 snow accumulation simulations. Isopleth interval is 0.1.

resolution of the data: the model performance is more dependent upon the mean melt rates involving a variety of weather situations, rather than upon short term rates, for which the relative roles of RMF, C1 and C2 would be better defined.

Table 5.3 summarizes the goodness of fit indices for calibration and verification periods. The DDF model using CF temperatures performed most poorly, and showed the greatest deterioration in fit between the 1967-68 and 1969-73 periods. The IEB model performed only marginally better than the DDF model using SB temperatures during both calibration periods, but displayed less decrease in performance during the verification period. The RMS errors for the simulations using SB temperatures are approximately 50 to 70 mm, roughly the same as the sampling errors of the snow course data.

The modelled and observed water equivalents are illustrated in Figs. 5.5 and 5.6. Little difference is visible between the IEB and DDF with SB temperature simulations. The DDF simulations using CF data are visually poorer fits than the other simulations, particularly during 1970. These plots show that the quality of simulation varies between years for all simulations. The variation is due to the differences in weather patterns between the years.

Table 5.3 - Performance indices from snow accumulation simulations.

		1967-68	1969-73	1967-73
1	E	.920	.686	.819
	R^2	.93	.75	.83
	A	33	75	54
	B	.86	.86	.83
	CE	318	1423	1301
	RMSE	65	105	90
2	E	.956	.867	.938
	R^2	.96	.90	.94
	A	-3.6	1.3	4.0
	B	.98	.85	1.0
	CE	-180	-1094	299
	RMSE	48	68	53
3	E	.958	.882	.942
	R^2	.96	.91	.94
	A	-0.7	0.8	-2.3
	B	.97	.86	.98
	CE	-124	-1003	-368
	RMSE	47	65	51

E - model efficiency (defined in text)
CE - cumulative error (mm)
RMSE - root mean square error (mm)
R^2, B, A - coefficient of determination, slope and intercept of linear regression of modelled on observed values

1 - Degree-day model using CF temperatures
2 - Degree-day model using SB temperatures
3 - Index energy budget model using SB temperatures

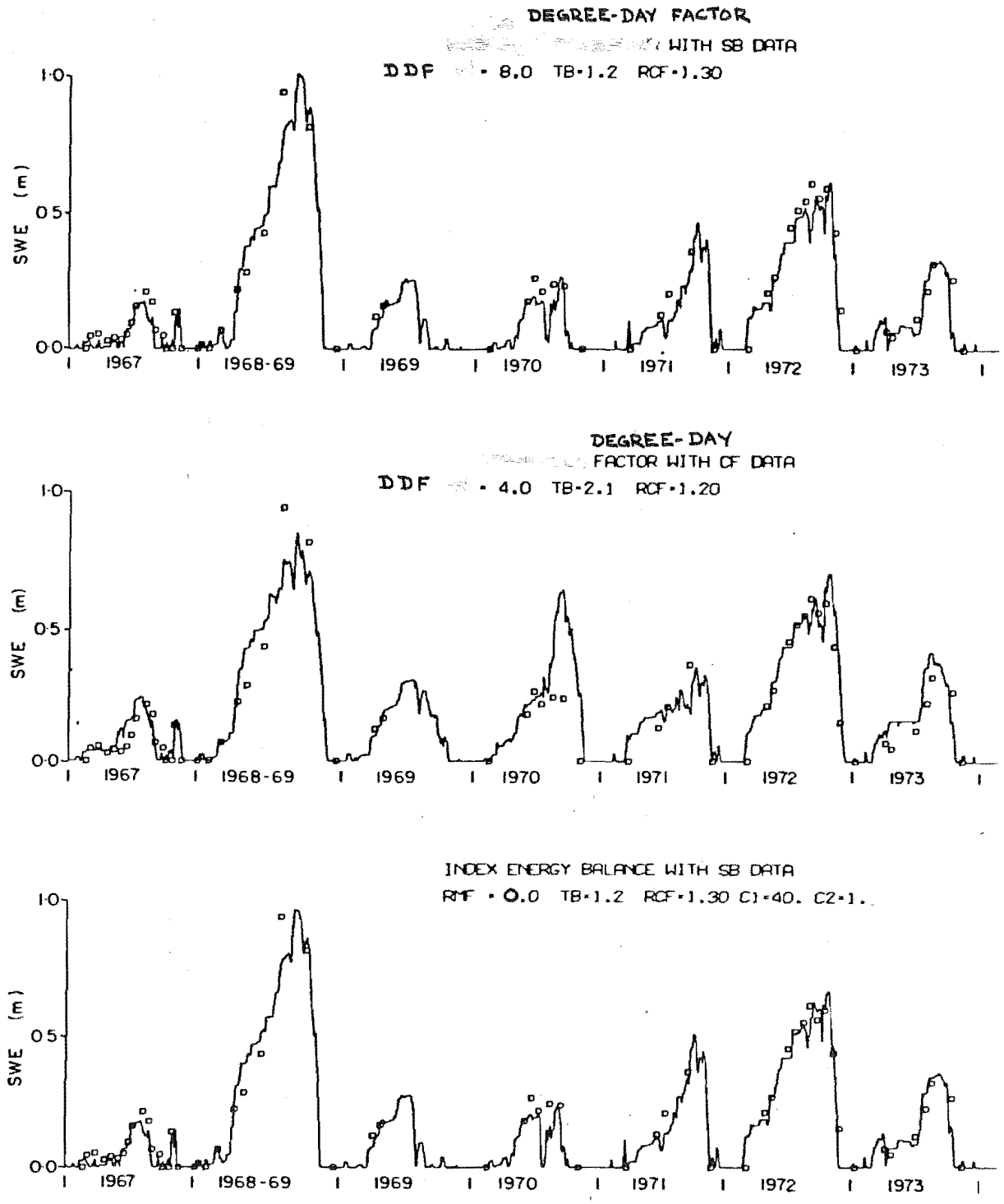

Fig. 5.5. Modelled (line) and observed (squares) snow accumulation. (1967, 1968-69 optimal parameters). Simulation period May to January for 1968-69; May to December for other years.

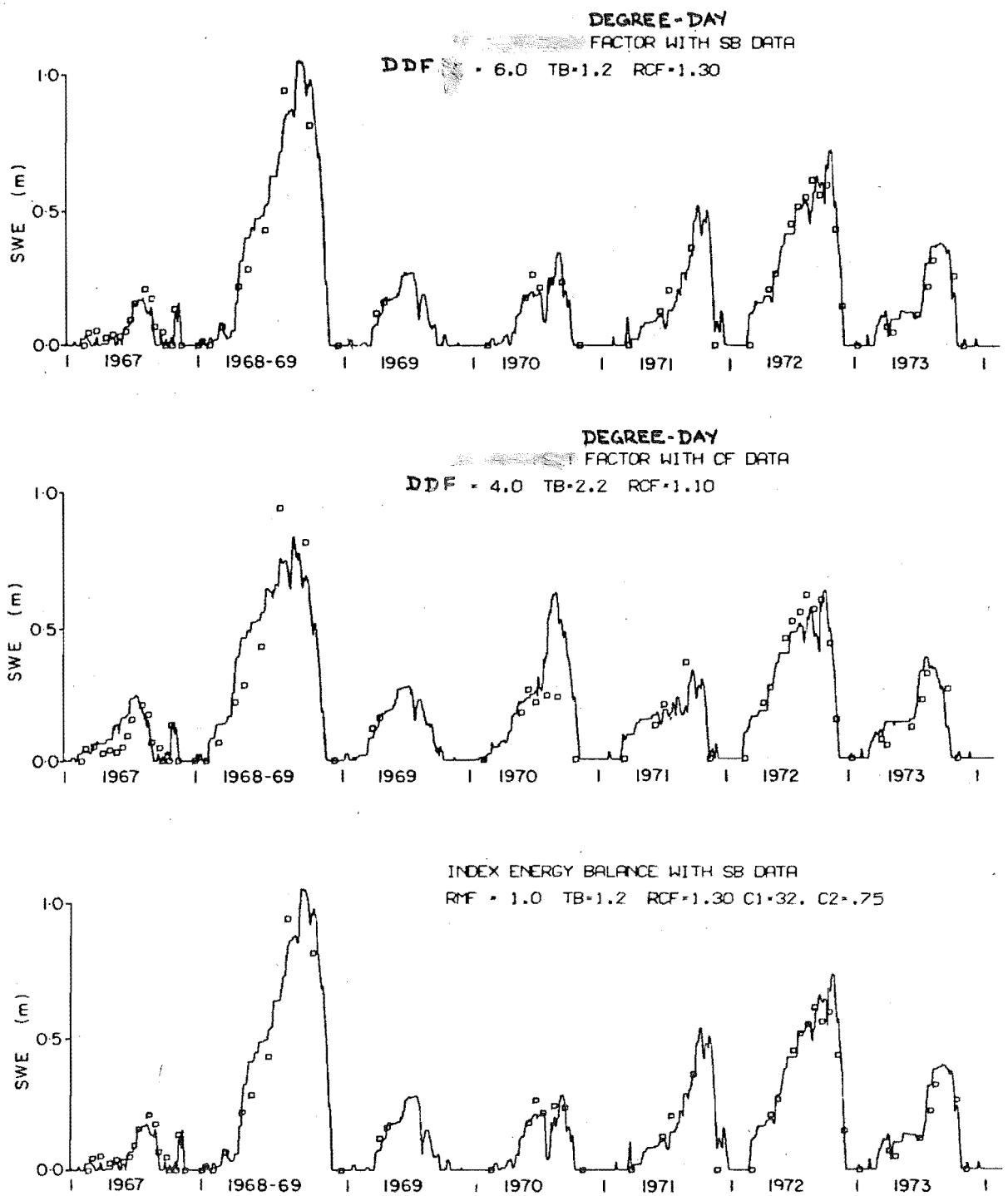

Fig. 5.6. Modelled (line) and observed (squares) snow accumulation simulations (1967 to 1973 optimal parameters). Simulation period May to January for 1968-69; May to December for other years.

5.6.4 Discussion

Low elevation precipitation measurements provided a good index of high altitude precipitation. However, model performance was substantially better when high elevation temperatures rather than when low elevation temperatures were used. The poor performance when using low elevation temperatures is due to the marked and systematic deviations of the lapse rates of near surface air temperature from the assumed rate of 6.5°C km^{-1}. When using high elevation temperatures the optimal parameters assumed physically reasonable, stable values; the use of low elevation temperatures resulted in less stable, unrealistic parameter values. These results illustrate the statement of Charbonneau *et al.* (1981) that errors in extrapolating data, particularly temperature, can have a greater effect on simulations than the choice of algorithm. The transition temperature and precipitation correction factor are unstable when using low elevation temperatures, so the main problem appears to be discriminating rain from snow events. If no high elevation temperature data are available, snow accumulation simulations could probably be improved if observations of new snow-line elevations following storms were used to determine the phase of precipitation at a given elevation, rather than an extrapolated temperature.

The IEB model, which requires surface pressure data, was found to perform only marginally better than the simpler DDF model. However, the greater flexibility of the IEB model appears to protect it somewhat from calibration bias. The IEB model may have performed better than the DDF model

if the snow course data had greater temporal resolution.

The inclusion of parameters which govern water retention and refreezing did not improve model fit. One reason may be that snow-water phenomena were unimportant given the temporal resolution of the data and the inherent errors in the data and in the simplified representations used in the model. Another possible reason is that the representations of the water retention and refreezing processes are inappropriate.

5.7 RUNOFF MODELLING

The process representations employed in the runoff model are described in sections 5.2 to 5.5, and a listing of the program is included in appendix B. The application of the model is discussed in this section.

5.7.1 Data Selection and Processing

The data required for model application are maximum and minimum temperatures at both SB and CF, daily precipitation and mean daily discharge from CS and the Auckland-Invercargill pressure difference. The data from the Camp Stream weir are of variable quality, and have been edited by the MWD (S.M. Thompson, pers. comm.). Periods in which any of the required data had large gaps or were of doubtful quality were discarded, leaving only 1981 and up to the end of November 1982. It was intended that the model would be calibrated on one set of data and verified on an independent set, so 1981 was selected as the calibration

period by flipping a coin.

Precipitation and runoff are averaged on a midnight to midnight time frame. Daily mean temperatures were therefore calculated from the extrema as recorded in the climate records. The pressure difference at 1200 local time was used each day, because it is a reasonable approximation to the daily mean (B.C. Ereckson, pers. comm.). The mean temperature at any elevation was normally calculated by linear interpolation between SB and CF. When one of the stations had missing data, temperatures were extrapolated using the lapse rates discussed in section 5.5.2.

5.7.2 Model Calibration

Calibration was performed on the basis of visual inspection of observed and modelled hydrographs supported by several numerical indices, including the model efficiency, the cumulative error and regression relationships between modelled and observed streamflow. The snow routine has four or six parameters, depending upon whether the DDF or the IEB melt routine is used, while the transformation routine has nine. In addition, initial values for the three state variables in the transformation routine (SM, SUZ and SLZ) must be specified.

Initial values for the snow routines were found by calibrating the routines against snow course data from AB. Camp Stream basin is well-drained and has no lakes, so PW was set to zero. Values for K0, K1, K2 and PERC were found through hydrograph analysis, as described by Bergström and Forsman (1973) and Bergström and Jönsson (1976). Initial

estimates of BETA, FC, CL and UZL were made in consideration of values reported by Bergström and Forsman (1973), Bergström (1975), Bergström and Jönsson (1976) and Svensson (1977). Initial values for SUZ and SLZ were set to correspond to the observed discharge on the first day of the simulation period, and SM was set to FC. Application of a snowfall correction factor and varying precipitation with elevation did not improve model fit.

During calibration, a problem was noted with respect to fitting the recession limbs. Parameter adjustment to maximize E tended to fit the larger peaks at the expense of fitting the recessions (Table 5.4; Fig. 5.7). When the parameters were adjusted to fit the recessions, E decreased markedly and the model tended to respond too rapidly to the smaller runoff events (Fig. 5.7). This problem is related to the significant cumulative error: the modelled runoff exceeded observed runoff during the calibration period by approximately 300 mm (Table 5.4). This cumulative error is equivalent to fifteen percent of the gross precipitation or thirty percent of observed runoff, and is almost the same magnitude as the estimated evapotranspiration. The choice of parameters in effect dictates when the excess water is routed through the basin.

5.7.3 Model Verification

Performance indices for the 1982 simulations using the IEB and DDF models are shown in Table 5.4. The DDF model provided the better fit according to the indices, but neither performed satisfactorily. Both simulations again

Table 5.4 - Parameter values and performance indices, runoff simulations.

	Run Number				
	1	2	3	4	5
TB	1.2	1.2	1.2	1.2	1.2
C1	10.0	-	10.0	10.0	-
C2	1.6	-	1.6	1.6	-
RMF	0.0	-	0.0	0.0	-
DDF	-	4.0	-	-	4.0
WRG	0.0	0.0	0.0	0.0	0.0
CRF	0.0	0.0	0.0	0.0	0.0
FC	150.	150.	150.	150.	150.
CL	90.	90.	90.	90.	90.
BETA	8.0	8.0	8.0	8.0	8.0
K0	0.5	0.5	0.5	0.5	0.5
K1	.06	.06	.10	.06	.06
K2	.025	.025	.025	.025	.025
PERC	3.0	3.0	3.0	3.0	3.0
UZL	75.	75.	50.	75.	75.
E	.739	.759	.561	.316	.361
CE	297.	300.	308.	223.	218.
RMSE	20.8	20.0	27.0	25.3	24.4
R^2	.79	.81	.72	.52	.53
A	1.2	14.0	9.5	13.2	13.8
B	.83	.84	1.0	.79	.77

1 - Calibration run, IEB model (1981)
2 - Calibration run, DDF model (1981)
3 - Calibration run, IEB model (1981)
4 - Verification run, IEB model (1982)
5 - Verification run, DDF model (1982)

E - model efficiency
CE - cumulative error (mm)
RMSE - root mean square error (L/s)

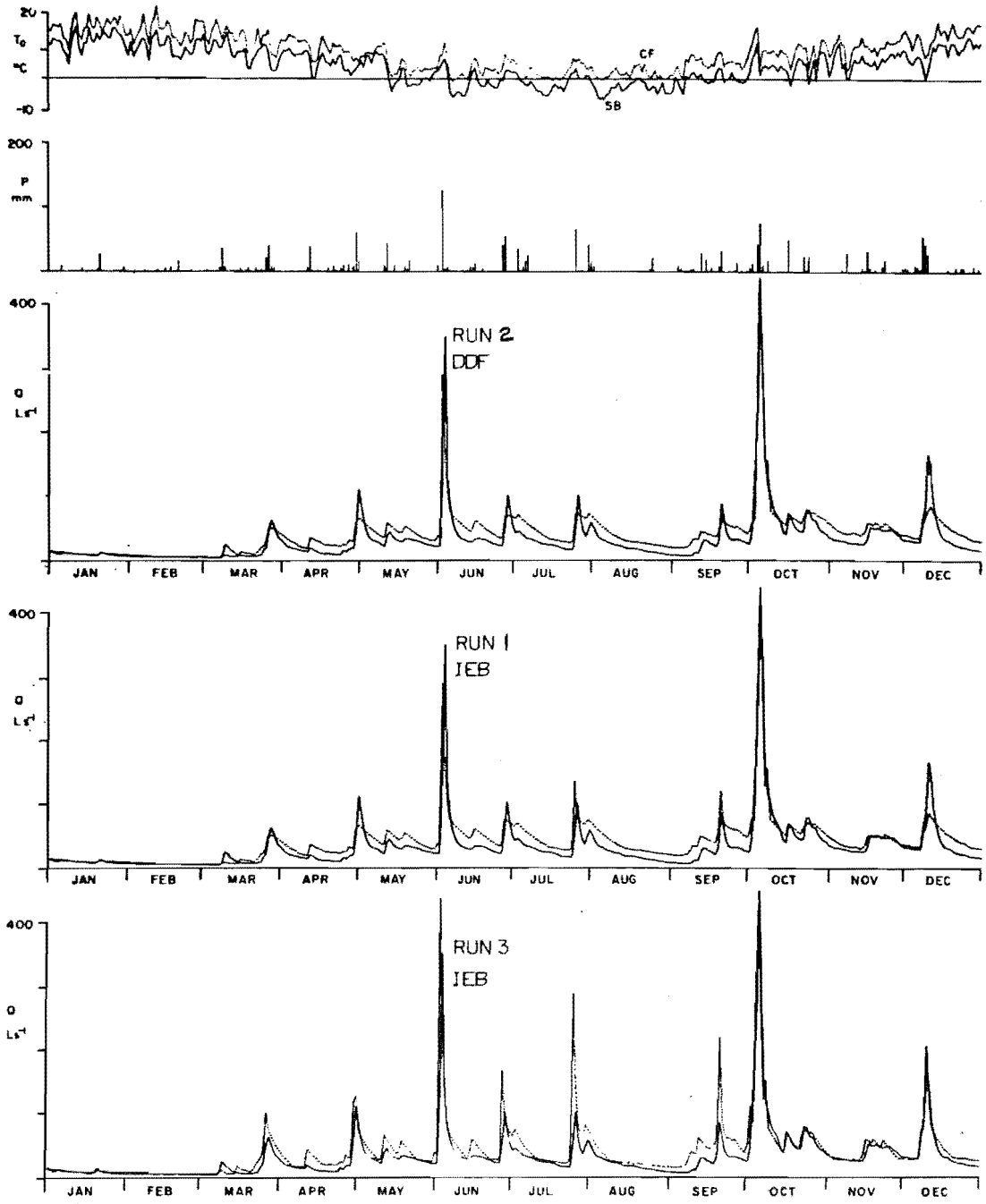

Fig. 5.7. Modelled (dotted line) and observed (solid line) hydrographs for 1981.

show a positive cumulative error. Fig. 5.8 illustrates the simulations. Visually, there is little to choose between the two. In particular, neither simulation reproduces the two hydrograph peaks during the snowmelt period between 28 October and 9 November; conditions leading up to and during this period are discussed in chapter three. Fig. 5.9 shows the snow storage in the open portions of the upper five elevation zones as modelled using the IEB melt routine. The accumulation at 1105 m, 1605 m and 1705 m appears reasonable compared to CF and SB climate records and personal observations, but the snow storage at 1295 m and particularly at 1450 m melts prematurely. Consequently, the modelled area contributing snowmelt runoff during the 28 October to 9 November melt period is underestimated, producing an underestimate of runoff.

An alternative approach has been taken to modelling the snowmelt period. Estimated snow-lines based on field observations during the melt period were used to calculate the snow covered area each day. To simplify the calculations, snowmelt under the beech forest has been neglected; the area contributing snowmelt was therefore derived from a plot of the non-forested area in Camp Stream above a given elevation against the elevation. The mean daily temperature at the median elevation of the snow covered area was used in the snowmelt calculations. Net precipitation was calculated by subtracting interception losses from rain falling onto the forested portion of the catchment. The daily totals of snowmelt averaged over the basin plus net precipitation were input to the transformation routine which has been used in this study.

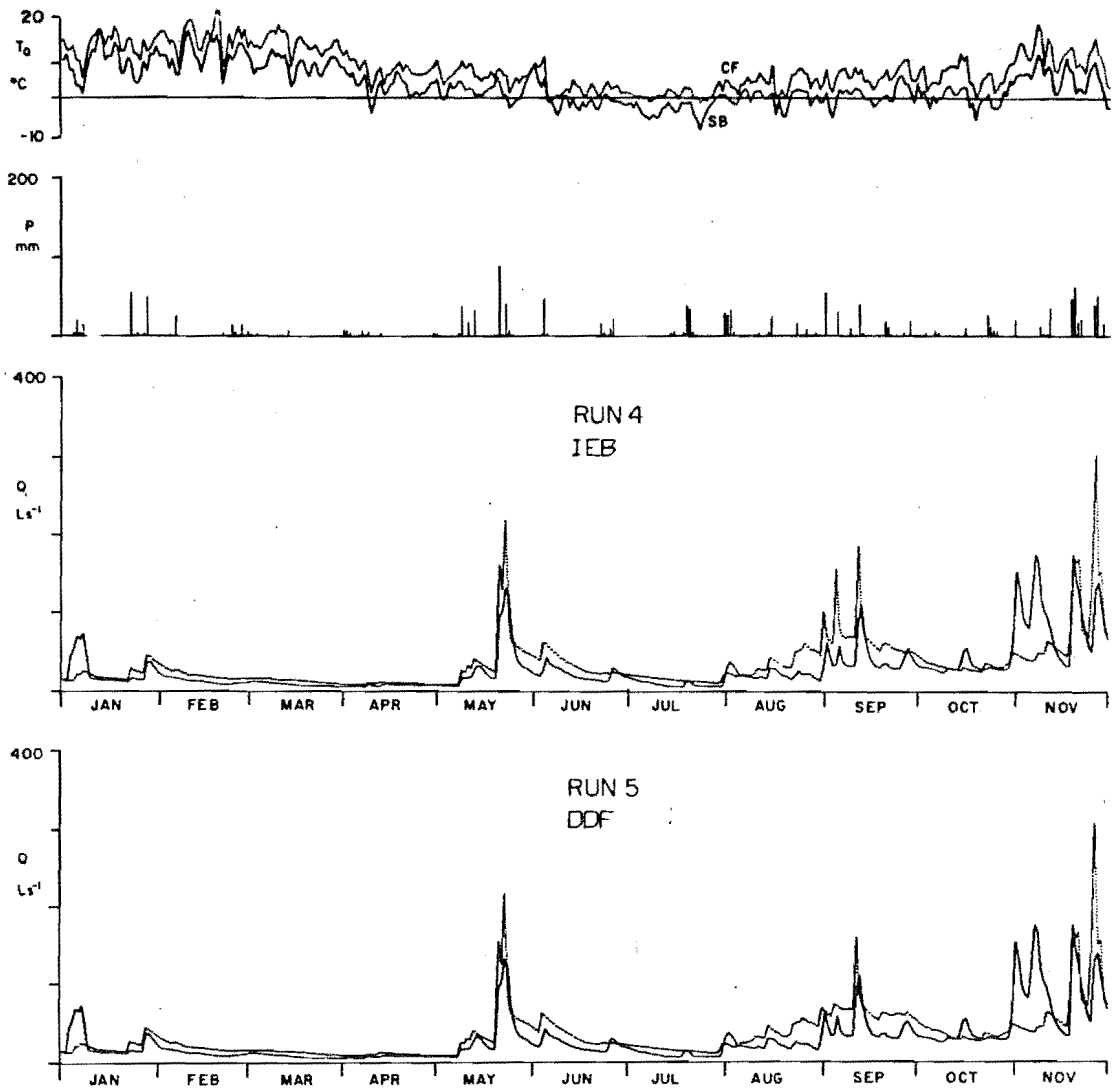

Fig. 5.8. Modelled (dotted line) and observed (solid line) hydrographs for 1982.

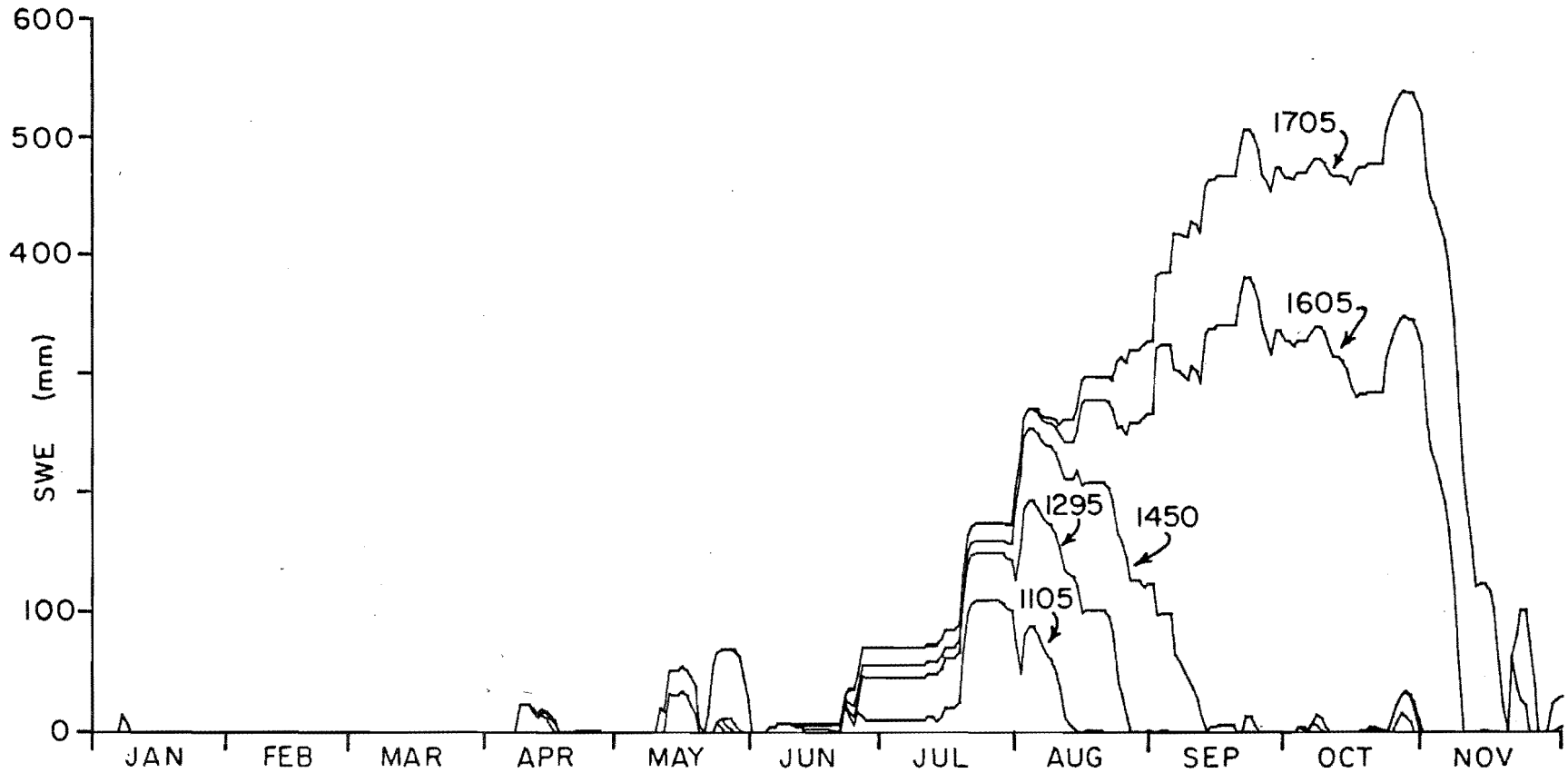

Fig. 5.9. Modelled snow accumulation in five elevation bands, 1982.

As before, soil moisture was initially set to field capacity, and hydrograph analysis indicated that the upper storage was almost empty. Therefore, SUZ was set to 0 mm and SLZ to 101 mm, to correspond to the discharge of 27.5 L s^{-1} on 28 October. When the model was run, however, basin response to the first rain-on-snow pulse was far too damped, suggesting either that the upper zone was not initially empty, or that either or both of UZL and K1 were inappropriate. Therefore, SUZ and SLZ were set arbitrarily such that each reservoir contributed equally to the discharge on 28 October.

Fig. 5.10 shows the results of simulations using the IEB melt routine and the DDF model, with two values for the melt factor, and Table 5.5 shows the snowmelt calculations. The IEB model provides a better reproduction of the variability of runoff. The DDF model does not adequately account for short term melt variations during changing weather situations. However, all simulations display an unrealistic response to the 32.5 mm of net rainfall on 11 November. This over-response is not as evident in the simulations shown in Fig. 5.8.

5.7.4 Discussion

Several problems were encountered in this modelling exercise. One was the substantial volume error, which made calibration of the response function parameters difficult. Assuming that the precipitation and streamflow data are reasonably accurate, the volume error could be caused by one or more of underestimation of evaporation and interception

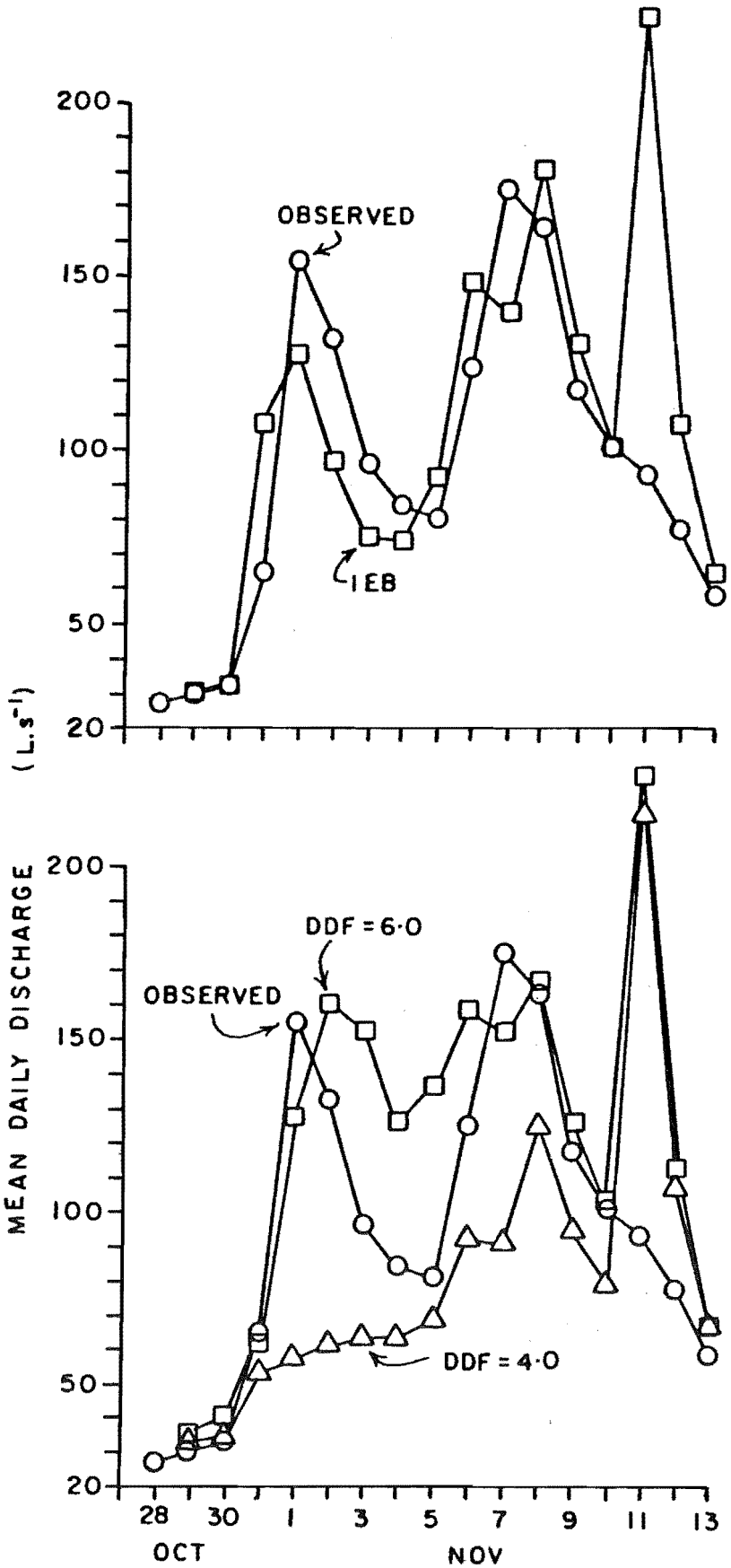

Fig. 5.10. Modelled and observed discharge, spring 1982.

Table 5.5 - Snowmelt calculations for spring 1982 melt period.

Date	SL	SCA	T	DP	P	M1	M2	M3
Oct 28	1200	.47	1.9	6.2	0.0			
29	1200	.47	5.2	6.1	0.0	20.8	31.2	14.9
30	1200	.47	4.2	8.8	0.0	16.8	25.2	14.7
31	1230	.46	6.3	20.1	23.1	25.2	37.8	79.9
Nov 1	1260	.44	7.4	13.0	0.0	29.6	44.4	33.1
2	1300	.42	7.1	5.6	0.0	28.4	42.6	19.5
3	1350	.38	6.4	3.1	0.0	25.6	38.4	13.9
4	1400	.32	5.6	7.4	0.0	22.4	33.6	17.7
5	1425	.28	8.9	16.8	0.0	35.6	53.4	47.6
6	1450	.24	12.1	22.7	0.0	48.4	72.6	81.3
7	1450	.24	10.4	16.5	0.0	41.6	62.4	54.9
8	1500	.15	6.1	15.0	14.5	24.4	36.6	62.2
9	1525	.10	9.1	17.6	5.8	36.4	54.6	50.4
10	1525	.10	7.5	19.1	5.8	30.0	45.0	44.1
11	1525	.10	1.6	6.6	37.6	6.4	9.6	10.0
12	1525	.10	1.3	8.6	2.9	5.2	7.8	4.5
13	1525	.10	3.5	0.9	0.0	14.0	21.0	5.8

SL - snow line elevation (m)
SCA - snow covered area (km^2)
T - temperature at median elevation of snow zone (°C)
P - daily precipitation at CS (mm)
DP - Auckland-Invercargill pressure difference (mb)
M1 - melt (mm/d) calculated with DDF = 4 mm/(d·°C)
M2 - melt (mm/d) calculated with DDF = 6 mm/(d·°C)
M3 - melt (mm/d) calculated with IEB model

losses, unrepresentative precipitation data, unaccounted blowing snow losses and subsurface losses. Considering that the precipitation gauge probably has a negative bias because it is not fitted with a wind shield of any sort and that it is only 60 m above the median basin elevation, precipitation overestimation appears unlikely to account for all of the volume error. Blowing snow losses are also unlikely to account for 300 mm averaged over the basin. Subsurface losses are possibly the main cause of the volume error, given that the evaporation and interception losses were based upon measurements and would have to be over fifty percent greater than the assumed values to account for the error. Mosley (1982) noted that much of the bedrock underlying Camp Stream is highly shattered, offering further evidence for subsurface losses.

Another problem was the misclassification of snow events below 1500 m. Analyses by O'Loughlin (1969a) and Prowse (1981) indicate that the magnitude of temperature variations preceding, during and following snow storms in the Craigieburn Range decreases with elevation, with freezing level fluctuations being confined mainly to the zone below 1500 m. Hence, snow events are more likely to be misclassified on the basis of daily temperature in this zone than at higher elevations. Large portions of Camp Stream and other South Island catchments lie below 1500 m, so precipitation and temperature data with a finer temporal resolution are required for successful modelling in this environment.

The IEB model reproduced the variation of melt more faithfully during the spring 1982 melt period than the DDF

model. This finding supports the inference from energy balance considerations that a wind speed index is required in melt calculations in the South Island. In this study, DP was used as the wind speed index because it is readily available, and the time frame of wind speed measurements at SB do not coincide with those of the precipitation and streamflow data. However, DP may not be the most appropriate index for use in the Craigieburn Range, which lies in the lee of the Main Divide mountains.

Some problems were encountered in transforming the calculated melt and net precipitation into streamflow. One explanation for this is that, as Sorooshian (1983) stressed, the lumped representations of soil moisture and upper zone storage are inaccurate. During the snowmelt period, the majority of runoff was generated on the upper portions of the basin, while the soil dried out in the areas below the snow-line. When the rain fell on 11 November, the response of the snow-free areas would have been damped as the soil moisture deficit was satisfied. However, the lumped transformation model appears to have misrepresented the equivalent antecedent moisture status of the basin, producing too rapid a response. Ferguson (1984) similarly found that rain inputs were routed less correctly than snowmelt in his application of a simple lumped model in the Cairngorm mountains, and postulated that not accounting for soil moisture conditions on areas below the snow-line caused the overestimation of basin response.

Inhomogeneity of response characteristics could also explain the problems with setting initial conditions for simulating the spring 1982 snowmelt period. The recession

constants were derived from a year which was dominated by rainfall, in which water inputs occurred over the entire catchment. However, snowmelt inputs occurred mainly over the upper portion of the catchment, which is dominated by tussock and scree, and on which runoff is generated differently compared to the lower, forested portions of the catchment (see chapter four).

Only one year was used for calibration. This presents a problem, because 1981 was a light snow year, and adequate activation of the snow routine parameters may not have occurred. Bergström (1975) found that four years of data were insufficient to fit stable parameter values in a Swedish catchment. Sorooshian (1983) stated that calibration data should be chosen to maximize hydrological variability; therefore, at least one light and one heavy snow year should be used for calibration.

5.8 SUMMARY

Snow accumulation in the seasonal snow zone was modelled using daily climate observations and compared to snow course data. A simple three parameter model using daily mean temperature and precipitation was found to reproduce reasonably the observed snow accumulation when high elevation temperatures were used. Model performance was less satisfactory when low elevation temperatures were used, because of the marked and systematic deviations of the actual from the assumed lapse rates. A more complicated melt algorithm incorporating a wind index did not perform significantly better than the simpler DDF model. The IEB

model may have performed better than the DDF model if the snow course data had greater temporal resolution.

A runoff model incorporating a distributed snow routine and a lumped transformation routine was developed for conditions in non-glacierized mountainous basins in the eastern South Island of New Zealand, and was applied in the Camp Stream catchment. A major problem was the over-estimation of runoff, which is thought to have been caused by unaccounted-for subsurface losses or underestimation of evaporative losses. Mean daily air temperature appears to be inadequate for discriminating rain from snow events at elevations lower than about 1500 m. The lumped transformation routine performs poorly in situations where runoff sources and mechanisms vary between events. The results from modelling a spring melt period by using observed rather than simulated snow coverage indicate that a wind speed index is required in melt calculations in this environment.

CHAPTER SIX

CHARACTERISTICS OF SNOW STORAGE AND RELEASE

Attempts are made in this chapter to synthesize the results of the present and other studies in order to assess the hydrological significance of snow in the Canterbury high country of New Zealand's South Island. The magnitude and variation of snow accumulation and melt are discussed, and some attention is paid to hydrological characteristics of the transient snow zone.

6.1 SNOW ACCUMULATION

Elevation zones having different accumulation characteristics can be defined, based upon the observations of O'Loughlin (1969a), Chinn (1969; 1981), Prowse (1981), Owens et al. (1983) and the present author. Below 1300 m, snow cover is transient, and the snow-line fluctuates throughout winter with the alternation of snowfall and snowmelt situations. The seasonal snow zone, in which snow cover is usually continuous both spatially and temporally during winter, lies above 1300 m. However, mid-winter melt significantly affects snow accumulation between 1300 and 1500 m, maintaining relatively thin, warm snow packs. Mid-winter melt events are less important above 1500 m, where only occasional events produce marked ablation. Above approximately 2200 m mid-winter melt is usually negligible, and many spring storms which produce rain and melt at lower

elevations bring snow to the higher elevations. One-third of the snow accumulation at 2340 m on the Tasman Glacier coincided with the ablation period at 1645 m in 1972 (Chinn, 1981). The elevations separating these zones refer to the Waimakariri catchment, and decrease to the south: Fitzharris and Grimmond (1982) noted that the seasonal snow-line in Central Otago is 1000 m. These transitional elevations also vary from year to year, and depend upon freezing level fluctuations during storms, which Prowse (1981) has shown to vary systematically with storm type.

Snow accumulation patterns also show a marked variation across the South Island, which is due to the variability of snowfall during different types of storms. Chinn (1981) calculated an integrated index of snow pack magnitude and persistence, which is the area under the water equivalent-time curve, for four snow course sites in the headwaters of the Waitaki catchment. He found that the snow pack index for a high elevation site (2340 m) was poorly correlated with lower elevation sites. This poor correlation is expected from the differences in accumulation characteristics. The degree of correlation observed between pairs of the lower elevation sites could be explained largely with respect to the relative exposures of the different sites to various storm types. The worst correlation was between the site with the greatest exposure to westerly snowstorms and the site with the greatest southerly exposure.

Several studies have investigated the relationship between snow accumulation and annual precipitation. Morris and O'Loughlin (1965) found that snowfall in the Craigieburn

Range represented approximately one-third and one-fifth of the annual precipitation at 1750 m and 1450 m elevation, respectively, between 1962 and 1964. Between 1965 and 1968, snow accumulation at 1750 m accounted for eighteen to fifty-six percent of annual precipitation, with a mean of thirty-six percent (O'Loughlin, 1969a). Prowse (1981) estimated that between twenty-six and forty-one percent of precipitation falls as snow at SB. Anderton and Chinn (1978) found that maximum snow accumulation on the Ivory Glacier (elevation range 1400 to 1700 m) in the period 1969 to 1974 was on average twenty-five percent of annual precipitation.

From the figures cited above, it appears reasonable to assume that on average thirty percent of precipitation above 1500 m is stored as seasonal snow throughout the Waimakariri catchment. Mean annual precipitation in the Waimakariri catchment is approximately 2300 mm. This figure is based upon measured discharges from 1967 to 1981, increased by fifteen percent to account for subsurface losses, and an estimated annual evaporative loss of 500 mm, which is the value assumed by Bowden (1983) for the Rakaia. Approximately fifteen percent of the Waimakariri catchment lies above 1500 m (Fig. 2.2), so if precipitation is spatially uniform, roughly five percent of the basin precipitation is stored as snow in the winter and released in the spring. However, precipitation increases with elevation, and a concentration factor of 1.5 should be a reasonable upper limit. Therefore, it appears that the mean magnitude of snow storage lies between 100 and 150 mm, or considerably less than half the magnitude of assumed

evaporative losses. A similar calculation for the Rakaia catchment, in which twenty-eight percent of the catchment lies above 1500 m (Bowden, 1977), yields an average snow storage of up to thirteen percent of annual precipitation for a concentration factor of 1.5. This figure compares favourably with water balance estimates of thirteen percent (Bowden, 1983) and eleven percent (M.J. McSaveney, pers. comm.).

Estimation of the long term average monthly water balance of the Waimakariri catchment was attempted. The change in storage term was critically sensitive to the monthly distribution of evaporation, particularly during the summer, when evaporation may be limited in the drier portions of the catchment. The results of this approach were probably also confounded by the variability of the magnitude and timing of snow storage and melt from year to year.

Snow storages equivalent to 100 and 150 mm in the Waimakariri catchment would respectively produce mean flows of 39 and 58 $m^3 s^{-1}$, averaged over a two month spring melt period and corrected for losses. The mean flow for the months October and November is 176 $m^3 s^{-1}$ (Bowden, 1977). Seasonal snow storage thus appears to account for twenty-two to thirty-three percent of the mean flow in October and November. These figures are averages over a number of years; snow accumulation in a particular year may be twice the mean (see section 2.1). The release of seasonal snow accumulation will maintain streamflow during inter-storm recession periods. The contribution of snowmelt to storm runoff will depend upon snowmelt rates and snow-covered area

during rain events.

6.2 SNOWMELT

Most snowmelt occurs at or near the upper snow pack surface, so the snow surface energy exchanges are the primary controls on melt rates (Male and Granger, 1981). The magnitudes of the various exchange mechanisms reflect the interactions between snow pack characteristics, site factors and meteorological conditions. Virtually all of the seasonal snow zone in the Canterbury high country is alpine in character, and, as discussed in chapters two and three, snowmelt is strongly controlled by the prevailing synoptic situation. Even in the transient snow zone, well less than half of the area is forested (see chapter two). Transient snow zone processes are discussed in more detail in section 6.3; snowmelt above the seasonal snow-line is the focus of this section.

During winter, incoming solar radiation is at a minimum, and net radiation gains can be important only on clear days. Even then, only north-facing slopes will exhibit appreciable melt. During periods of clear winter weather at Temple Basin, it was observed that while the snow surface on north-facing slopes had a spring snow texture, the snow on slopes of other aspects remained dry and powdery. Mid-winter clear weather melt is maximized when air temperatures are above freezing. If air temperatures are below freezing and the air is dry relative to the snow surface, the loss of sensible and latent heat can offset the radiative exchange even on the clearest days, particularly

if a strong southerly wind is blowing. Granger and Male (1978) noted similar offsetting of radiation by the turbulent exchanges in a prairie environment. Prowse (1981) estimated net radiation during several winter melt events at SB, and found that Q* averaged -4.5 MJ m^{-2} d^{-1}. This value is probably too large in magnitude, for it was calculated by assuming a snow surface temperature of 0°C, which was likely not always the case. However, this estimate does illustrate the fact that net radiation usually represents a heat loss during winter at this south-east facing site. Therefore, mid-winter melt must be generated mainly by the turbulent exchanges of sensible and latent heat.

Because mid-winter melt is generated mainly by sensible and latent heat exchanges, the magnitude and frequency of melt at any elevation depends strongly upon freezing level fluctuations, particularly during precipitation events. As noted previously, these fluctuations are such that mid-winter melt frequently occurs below 1500 m, but less often above 1500 m. However, occasional mid-winter events can cause rapid melt throughout most of the seasonal snow zone in the Waimakariri catchment, that is, up to 2000 m or higher. Prowse's (1981) estimated energy budgets during winter melt events indicate that winter melt rates at SB can range at least up to 64 mm d^{-1}. Melt rates would be greater at sites which are more exposed to the wind.

In spring, and in summer if a snow cover persists, the controls on the energy balance climate over snow change. Net radiation increases because of the increased insolation and decreased albedo, and on a clear day, slopes of almost all aspects will experience melt. In addition, lower slopes

are often free of snow, and radiative heating of the bare slopes on clear days warms the air and can generate local winds, enhancing turbulent exchange over adjacent snow fields. However, the spring months in the South Island are characterized by an increased frequency of strong winds from the north-west quarter, which produce regional scale advection of heat and moisture. The dominance of warm, windy weather is reflected in the energy budget estimates at SB and TB, as presented by Prowse and Owens (1982) and in this study. Prowse and Owens (1982) found that sensible heat contributed fifty-seven percent of the heat input at SB during spring melt periods between 1976 and 1980. The turbulent exchanges also dominated the energy budgets at both TB and SB during the spring melt period of 1982, as discussed in chapter three.

The storms which produce rapid spring melt at lower elevations often produce accumulation at higher elevations. Most of the ablation of these higher elevation snow packs thus occurs in summer, when the weather is often more settled than in spring (Anderton and Chinn, 1978). The combination of lower temperatures at higher elevations and more settled weather would tend to minimize sensible and latent heat inputs, increasing the importance of radiation. Chinn (1981) showed that ablation on the Tasman Glacier during the 1972-73 glacial year ranged from approximately 2.3 m water equivalent of snow at 2340 m to over 7 m (mostly glacier ice) at 1645 m. The greater melt at the lower elevation is due to both the lower albedo of glacier ice as compared to snow, and the greater turbulent fluxes.

Detailed frequency-magnitude-duration relationships,

such as those derived for rainfall, cannot be calculated for melt in New Zealand. However, some semi-quantitative characteristics of short term melt rates in the Craigieburn Range can be inferred from climatic and hydrological evidence. The results of Prowse and Owens (1982) and chapter three indicate that daily melt totals at SB can range at least up to 100 mm. These melt totals can be compared to the twenty-four hour two year return period rainfall at CF, which is 92 mm (NZMS, 1980). Another indication of the hydrological significance of rapid snowmelt in the Craigieburn Range is the daily flow of 176 L s^{-1} at Camp Stream on 8 November 1982. This flow was the maximum daily flow in 1982, and was generated purely by snowmelt over less than half the basin area (see section 5.7). The highest daily flow in 1982 caused by rain was 175 L s^{-1}. This flow occurred on 19 November when over 50 mm of rain fell.

Snowmelt during rainfall can potentially increase the effective return period of a runoff event compared to that expected from rainfall alone. To investigate whether atmospheric conditions during rainfall are conducive to rapid snowmelt, an index related to sensible heat transfer was calculated from daily climatological observations at SB for the period 1972 to 1981. The convective melt index, CMI, was calculated as

$$CMI = u_a T_a/(1 + 10\ Rb)$$

where u_a is the daily mean wind speed (m s^{-1}), T_a is the mean of maximum and minimum air temperatures (°C) and Rb is the bulk Richardson number, which is defined in chapter three and was calculated using a nominal instrument height

of 1.2 m. Values of CMI can be approximately converted to mm d^{-1} of melt by multiplying by 1.3, although variations of instrument heights with snow depth will influence the conversion. CMI neglects net radiation and latent heat exchange, the latter of which may strongly augment sensible heat exchange when the air is warm and humid. To exclude most non-melt days, CMI was calculated only for days with snow lying and T_a greater than 1.2°C on rain days, and T_a greater than 0°C on non-rain days.

Fig. 6.1 shows scattergrams of CMI, T_a and u_a against daily precipitation at CF. The envelope curve of the scattergram of CMI decreases with precipitation. Inspection of the scattergrams of wind speed and temperature against precipitation indicates that depressed temperatures, not wind speeds, account for the shape of the envelope. It appears, then, that rapid snowmelt in the seasonal snow zone is not likely to coincide with extreme rainfalls in the Craigieburn Range, at least for shorter durations. However, rapid melt conditions could precede, follow or occur between episodes of intense rain, and would effectively increase the duration of the event, or increase the effective magnitude of the equivalent longer duration event. Melt preceding rainfall would act to prime a catchment and increase the catchment's response to the rainfall. Fitzharris *et al.* (1980) and Thomson (1983) respectively reported this priming function of snowmelt in catchments in Central Otago and the northern South Island. A more detailed analysis of weather patterns associated with rain-on-snow on a finer time scale would be required to define the temporal relationships of snowmelt and rainfall rates.

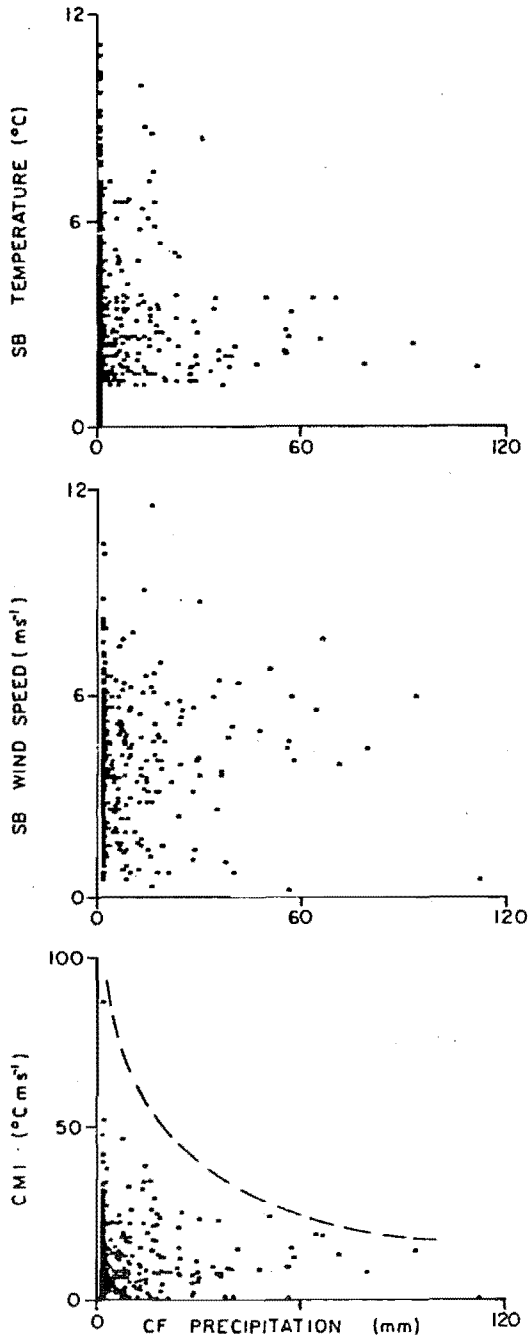

Fig. 6.1. Scattergrams of mean daily temperature, wind speed and convective melt index (CMI) at SB against daily precipitation at CF.

Because of the lack of a data base, even a superficial analysis like that just described cannot be carried out for areas near the Main Divide. Following the approach of Harr (1981), some conjectures can be made based upon the relationships between melt and meteorological variables. Fig. 6.2 illustrates the dependence of snowmelt upon rainfall, temperature and wind speed. Melt was calculated from Eqs. (3.5), (3.8) and (5.2) with the assumptions made that the air is saturated and the rain drops are at air temperature. As can be seen, some combinations of meteorological conditions could produce sufficient snowmelt to augment rainfall. For example, for T_a = 4°C, u_a= 6 m s^{-1} and P = 250 mm, which is the twenty-four hour five year return period rainfall (Tomlinson, 1980), melt would be 70 mm, which would increase the water input to 320 mm, or only 10 mm less than the twenty year return period rainfall. The combination of T_a = 4°C and u_a= 6 m s^{-1} probably occurs frequently; it was observed in the spring melt period of 1982. The coincidence of high wind speeds and heavy rain has also been observed. Therefore, the main factor limiting the magnitude of snowmelt during heavy rain would be the air temperature, just as it appears to be in the Craigieburn Range. However, rainfall intensities of 10 mm h^{-1} coincided with air temperatures of 5 to 6°C during the spring 1982 melt period, and Anderton and Chinn (1978) recorded that 62 mm water equivalent of snowmelt occurred during a 400 mm rainfall event on the Ivory Glacier, on the west coast (see Fig. 1.1). More climatic data regarding temperatures during rainfall near the Main Divide are required.

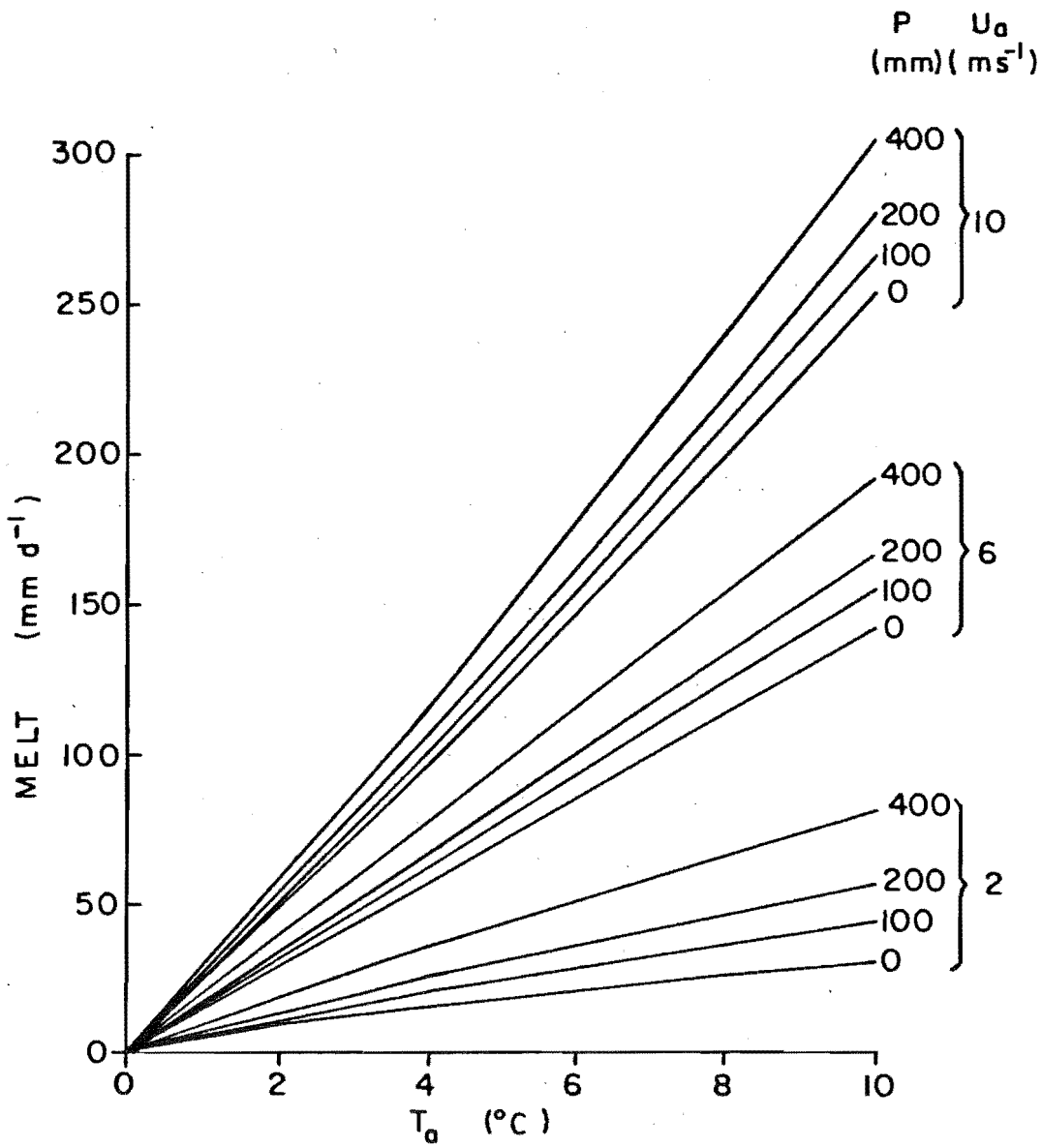

Fig. 6.2. Snowmelt as a function of temperature, wind speed and precipitation.

6.3 TRANSIENT SNOW ZONE PROCESSES

Standard meteorological observations do not have sufficient temporal resolution to be of use in studying or modelling transient snow zone processes. This difficulty is probably the main reason why much attention has only recently been focused upon the transient snow zone. Harr (1981) and Christner and Harr (1982) related annual flood characteristics of a number of basins in western Oregon to basin elevations and land use patterns to infer the nature of rain-on-snow processes. Harr and Berris (1983), Beaudry and Golding (1983) and Zuzel et al. (1983) used detailed meteorological observations and lysimeter runoff to study transient snow events. Cooley and Robertson (1983) added time lapse terrestrial photography of snow cover to meteorological and lysimeter runoff data, while Braun and Zuidema (1982) combined meteorological and profiling snow gauge data with streamflow from a small experimental basin in a modelling study of transient snow zone hydrology.

The consensus from these studies is that temperatures during heavy rainfalls can be high enough so as not to limit snowmelt, so melt may effectively increase water input. The characteristically thin, warm snow packs have little effect on runoff production. The main problem with most of the studies cited above is that they present a limited number of case studies, from which it is difficult to extrapolate frequency-magnitude-duration statistics which would be of practical interest. A large portion of the Canterbury high country, including fifty percent of the Waimakariri catchment, lies between 700 and 1300 m elevation.

Therefore, the hydrological aspects of transient snow events warrant some attention.

The Hut Creek catchment lies entirely within the transient snow zone. The flow record is not long or complete enough to compare flood frequencies for rain and rain-on-snow events, as was done by Harr (1981) and Waylen (1982). Pearce and McKerchar (1979) separated a seven year long record of runoff events into quickflow and delayed flow according to the method of Hewlett and Hibbert (1967). An examination of their data revealed no systematic differences in event characteristics such as time to peak, peak runoff rate and quickflow to precipitation ratio between rain on bare ground and rain-on-snow events. This finding contrasts with that of Harr (1981), who found significant differences in rate of hydrograph rise and runoff rates between the two types of events. Reasons for the lack of systematic differences include the dependence of basin response on antecedent soil moisture conditions (Taylor and Pearce, 1982), groundwater influx in an area of fractured bedrock, which can occasionally produce greater than one-hundred percent runoff (Taylor and Pearce, 1982), and variation of the phase of precipitation during an event.

A detailed case by case analysis of runoff events at Hut Creek would be required to define the hydrological significance of transient snow cover. Time constraints prevented the inclusion of such analyses in this project. However, an analysis has been made of one event which resulted in flooding and road washouts in the Craigieburn area. Road washouts occur on average about every five years (A.J. Pearce, pers. comm.). This event occurred between 8

and 10 July 1983. A reconstruction of the event has been performed using the chart records of wind speed, temperature, humidity, and precipitation at CF. Several hours of the precipitation record were lost because the Belfort rain gauge overflowed; the missing record was estimated from the manual rain gauge total at CF and the precipitation record from the Camp Stream gauge. An attempt to synthesize the streamflow from Hut Creek during the event would have been made, but, unfortunately, the water level recorder clock stopped prior to the event and was not re-started until some time after the event.

The phase of precipitation during the event was determined from the recorded six-hourly observations and the temperature record. Initial snow pack water equivalent was estimated from the observed snow depth and an assumed density of 300 kg m^{-3} (the snow had been lying for several days). Snowmelt was calculated from the USACE (1956) equation for melt during heavy rain, which can be expressed as

$$M = T_a \cdot (.055 + .036\ u + .005\ P) + .096 \qquad (6.1)$$

where M is melt (mm h^{-1}), T_a is air temperature (°C), u is wind speed at 15 m (m s^{-1}) and P is precipitation (mm). The wind speed measurement was adjusted to a height of 15 m by using a one-sixth power law as recommended by USACE (1956) and Anderson (1976). It is not known how applicable Eq. (6.1) is at CF. Eq. (6.1) may underestimate melt because the convection-condensation melt term was derived over a deep seasonal snow pack, which would have a lower surface roughness than a shallow snow pack with vegetation protruding through. The ground heat flux term may also be

greater at CF than at the site at which the equation was derived.

Fig. 6.3 shows the input data and estimated snow storage and water inputs for the rain-on-snow event. Changes in snow storage have a marked effect on the short term distribution of water input. Not accounting for snow influences would certainly perturb the results of rainfall-runoff analyses such as the derivation of unit hydrographs. The snowmelt significantly increased the water input during periods of intense rain. For example, the precipitation total for 9 July is 123 mm, while the estimated water input is 155 mm, an increase of over twenty-five percent. These figures can be compared to the twenty-four hour duration precipitation totals at CF, which are 129 and 153 mm for return periods of five and ten years, respectively.

6.4 DISCUSSION

Although the processes of snow accumulation and melt vary with position across the Southern Alps, the hydrological impact of snow depends mainly upon elevation. In the transient snow zone, snow storage acts to delay runoff on time scales ranging from the order of an hour to several weeks. The snow may melt slowly, resulting in flooding only locally in areas with poor drainage; or melt may be rapid, and can considerably increase water input to the soil during rain-on-snow situations. In either case, transient snow storage influences short term rainfall-runoff relationships, but should usually not be important on

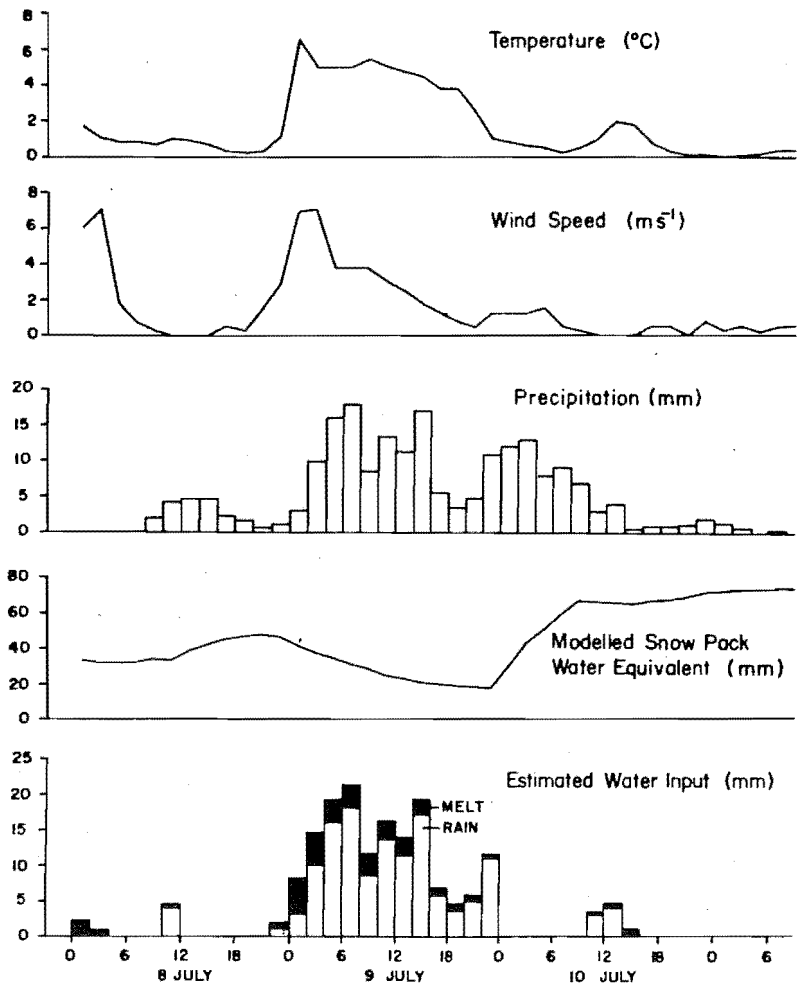

Fig. 6.3. Meteorological data and estimated snow storage and water input at CF during a rain-on-snow event, 8 to 10 July 1983.

monthly or longer time scales.

In the lower 200 m or so of the seasonal snow zone, runoff lag times due to snow storage should be characteristically on the order of days to months, although some events with rapid freezing level fluctuations may produce shorter lag times. The snow storage throughout the rest of the seasonal snow zone should range from weeks to months. Although rapid snowmelt can coincide with rainfall, the relationship between temperature and precipitation may limit the extent to which snowmelt can contribute to water input during the less frequent events. At the highest elevations, above approximately 2200 m, lower air temperatures limit snowmelt rates, and the time lag between snow deposition in the accumulation zones of glaciers and melt may be years or even centuries.

Most basins in the Canterbury high country have steep slopes and a great amount of relief, with valley bottoms approximately 600 to 800 m elevation and ridgetops from 1800 to over 3000 m. Even a first order catchment like Camp Stream, with an area of less than 1 km^2 , has over 700 m of relief. Accordingly, snowmelt and accumulation can occur simultaneously in the same basin at different elevations. The net influence of snow on basin response will vary with the basin's hypsography and thus, to some extent, on basin scale, since the higher basins often tend to be headwater basins in larger catchments. Snow influences may therefore represent another difficulty in extrapolating results from small to large basins, in addition to those discussed by Pilgrim et al. (1982).

The magnitude of seasonal snow storage varies greatly,

but in some years can probably significantly contribute to runoff during the short spring melt period. The coincidence of rapid melt in the seasonal snow zone with intense rain episodes is uncertain given the present data availability. Rapid snowmelt preceding or occurring between intense rainstorms may enhance a basin's response to rain inputs.

Rapid melting of snow during heavy rain in the transient zone may possibly contribute significantly to flood runoff. The snowfalls of November 1967 and August 1973, which both produced substantial snow accumulation down to low elevations, were followed by heavy rain (Ministry of Works, 1970; Hughes, 1976). The resultant floods in 1967 deposited large quantities of sediment in the Camp Stream flume (Ministry of Works, 1970). The magnitude of snowmelt during these and similar events deserves further investigation. Much of the transient snow zone comprises valley bottom areas, which are less exposed to wind than the seasonal snow zone. Hence, wind may be the main factor limiting snowmelt during rainfall, rather than temperature, as appears to be the case in the seasonal snow zone.

CHAPTER SEVEN

CONCLUSIONS

7.1 SUMMARY OF MAJOR FINDINGS

Field studies of snowmelt processes in the seasonal snow zone were carried out at two sites in the Waimakariri catchment. Regional air mass and circulation characteristics appear to provide stronger controls on the turbulent exchanges of sensible and latent heat at Temple Basin (TB) than local advection and locally-generated winds. Daily estimates of the sensible and latent heat fluxes are correlated with indices of regional air mass characteristics and circulation. Estimates of sensible and latent heat exchanges at Ski Basin are less well correlated with the large scale indices, and display marked differences to the estimates at TB. This variation in snowmelt climate across the Southern Alps appears to be related to air mass modification and interactions between the regional air flow and the mountains.

Snow surface lowering, which is used as a surrogate for melt, displays within TB a systematic and statistically significant spatial variation with weather type. During anticyclonic, clear weather, sunny slopes showed the greatest lowering. However, during strong regional advective melt conditions,

surface lowering was greater at the crest of a small rise than at sites with rectilinear slopes. It is suggested that this pattern is caused by increased shear and, hence, greater turbulent exchange on the rise. This finding qualitatively accords with the theory of Jackson and Hunt (1975).

Observations of snow pack structure, water movement and considerations of climatic factors suggest that the routing properties of snow cover vary across the South Island. In the western areas below about 2200 m, where rain-on-snow is relatively frequent, the snow pack matures throughout the winter and ice layers are relatively permeable. Calculations based upon Colbeck's kinematic wave theory show that water movement in snow should not have a great influence on routing during flood-producing events. However, rain-on-snow is not as frequent or as great in magnitude in the eastern mountain areas such as the Craigieburn Range. Observations made by Prowse (1981) indicate that ice layers may have a stronger impeding effect on water percolation in the drier, colder climate typical of the eastern ranges than nearer the Main Divide.

The effect of snow cover on routing water from the ground surface to the stream channel is difficult to predict because of the great variability of runoff mechanisms and lack of knowledge about ground ice characteristics. Snow cover effects are particularly uncertain for scree surfaces and under beech forests. However, snow cover should not have so great an effect

on runoff generation from alpine tussock grassland, because the vegetation cover provides a porous zone between the ground surface and the snow, in which turbulent overland flow could occur.

Conceptual parametric models of snow accumulation, melt and runoff were developed and tested against snow course and streamflow data. A simple model based upon daily air temperature and precipitation produced reasonable simulations of snow accumulation at 1750 m when temperatures measured at 1550 m were used. The quality of simulation was less satisfactory when low elevation temperatures were used, because of the marked and systematic deviations of the actual from the assumed lapse rates. A more complicated snowmelt algorithm did not perform significantly better than the simpler model, possibly because of the limitations of temporal resolution and precision inherent in the snow course data. Low elevation precipitation appears to be a reasonable index of high elevation precipitation.

A runoff model using a distributed snow routine and a lumped transformation routine was developed for vegetative and terrain conditions in South Island catchments. The model overestimated runoff, probably because of significant subsurface losses from Camp Stream catchment. Snow accumulation was reproduced reasonably well in the elevation zones above 1500 m, but between 1100 m and 1500 m many snow events were misclassified because of the inadequacy of daily temperature as a rain-snow discriminator. A spring melt event was simulated using observed snow line

elevations rather than simulated snow cover. An index energy budget melt routine which incorporates an index of regional circulation provided a better reproduction of runoff variations than did a simple temperature index. Some problems were encountered in transforming surface water inputs into runoff. These problems could be caused by improper specification of the runoff parameters, or, more fundamentally, by the inadequacy of a lumped transformation routine in situations where runoff sources and mechanisms vary from event to event.

Based upon estimates of total basin precipitation and the relationship between snow accumulation and annual precipitation, mean seasonal snow accumulation in the Waimakariri catchment is estimated at 100 to 150 mm, or roughly twenty to thirty percent of the streamflow during October and November. However, snow accumulation in a given year may be up to twice the mean value. The impact of snow cover on a basin's streamflow pattern depends upon its hypsography. Rivers such as the Rakaia, which have a greater portion of their catchment above the seasonal snow line, will have a greater seasonal snow storage influence. The magnitude of snow storage and release apears to be significant enough to require inclusion into streamflow models of rivers draining mountainous catchments.

The existing data base is insufficient to define frequency-magnitude-duration characteristics of snowmelt. Energy budget estimates of daily melt totals suggest that melt can range at least up to 100 $mm \cdot d^{-1}$, which is roughly equal to the one year return period

twenty-four hour rainfall at Arthur's Pass (Tomlinson, 1980) or the two year rainfall at Craigieburn Forest (NZMS, 1980). The magnitude of snowmelt during heavy rain is uncertain, but available evidence indicates that it may vary with position with respect to the Main Divide. Anderton and Chinn (1978) found that 62 mm of melt occurred during a 400 mm rainfall at a west coast site, while analysis of climatic data at SB indicates that depressed temperatures during heavy rain may limit snowmelt there. These differences may be caused by systematic geographic variation in storm types producing heavy precipitation during rain-on-snow events. Wind speed rather than air temperature appears to be the probable major limit to snowmelt rates in the transient snow zone, but analysis of one event suggests that snowmelt can contribute to storm runoff during heavy rain.

7.2 SUGGESTIONS FOR FUTURE RESEARCH

Through the course of this study many gaps in knowledge concerning the environment of the Southern Alps became apparent. Basic climatological data are lacking, particularly for the alpine areas near and west of the Main Divide. Air temperature in the alpine zone is a crucial variable for snow hydrological studies because of its relationships to the phase of precipitation and the energy available for melt. Lack of this sort of data precluded even a superficial attempt to assess long term features of snow

hydrological processes in this region. Data collected from a site such as TB would be valuable not only for hydrological purposes, but also for meteorological and ecological investigations and avalanche forecasting.

More work is required on hydrological processes in the Southern Alps. Several distinct hydrological regions exist within the Alps and adjacent ranges, and a better understanding of the processes within these regions would increase the efficiency of regional prediction methods. Evaporation is an important hydrological component in the eastern portions of the South Island high country, but little is known about its magnitude or variability. The magnitude of subsurface losses from mountain catchments is not known, although model results in Camp Stream indicate that such losses may represent an important component of the water balance. Investigation into runoff processes, particularly in scree basins, would find application in understanding streamflow generation and erosion. Very little is known about the control of soil moisture conditions on rainfall-runoff relationships, although the modelling exercise in Camp Stream suggests they may be important. The range of environmental processes operating in the South Island mountain regions makes them a challenging and rewarding natural laboratory.

The thrust of the present study has been primarily exploratory, but the results have implications for research approaches. Much of the previous snow hydrological research in New Zealand concentrated on

defining the magnitude of the seasonal snow resource, usually through a basin water balance approach. The temporal and spatial lumping inherent in such approaches limits the amount of information that can be derived, particularly in view of the elevational variation of snow storage characteristics. Basin outflow by itself carries no information on the spatial or temporal origin of runoff, and the commonly-used monthly time frame yields no information concerning the transient snow zone, where snowmelt may have significance for flood generation. Future research in New Zealand will have to address the great spatial and temporal variability of snow hydrological processes.

One approach to the spatial variability problem is to conduct "point" studies of processes within small basins. For example, TB represents a basin lying entirely within the lower seasonal snow zone of western Canterbury, while Hut Creek lies entirely within the transient snow zone of eastern Canterbury. Results from such studies could be synthesized to understand the snow hydrology of larger catchments.

Another approach is the use of conceptual runoff models such as that developed in chapter five, which are essentially sequential water balance models with as fine a temporal and spatial resolution as data availability and quality will allow. These models have potential as tools for snow investigations in South Island catchments. They can be used for assessing snowmelt contributions to streamflow in both water resources applications and real-time flood forecasting.

Further efforts should be made to apply a conceptual model to catchments like Camp Stream, where snow has a marked impact on streamflow.

In the particular case of Camp Stream, some work should concentrate on the reasons for the volume errors. It may be that the scheme for estimating evaporation needs alteration. If subsurface flow is the cause of losses, the transformation routine could be amended to include a subsurface discharge component. Meteorological data at a finer time scale are available on chart records in the Craigieburn Range, and should be used in further model testing. Distributing the soil moisture representation should be attempted. Methods for incorporating external snow cover observations, either ground-based or remotely-sensed, should be developed.

Model application should be extended to the major glacial catchments, such as those in the Mount Cook region, where ice- and snowmelt are important for hydro-electric power generation. Little work appears to have been carried out since Anderton's (1974) promising initial water balance and storage index study in the Pukaki catchment. Hydrological modelling of glacierized catchments presents many problems which are not yet solved, though many regions in Asia and other parts of the world depend upon glacial catchments for water supply.

The climatic characteristics of the South Island mountain regions have important implications for appropriate methodology and logistics of future

research. Snowmelt studies must be designed to collect data with a high temporal resolution when required throughout the months of June to December, because of the unpredictable, irregular and often fleeting nature of melt events. Meteorological and runoff data should have a temporal resolution of at least an hour, and changes in snow depth, density and/or water equivalent at least a day, depending upon whether manual or automatic methods are used. These requirements demand either relatively sophisticated instrumentation and data-logging capability or intensive manual observations. Melt events often coincide with strong winds and driving rain, while extreme riming is common at alpine sites during winter. Both the instrumentation and observers engaged in snowmelt research must be carefully protected from the harsh conditions in the Southern Alps, and should be as robust as possible while maintaining the required level of accuracy.

The possibility of flood runoff being augmented by melt during heavy rain requires investigation. This augmentation may be limited by the snow-covered area in large catchments, as it was in the Pomahaka River in Central Otago in 1978 (Fitzharris et al., 1980). However, ski field, highway and other development in mountain areas involves bridge construction over and culvert emplacement in mountain streams. On these streams, the limit to snowmelt contributions could be snowmelt rates rather than coverage. The assessment of potential snowmelt inputs for design purposes requires

both the collection of climatological data and the development of suitable melt indices.

The energy balance aproach could be used to estimate melt at sites where wind speed, temperature, humidity and solar radiation are measured. However, input data for most practical applications are usually limited, and index methods which use incomplete data and rest upon assumptions are required. As demonstrated in chapter three, differences in snowmelt climate across the Alps imply that separate assumptions are appropriate for different sites, especially concerning the role of latent heat inputs. The importance of turbulent exchange and the results from chapter five indicate that snowmelt indices need to include a variable related to wind speed. Such a variable could be wind speed measured at a point, a pressure difference index similar to that used in chapters three and five, an upper air wind speed derived from radiosonde ascents or upper air pressure analyses, or output from a numerical wind model.

Snowmelt models could be calibrated using measured ablation or runoff data, as was done in chapter five. However, parameter values derived in such a way would be local values, applicable only within the basin or at the site for which they were derived. Studies of the spatial variability of melt would be required to define the domain of applicability of empirical coefficients.

A related problem is the difficulty involved in extrapolating input data to the site of interest. Temperature and humidity vary mainly with elevation,

particularly when the ground is snow-covered. A point measurement of these quantities above the snow line should be representative of a larger area. However, wind speed is highly variable, and a point measurement of wind speed may not be representative beyond that site. Tesche and Yocke (1976) have discussed the use of inexpensive kinematic wind models for use in mountainous terrain. Such models may have promise in indicating at least the regional variability of wind speed and, hence, turbulent exchange relative to a point, if not the actual magnitude. Quantifying wind speed and turbulent exchange in mountainous environments is an important and fundamental problem. Any approaches found successful in New Zealand would have application elsewhere.

Further work should be carried out on the thermal and hydrological properties of snow cover and their regional variability. The heterogeneous snow pack structure of the Craigieburn Range makes it a good site in which to investigate heat and mass transfers in layered snow. Although water movement in snow may not have much impact upon streamflow generation in many cases, an understanding of the variability of snow pack structure and its hydrological properties may improve efforts at regional avalanche forecasting.

The implementation of most of these suggestions would require the expansion and integration of the hydrological and climatological data collection networks. In particular, further climatological data should be collected in the mountain catchments which

are presently gauged. Recently, a greater effort has been made to collect mountain meteorological data (I. Miller, pers. comm.). However, much of this data is collected for purposes of avalanche forecasting schemes, and often is discontinued before the major spring melt periods and not carried through summer. Greater cooperation is required between the agencies which are responsible for the collection of hydrological and meteorological data to maximize the value of data, which are expensive to collect in the mountain regions. An appropriate action may be the setting-up of an integrated committee on alpine studies, which would coordinate the research and data collection efforts of the Ministry of Works and Development, the N.Z. Meteorological Service, Catchment Boards and University and other workers.

REFERENCES

Anderson, E.A. 1973. National Weather Service river forecast system - snow accumulation and ablation model, NOAA Tech. Memo. No. NWS 17. U.S. Department of Commerce, Washington, D.C.

Anderson, E.A. 1976. A point energy and mass balance model of a snow cover, NOAA Tech. Rep. No. NWS 19. U.S. Department of Commerce, Washington, D.C.

Anderson, E.A. 1979. Streamflow simulation models for use on snow covered watersheds. Modeling of Snowcover Runoff (S.C. Colbeck and M. Ray, ed.): 336-50. U.S. Army Cold Regions Research and Engineering Laboratory, Hanover, New Hampshire.

Anderton, P.W. 1973. The significance of perennial snow and ice to the water resources of the South Island, New Zealand. J. Hydrol. (N.Z.) 12: 6-18.

Anderton, P.W. 1974. Estimation of snow storage and melt in the catchment of Lake Pukaki. Presented at: N.Z. Hydrological Society Annual Symposium, Dunedin.

Anderton, P.W. and Chinn, T.J. 1978. Ivory Glacier, New Zealand, an I.H.D. representative basin study. J. Glaciol. 20: 67-84.

Archer, A.C. 1970. Studies of snow characteristics in the north-eastern Ben Ohau Mountains, New Zealand. J. Hydrol. (N.Z.) 9: 4-21.

Arnfield, A.J. 1979. Evaluation of empirical expressions for the estimation of hourly and daily totals of atmospheric longwave emission under all sky conditions.

Quart. J. Roy. Meteor. Soc. 105: 1041-52.

Bagchi, A.K. 1982. Orographic variation of precipitation in a high-rise Himalayan basin. Hydrological aspects of alpine and high-mountain areas, IAHS Publ. No. 138: 3-9. International Association of Hydrological Sciences, Washington, D.C.

Bagchi, A.K. 1983. Areal value of degree-day factor. Hydrol. Sci. J. 28: 499-511.

Beaudry, P. and Golding, D.L. 1983. Snowmelt during rain-on-snow in coastal British Columbia. Proceedings, 51st Western Snow Conference: 55-66.

Beaumont, R.T. 1965. Mount Hood pressure pillow snow gage. J. Appl. Meteor. 4: 626-31.

Bengtsson, L. 1980. Evaporation from a snow cover: review and discussion of measurements. Nordic Hydrol. 11: 221-34.

Bengtsson, L. 1982. The importance of refreezing on the diurnal snowmelt cycle with application to a Northern Swedish catchment. Nordic Hydrol. 13: 1-12.

Bergman, J.A. 1983. Hydrological response of central Sierra Nevada snowpacks to rainfall. Proceedings, 51st Western Snow Conference: 141-4.

Bergström, S. 1975. The development of a snow routine for the HBV-2 model. Nordic Hydrol. 6: 73-92.

Bergström, S. 1979. Springflood forecasting by conceptual models in Sweden. Modeling of Snowcover Runoff (S.C. Colbeck and M. Ray, ed.): 397-405. U.S. Army Cold Regions Research and Engineering Laboratory, Hanover, New Hampshire.

Bergström, S. and Forsman, A. 1973. Development of a

conceptual deterministic rainfall-runoff model. Nordic Hydrol. 4: 147-70.

Bergström, S. and Jönsson, S. 1976. The application of the HBV runoff model to the Filefjell research basin, Rapporter Nr RHO 5. Swedish Meteorological and Hydrological Institute, Norrkoping.

Bergström, S. and Sandberg, G. 1983. Simulation of groundwater response by conceptual models - three case studies. Nordic Hydrol. 14: 71-84.

Berkowicz, R. and Prahm, L.P. 1982. Evaluation of the profile method for estimation of surface fluxes of momentum and heat. Atmos. Environ. 16: 2809-19.

Bernard, M. and Wilson, W.T. 1941. A new technique for the determination of heat necessary to melt snow. Trans. Am. Geophys. Union 22: 178-81.

Bhatia, P.K., Bergström, S. and Persson, M. 1984. Application of the distributed HBV-6 model to the upper Narmada basin in India, Rapporter Nr RHO 35. Swedish Meteorological and Hydrological Institute, Norrkoping.

Bowden, M.J. 1974. The Water Resources of the Waiau Catchment. North Canterbury Catchment Board, Christchurch.

Bowden, M.J. 1977. The Water Resources of the Hurunui River. North Canterbury Catchment and Regional Water Board, Christchurch.

Bowden, M.J. 1983. Ice and snowfields. Rakaia Resource Report, Vol. 2: 7-10. North Canterbury Catchment and Regional Water Board, Christchurch.

Bradley, E.F. 1980. An experimental study of the profiles of wind speed, shearing stress and turbulence at the

crest of a large hill. Quart. J. Roy. Meteor. Soc. 106: 101-23.

Braun, L.N. and Zuidema, P.K. 1982. Modelling snowmelt during advection-melt situations in a small basin (Reitholzbach). Presented at: International symposium on hydrological research basins and their use in water resources planning, 21-23 September, Berne, Switzerland.

Braun, L.N. (in prep.). Simulation of snowmelt runoff in the lowland and low alpine zones of Switzerland. Ph.D. thesis, Eidgenossische Technische Hochschule, Zurich.

Brutsaert, W. and Maudsley, J.A. 1976. The applicability of planetary boundary layer theory to calculate regional evapotranspiration. Water Resour. Res. 12: 852-8.

Burrows, C.J. 1976. Exceptional snow storms in the South Island High Country. Tussock Grasslands and Mountain Lands Institute Review 32: 43-7.

Carroll, T. 1979. A procedure to incorporate snow course data into the NWS river forecast system. Modeling of Snow Cover Runoff (S.C. Colbeck and M. Ray, ed.): 351-8. U.S. Army Cold Regions Research and Engineering Laboratory, Hanover, New Hampshire.

Charbonneau, R., Lardeau, J.-P. and Obled, C. 1981. Problems of modelling a high mountainous basin with predominant snow yield. Hydrol. Sci. Bull. 26: 345-61.

Chinn, T.J.H. 1969. Snow survey techniques in the Waitaki catchment, South Canterbury. J. Hydrol. (N.Z.) 8: 68-76.

Chinn, T.J. 1981. Snowfall variations, hazards and snowmelt. Presented at: Mountain Lands Workshop, 11-12 November 1981, Lincoln College, Lincoln.

Chinn, T.J. and Whitehouse, I.E. 1980. Glacier snow line variations in the Southern Alps, New Zealand. World glacier inventory, IAHS Publ. No. 126: 219-28. International Association of Hydrological Sciences, Washington, D.C.

Christner, J. and Harr, R.D. 1982. Peak streamflows from the transient snow zone, western Cascades, Oregon. Proceedings, 50th Western Snow Conference: 27-38.

Church, J.E. 1933. Snow surveying, principles and possibilities. Geog. Rev. 23: 539-60.

Colbeck, S.C. 1972. A theory of water percolation in snow. J. Glaciol. 11: 369-85.

Colbeck, S.C. 1973. Theory of metamorphism of wet snow, Res. Rep. 313. Cold Regions Research and Engineering Laboratory, Hanover, New Hampshire.

Colbeck, S.C. 1974. The capillary effects on water percolation in homogeneous snow. J. Glaciol. 13: 85-97.

Colbeck, S.C. 1975. A theory for water flow through a layered snowpack. Water Resour. Res. 11: 261-66.

Colbeck, S.C. 1976. An analysis of water flow in dry snow. Water Resour. Res. 12: 523-7.

Colbeck, S.C. 1978a. The physical aspects of water flow through snow. Advances in Hydrosciences 11: 165-206.

Colbeck, S.C. 1978b. The difficulties of measuring the water saturation and porosity of snow. J. Glaciol. 20: 189-201.

Colbeck, S.C. 1979a. Water flow through heterogeneous snow. Cold Regions Sci. Tech. 1: 37-45.

Colbeck, S.C. 1979b. Introductory remarks. Modeling of Snow Cover Runoff (S.C. Colbeck and M. Ray, ed.): 1-2. U.S. Army Cold Regions Research and Engineering Laboratory, Hanover, New Hampshire.

Colbeck, S.C. 1982. An overview of seasonal snow metamorphism. Rev. Geophys. Space Phys. 20: 45-61.

Colbeck, S.C. and Anderson, E.A. 1982. The permeability of a melting snow cover. Water Resour. Res. 18: 904-9.

Colbeck, S.C., Anderson, E.A., Bisell, V.C., Crook, A.G., Male, D.H., Slaughter, C.W. and Wiesnet, D.R. 1979. Snow accumulation, distribution, melt and runoff. EOS, Trans. Am. Geophys. Union 60: 465-8.

Collins, E.H. 1934. Relationship of degree-days above freezing to runoff. Trans. Am. Geophys. Union 15: 624-9.

Cooley, K.R. and Robertson, D.C. 1983. Monitoring a rain-on-snow event. Proceedings, 51st Western Snow Conference: 19-26.

Dalmer, E. 1971. The Waimakariri as a Water Resource. North Canterbury Catchment Board, Christchurch.

Deardorff, J.W. 1968. Dependence of air-sea transfer coefficients on bulk stability. J. Geophys. Res. 73: 2549-57.

de la Casiniere, A.C. 1974. Heat exchange over a melting snow surface. J. Glaciol. 13: 55-72.

de Quervain, M. 1973. Snow structure, heat and mass flux through snow. The role of snow and ice in hydrology,

Proceedings of the Banff Symposia 1972: 203-26. UNESCO-WMO-IASH, Paris.

Dreaver, K.R. and Hutchinson, P. 1974. Random and systematic errors in precipitation at an exposed site. J. Hydrol. (N.Z.) 13: 54-63.

Dunne, T. 1983. Relation of field studies and modeling in the prediction of storm runoff. J. Hydrol. 65: 25-48.

Dunne, T. and Price, A.G. 1975. Estimating daily net radiation over a snowpack. Climatol. Bull. 18: 40-8.

Dunne, T., Price, A.G. and Colbeck, S.C. 1976. The generation of runoff from subarctic snowpacks. Water Resour. Res. 12: 677-85.

Ebaugh, W.P. and DeWalle, D.R. 1977. Retention and transmission of liquid water in fresh snow. Preprints, Second Conference on Hydrometeorology: 255-60. American Meteorological Society and Canadian Meteorological and Oceanographic Society.

Ferguson, R.I. 1984. Magnitude and modelling of snowmelt runoff in the Cairngorm mountains, Scotland. Hydrol. Sci. J. 29: 49-62.

Ffolliott, P.F. and Brooks, K.N. 1983. Rain-on-snow flood event in central Arizona. Proceedings, 51st Western Snow Conference: 130-8.

Fitzgibbon, J.E. 1977. Generation of the snowmelt flood in a subarctic area, Schefferville, Quebec. Unpublished Ph.D. thesis, McGill University, Montreal.

Fitzgibbon, J.E. and Dunne, T. 1980. Snowmelt prediction in a subarctic drainage area. Nordic Hydrol. 11: 243-54.

Fitzgibbon, J.E. and Dunne, T. 1983. Influence of subarctic vegetation cover on snowmelt. Phys. Geog. 4: 61-70.

Fitzharris, B.B. 1976. Spatial variations in snow accumulation on Central Otago Mountains. Proceedings, N.Z. Hydrological Society Annual Symposium (Rotorua): 165-77.

Fitzharris, B.B. 1977. Estimating maximum snow storage capacity of central Otago terrain. Presented at: N.Z. Hydrological Society Annual Symposium, 22-24 November, Christchurch.

Fitzharris, B.B. 1978. Problems in estimating snow accumulation with elevation on New Zealand mountains. J. Hydrol. (N.Z.) 17: 78-90.

Fitzharris, B.B. 1979. Snow hydrology. Physical Hydrology - New Zealand Experience (D.L. Murray and P. Ackroyd, ed.): 23-43. N.Z. Hydrological Society, Wellington.

Fitzharris, B.B. and Grimmond, C.S.B. 1982. Assessing snow storage and melt in a New Zealand mountain environment. Hydrological aspects of alpine and high mountain areas, IAHS Publ. No. 138: 161-8. International Association of Hydrological Sciences, Washington, D.C.

Fitzharris, B.B., Stewart, D. and Hutchinson, W. 1980. Contribution of snowmelt to the October 1978 flood of the Pomahaka and Fraser Rivers, Otago. J. Hydrol. (N.Z.) 19: 84-93.

Fitzsimmons, S. 1983. Modelling snowmelt runoff in Camp Stream catchment. Unpublished B.Sc. (Hons) project, University of Canterbury, Christchurch.

Fletcher, N.H. 1962. The Physics of Rainclouds. Cambridge University Press.

Fohn, P.M.B. 1973. Short-term snow melt and ablation derived from heat- and mass-balance measurements. J. Glaciol. 12: 275-89.

Gerdel, R.W. 1954. The transmission of water through snow. Trans. Am. Geophys. Union 35: 475-85.

Gillies, A.J. 1964. Review of snow survey methods, and snow surveys in the Fraser catchment, Central Otago. J. Hydrol. (N.Z.) 3: 3-16.

Goring, D.G. 1984. Flood routing by a linear systems technique. J. Hydrol. 69: 59-76.

Granberg, H.B. 1979. Measured thermal regime within a snow cover just before the onset of melt. Modeling of Snowcover Runoff (S.C. Colbeck and M. Ray, ed.): 279-87. U.S. Army Cold Regions Research and Engineering Laboratory, Hanover, New Hampshire.

Granger, R.J. and Male, D.H. 1978. Melting of a prairie snowpack. J. Appl. Meteor. 17: 1833-42.

Griffiths, G.A. and McSaveney, M.J. 1983a. Distribution of mean annual precipitation across some steepland regions of New Zealand. N.Z. J. Sci. 26: 197-209.

Griffiths, G.A. and McSaveney, M.J. 1983b. Hydrology of a basin with extreme rainfalls - Cropp River, New Zealand. N.Z. J. Sci. 26: 293-306.

Grimmond, C.S.B. 1980. Runoff from seasonal snow in the Fraser catchment, Central Otago. Unpublished B.Sc. Hons dissertation, University of Otago, Dunedin.

Halberstam, I. and Schieldge, J. 1979. Interactions between the atmospheric boundary layer and a snow

surface, part I. Modelling. Modeling of Snow Cover Runoff (S.C. Colbeck and M. Ray, ed.): 154-60. U.S. Army Cold Regions Research and Engineering Laboratory, Hanover, New Hampshire.

Harding, F.B. 1972. Micro-meteorological investigations over a mid-latitude temperate glacier - the Ivory Glacier. Unpublished M.A. thesis, University of Canterbury, Christchurch.

Harr, R.D. 1981. Some characteristics and consequences of snowmelt during rainfall in Western Oregon. J. Hydrol. 53: 277-304.

Harr, R.D. and Berris, S.N. 1983. Snow accumulation and subsequent melt during rainfall in forested and clearcut plots in western Oregon. Proceedings, 51st Western Snow Conference: 38-45.

Hayward, J.A. 1967. The Waimakariri catchment, Special Publication No. 5. Tussock Grasslands and Mountain Lands Institute, Lincoln.

Hendrick, R.L., DeAngelis, R.J. and Dingman, S.L. 1979. The role of elevation in determining spatial distribution of precipitation, snow, and water input at Mt. Mansfield, Vermont. Modeling of Snow Cover Runoff (S.C. Colbeck and M. Ray, ed.): 63-70. U.S. Army Cold Regions Research and Engineering Laboratory, Hanover, New Hampshire.

Hendrick, R.L., Filgate, B.D. and Adams, W.D. 1971. Application of environmental analysis to watershed snowmelt. J. Appl. Meteor. 10: 418-29.

Heron, R. and Woo, M.-K. 1978. Snowmelt computations for a high Arctic site. Proceedings, 35th Eastern Snow

Conference: 162-72.

Hessel, J.W.D. 1983. Climatic effects on the recession of the Franz Josef Glacier. N.Z. J. Sci. 26: 315-20.

Hewlett, J.D. and Hibbert, A.R. 1967. Factors affecting the response of small watersheds to precipitation in humid areas. Forest Hydrology (W.E. Sopper and H.W. Lull, ed.): 275-90. Pergamon, Oxford.

Hickman, J.S. 1972. Estimates of snowline from meteorological satellite pictures 1968-1971. N.Z. Meteorological Service Research Report.

Ho, Chiuh Wah 1982. Snow avalanche studies in the Mount Cook Region. Unpublished M.Sc. thesis, University of Otago, Dunedin.

Hogg, I.G., Paren, J.G. and Timmis, R.J. 1982. Summer heat and ice balances on Hodges Glacier, South Georgia, Falkland Islands Dependencies. J. Glaciol. 28: 221-38.

Huber, A.L. 1983. A comparison of several snow accumulation and ablation algorithms used in watershed modeling. Proceedings, 51st Western Snow Conference: 76-88.

Hubley, R.C. 1954. The problem of short period measurements of snow ablation. J. Glaciol. 2: 437-40.

Hughes, J.G. 1976. The snow of August 1973, Special Publication No. 10. Tussock Grasslands and Mountain Lands Institute, Lincoln.

Jackson, P.S. and Hunt, J.C.R. 1975. Turbulent wind flow over a low hill. Quart. J. Roy. Meteor. Soc. 101: 929-55.

Jensen, N.O. and Peterson, E.W. 1978. On the escarpment wind profile. Quart. J. Roy. Meteor. Soc. 104: 719-28.

Johnson, P. and Archer, D.R. 1973. The significance of snow in Britain. The role of snow and ice in hydrology, Proceedings of the Banff Symposia 1972: 1098-1110. UNESCO-WMO-IASH, Paris.

Jordan, R.P. 1978. The snowmelt hydrology of a small alpine watershed. Unpublished M.Sc. thesis, University of British Columbia, Vancouver, Canada.

Jordan, R.P. 1983. Meltwater movement in a deep snowpack, 1, field observations. Water Resour. Res. 19: 971-8.

Kojima, K., Kobayashi, D., Aburakawa, H., Ishimoto, K., Takahashi, S. and Fujii, T. 1973. Studies of snowmelt, runoff and heat balance in a small drainage area in Moshiri, Hokkaido, III. (The influence of rainy weather). Low Temp. Sci., Ser. A 31: 159-77. (Japanese with English summary).

Kraus, H. 1973. Energy exchange at air-ice interface. The role of snow and ice in hydrology, Proceedings of the Banff Symposia 1972: 128-51. UNESCO-WMO-IASH, Paris.

Kuz'min, P.P. 1972. Melting of Snow Cover. Israel Program for Scientific Translations, Jerusalem.

LaChapelle, E.R. 1979. An assessment of avalanche problems in New Zealand, Avalanche Committee Report No. 2. N.Z. Mountain Safety Council, Wellington.

Lang, H. 1981. Is evaporation an important component in high alpine hydrology? Nordic Hydrol. 12: 217-24.

Lemmela, R. 1973. Measurements of evaporation-condensation and melting from a snow cover. The role of snow and

ice in hydrology, Proceedings of the Banff Symposia 1972: 670-9. UNESCO-WMO-IASH, Paris.

Light, P. 1941. Analysis of high rates of snow melting. Trans. Am. Geophys. Union 22: 195-205.

Linsley, R.K., Kohler, M.A. and Paulhus, J.L.H. 1949. Applied Hydrology. McGraw-Hill, New York.

Lowe, P.R. 1977. An approximating polynomial for the computation of saturation vapour pressure. J. Appl. Meteor. 16: 100-3.

Lundquist, D. 1982. Modelling runoff from a glacierized basin. Hydrological aspects of alpine and high-mountain areas, IAHS Publ. No. 138: 131-6. International Association of Hydrological Sciences, Washington, D.C.

Male, D.H. and Granger, R.J. 1981. Snow surface energy exchange. Water Resour. Res. 17: 609-27.

Male, D.H. and Gray, D.M. 1981. Snowcover ablation and runoff. Handbook of Snow (D.M. Gray and D.H. Male, ed.): 360-426. Pergamon, Toronto.

Marcus, M.G. and Moore, R.D. 1983. Snowpack structure and climate, Mount Egmont, New Zealand. Weather and Climate 3: 42-51.

Marcus, M.G., Moore, R.D. and Owens, I.F. (in prep.) Energy balance and ablation, lower Franz Josef Glacier, South Westland, New Zealand.

Marks, D. 1979. An atmospheric radiation model for general alpine application. Modeling of Snowcover Runoff (S.C. Colbeck and M. Ray, ed.): 101-124. U.S. Army Cold Regions Research and Engineering Laboratory, Hanover, New Hampshire.

Martinec, J. 1975. Snowmelt-runoff model for streamflow forecasts. Nordic Hydrol. 6: 145-53.

Martinec, J. and de Quervain, M.R. 1975. The effect of snow displacement by avalanches on snow melt and runoff. Interdisciplinary studies of snow and ice in mountain regions, IAHS Publ. No. 104: 364-77. International Association of Hydrological Sciences, Washington.

McCracken, I.J. 1980. Mountain climate in the Craigieburn Range, New Zealand. Mountain environments and subalpine tree growth, Technical Paper No. 70: 41-60. N.Z. Forest Service, Forest Research Institute, Christchurch.

McGregor, G.R. (in prep.). Snow avalanche phenomena in the Craigieburn Range, New Zealand. Ph.D. thesis, University of Canterbury, Christchurch.

McGurk, B.J. 1983. Snow temperature profiles in the central Sierra Nevada. Proceedings, 51st Western Snow Conference: 9-18.

McKay, D.C. and Thurtell, G.W. 1978. Measurements of the energy fluxes involved in the energy budget of a snow cover. J. Appl. Meteor. 17: 339-49.

McNulty, D. and Fitzharris, B.B. 1980. Winter avalanche activity and weather in a Canterbury alpine basin. N.Z. J. Geol. Geophys. 23: 103-11.

Ministry of Works 1968. Camp Stream, I.H.D. experimental basin no. 12, Annual Hydrological Research Report No. 1. Water and Soil Division, Wellington.

Ministry of Works 1970. Camp Stream, I.H.D. experimental basin no. 12, Annual Hydrological Research Report No.

2. Water and Soil Division, Wellington.

Monteith, J.L. 1957. Dew. Quart. J. Roy. Meteor. Soc. 83: 322-41.

Moore, R.D. 1983. On the use of bulk aerodynamic formulae over melting snow. Nordic Hydrol. 14: 193-206.

Morris, J.Y. 1965. Climate investigations in the Craigieburn Range. N.Z. J. Sci. 8: 556-82.

Morris, J.Y. and O'Loughlin, C.L. 1965. Snow investigations in the Craigieburn Range. J. Hydrol. (N.Z.) 4: 2-16.

Mosley, M.P. 1979. Streamflow generation in a forested watershed, New Zealand. Water Resour. Res. 15: 795-806.

Mosley, M.P. 1982. Subsurface flow velocities through selected forest soils, South Island New Zealand. J. Hydrol. 55: 65-92.

Nash, J.E. and Sutcliffe, J.V. 1970. River flow forecasting through conceptual models: Part I - A discussion of principles. J. Hydrol. 10: 282-90.

Neale, A.A. and Thompson, G.H. 1977. Meteorological conditions accompanying heavy snowfalls in Southern New Zealand, Technical Information Circular 155. N.Z. Meteorological Service, Wellington.

NZMS (N.Z. Meteorological Service) 1980. Depth-duration-frequency tables based on daily rainfalls, Miscellaneous Publication No. 162 Supplement 1. N.Z. Meteorological Service, Wellington.

Obled, Ch. and Harder, H. 1979. A review of snowmelt in the mountain environment. Modeling of Snowcover Runoff

(S.C. Colbeck and M. Ray, ed.): 179-204. U.S. Army Cold Regions Research and Engineering Laboratory, Hanover, New Hampshire.

Ohmura, A. 1972. Ocean-tundra-glacier interaction model. International Geography 1972 (W.P. Adams and F.M. Helleiner, ed.): 919-20. University of Toronto Press, Toronto.

O'Loughlin, C.L. 1964. Notes on the occurrence of concrete frost and other forms of soil-ice in Canterbury beech forests, Protection Forestry Report No. 5. N.Z. Forest Service, Forest and Range Experiment Station, Rangiora (unpublished).

O'Loughlin, C.L. 1965. The occurrence, classification and physical properties of unvegetated scree accumulations in the Craigieburn Range. Protection Forestry Report No. 19. N.Z. Forest Service, Forest and Range Experiment Station, Rangiora (unpublished).

O'Loughlin, C.L. 1969a. Further snow investigations in the Craigieburn Range, Protection Forestry Report No. 52. N.Z. Forest Service, Forest and Range Experiment Station, Rangiora (unpublished).

O'Loughlin, C.L. 1969b. The influence of snow on streamflow. Watershed management, part 1, Lincoln Papers in Water Resources No. 8: 112-27. Lincoln College, Lincoln.

Owens, I., McGregor, G. and Prowse, T. 1983. Snow avalanche hazards in the Canterbury high country. Canterbury at the crossroads, Miscellaneous Series No. 8 (R.D. Bedford and A.P. Sturman, ed.): 166-81. N.Z. Geographical Society, Christchurch.

Pearce, A.J. and McKerchar, A.I. 1979. Upstream generation of storm runoff. Physical Hydrology - New Zealand Experience (D.L. Murray and P. Ackroyd, ed.): 165-93. N.Z. Hydrological Society, Wellington.

Pierson, T.C. 1982. Classification and hydrological characteristics of scree slope deposits in the northern Craigieburn Range, New Zealand. J. Hydrol. (N.Z.) 21: 34-60.

Pilgrim, D.H., Cordery, I. and Baron, B.C. 1982. Effects of catchment size on runoff relationships. J. Hydrol. 58: 205-21.

Price, A.G. 1977. Snowmelt runoff processes in a subarctic area, Climatology Research Series No. 10. McGill University, Montreal.

Price, A.G. and Dunne, T. 1976. Energy balance computations of snowmelt in a subarctic area. Water Resour. Res. 12: 686-94.

Price, A.G., Hendrie, L.K. and Dunne, T. 1979. Controls on the production of snowmelt runoff. Modeling of Snow Cover Runoff (S.C. Colbeck and M. Ray, ed.): 257-68. U.S. Army Cold Regions Research and Engineering Laboratory, Hanover, New Hampshire.

Prowse, T.D. 1981. The snow environment of the Craigieburn Range. Unpublished Ph.D. thesis, University of Canterbury, Christchurch, New Zealand.

Prowse, T.D. and Owens, I.F. 1982. Energy balance over melting snow, Craigieburn Range, New Zealand. J. Hydrol. (N.Z.) 21: 133-47.

Prowse, T.D. and Owens, I.F. 1984. Characteristics of snowfalls, snow metamorphism, and snowpack structure

with implications for avalanching, Craigieburn Range, New Zealand. Arctic and Alpine Res. 16: 107-18.

Rango, A. and Martinec, J. 1979. Application of a snowmelt-runoff model using Landsat data. Nordic Hydrol. 12: 265-74.

Rowe, L.K. 1975. Rainfall interception by mountain beech. N.Z. J. For. Sci. 5: 45-61.

Rowe, L.K. 1983. Rainfall interception by an evergreen beech forest, Nelson, New Zealand. J. Hydrol. 66: 143-58.

Saelthun, N.R. 1979. Use of integrated hydrological models with distributed snowcover description for hydrological forecasting in Norway. Modeling of Snow Cover Runoff (S.C. Colbeck and M. Ray, ed.): 406-13. U.S. Army Cold Regions Research and Engineering Laboratory, Hanover, New Hampshire.

Saucier, W.J. 1955. Principles of Meteorological Analysis. University of Chicago Press, Chicago.

Sellers, W.D. 1965. Physical Climatology. University of Chicago Press, Chicago.

Shimizu, H. 1970. Air permeability of deposited snow. Low Temp. Sci. Ser. A. 22: 1-32. (Japanese with English summary).

Smith, J.L. 1974. Hydrology of warm snowpacks and their effects upon water delivery - some new concepts. Advanced Concepts and Techniques in the Study of Snow and Ice Resources: 76-89. American Academy of Science, Washington, D.C.

Smith, J.L. and Halverson, H.G. 1969. Hydrology of snow profiles obtained with the profiling snow gauge.

Proceedings, 37th Western Snow Conference: 41-8.

Sommerfeld, R.A. and LaChapelle, E.R. 1970. The classification of snow metamorphism. J. Glaciol. 9: 3-17.

Sorooshian, S. 1983. Surface water hydrology: on-line estimation. Rev. Geophys. Space Phys. 21: 706-21.

Speers, D., Kuehl, K. and Schermerhorn, V. 1979. Development of the operational snow band SSARR model. Modeling of Snow Cover Runoff (S.C. Colbeck and M. Ray, ed.): 369-78. U.S. Army Cold Regions Research and Engineering Laboratory, Hanover, New Hampshire.

Sturman, A.P. and Soons, J.M. 1983. Precipitation intensity and variablility at Chilton Valley near Cass, Southern Alps. Presented at: the joint meeting of the N.Z. Hydrological Society and the Meteorological Society of N.Z., 28 November to 2 December, Dunedin.

Sulahria, M. 1972. Prediction of water retentive capacity of high elevation snowpacks on the east side of the Sierra Nevada. Unpublished Ph.D. thesis, University of Nevada, Reno.

Svensson, S. 1977. A statistical study for automatic calibration of a conceptual runoff model, Rapporter Nr RHO 10. Swedish Meteorological and Hydrological Institute, Norrkoping.

Sverdrup, H.U. 1936. The eddy conductivity of the air over a smooth snow field. Geofys. Publ. 11: 1-69.

Taylor, C.H. and Pearce, A.J. 1982. Storm runoff processes and subcatchment characteristics in a New Zealand hill country catchment. Earth Surf. Proc. Landforms 7: 439-47.

Taylor, M.A. 1972. Assessment of a mathematical model for runoff prediction in New Zealand. Unpublished M.E. thesis, University of Canterbury, Christchurch.

Tesche, T.W. and Yocke, M.A. 1976. Application of numerical wind models to snow avalanche forecasting: theoretical considerations and preliminary investigations. Presented at: Avalanche Workship, November 1976, Banff, Canada.

Thomson, P.A. 1983. Report on the 10th July 1983 flood - Part A. Unpublished report for the Marlborough Catchment Board, Blenheim.

Tomlinson, A.I. 1970. The Canterbury snowfall of November 1967. N.Z. Geog. 26: 20-35.

Tomlinson, A.I. 1980. The frequency of high intensity rainfalls in New Zealand, Part I, Water and Soil Tech. Pub. No. 19. National Water and Soil Conservation Organisation, Wellington.

Trenberth, K.E. 1977. Relationships between inflow to Clutha Lakes, broad-scale atmospheric circulation parameters, and rainfall. N.Z. J. Sci. 20: 63-71.

Tucker, W.B. III and Colbeck, S.C. 1977. A computer routing of unsaturated flow through snow, Special Report 77-10. U.S. Army Cold Regions Research and Engineering Laboratory, New Hampshire.

USACE (U.S. Army Corps of Engineers) 1954. Analysis of January 1953 rain on snow observations at Central Sierra Snow Laboratory Soda Springs, California, Research Note No. 18. North Pacific Division, U.S. Army Corps of Engineers, Portland, Oregon.

USACE (U.S. Army Corps of Engineers) 1956. Snow Hydrology.

North Pacific Division, U.S. Army Corps of Engineers, Portland, Oregon.

USACE (U.S. Army Corps of Engineers) 1960. Runoff From Snowmelt. North Pacific Division, U.S. Army Corps of Engineers, Portland, Oregon.

Viessman, W., Knapp, J.W., Lewis, G.L. and Harbaugh, T.E. 1977. Introduction to Hydrology, 2nd Edition. Harper and Row, New York.

Wankiewicz, A. 1978. Water pressure in ripe snowpacks. Water Resour. Res. 14: 593-9.

Wankiewicz, A.C. 1979. A review of water movement in snow. Modeling of Snow Cover Runoff (S.C. Colbeck and M. Ray, ed.): 222-52. U.S. Army Cold Regions Research and Engineering Laboratory, New Hampshire.

Wankiewicz, A.C. and de Vries, J. 1978. An inexpensive tensiometer for snowmelt research. J. Glaciol. 20: 577-84.

Watt, J.P.C. 1979. Soil water: a catalogue, review, and commentary of New Zealand research and knowledge of water in New Zealand soils. Physical Hydrology - New Zealand Experience (D.L. Murray and P. Ackroyd, ed.): 44-83. N.Z. Hydrological Society, Wellington.

Waylen, P. 1982. Some characteristics and consequences of snowmelt during rainfall in western Oregon - a comment. J. Hydrol. 58: 185-8.

Webb, E.K. 1970. Profile relationships: the log-linear range and extension to strong stability. Quart. J. Roy. Meteor. Soc. 96: 67-90.

Weir, P.L. 1979. Topographic influences on snow accumulation at Mount Hutt. Unpublished M.Sc. thesis,

University of Canterbury, Christchurch.

Weir, P.L. 1983. Snowpack investigation, Craigieburn Range - winter 1983. Unpublished report for the Forest Research Institute, Christchurch.

Weir, P.L. and Owens, I.F. 1981. Snowpack structure at Mount Hutt, Canterbury, in 1979. N.Z. J. Sci. 24: 95-102.

Weisman, R.N. 1977. Snowmelt: a two-dimensional turbulent diffusion model. Water Resour. Res. 13: 337-42.

Woo, M.-K. 1972. A predictive model for snow storage in the temperate forest zone of the coastal mountains. Mountain Geomorphology (O. Slaymaker and H.J. MacPherson, ed.): 207-14. Tantalus, Vancouver.

Woo, M.-K. 1982. Snow hydrology of the high Arctic. Proceedings, 50th Western Snow Conference: 63-74.

Work, R.A., Stockwell, H.J., Freeman, T.J. and Beaumont, R.T. 1965. Accuracy of field snow surveys: western United States, including Alaska, Tech. Rep. No. 163. U.S. Army Cold Regions Research and Engineering Laboratory, Hanover, New Hampshire.

WMO (World Meteorological Organization) 1982. WMO project for the intercomparison of conceptual models of snowmelt runoff. Hydrological aspects of alpine and high mountain areas, IAHS Publ. No. 138: 193-202. International Association of Hydrological Sciences, Washington, D.C.

Yosida, Z. 1960. A calorimeter for measuring the free water content of wet snow. J. Glaciol. 3: 574-6.

Young, G.J. 1982. Hydrological relationships in a glacierized mountain basin. Hydrological aspects of

alpine and high-mountain areas, IAHS Publ. No. 138: 51-9. International Association of Hydrological Sciences, Washington, D.C.

Zuzel, J.F. and Cox, L.M. 1975. Relative importance of meteorological variables in snowmelt. Water Resour. Res. 11: 174-6.

Zuzel, J.F., Greenwalt, R.N. and Allmaras, R.R. 1983. Rain on snow: shallow transient snowpacks with frozen soils. Proceedings, 51st Western Snow Conference: 67-75.

Nordic Hydrology, 1983, 193-206

Appendix A - Discussion of bulk aerodynamic formulae

On the Use of Bulk Aerodynamic Formulae Over Melting Snow

R. Daniel Moore

Univ. of Canterbury, Christchurch, New Zealand

Bulk aerodynamic formulae which relate the turbulent exchanges of sensible and latent heat over melting snow to measurements of windspeed, temperature and humidity at one level can be derived from flux-gradient relationships and assumed log-linear profiles. Recent analyses of local advection over snow and wind flow over complex terrain suggest that the bulk aerodynamic formulae should apply in non-ideal field situations. The assumption that the scaling lengths for temperature and humidity equal the roughness length is problematic, since theoretical analyses indicate they should be much less than the roughness length. However, the effect of scale length inequality on the stability correction tends to compensate for the effect on the neutral-case transfer coefficient. Field experience indicates that the bulk aerodynamic formulae are adequate for use in energy balance estimates of daily or shorter term snowmelt.

Introduction

Hydrologists are often required to make estimates of snowmelt. The most rigorous method of calculating snowmelt at a point is through the energy balance, in which estimates or measurements are made of the energy exchanges at the snowpack interfaces. Generally, the net radiative exchange provides the greatest portion of the energy disposed of in melt (Male and Granger 1981). However, during weather conditions characterised by strong winds and warm, humid air, the sensible and latent heat fluxes dominate the snowpack energy budget, and produce the

highest short-term rates of melt (Hendrick, Filgate and Adams 1971; Light 1941). Thus, accurate and practical methods of evaluating these fluxes are required. The two most accurate methods of determining the turbulent fluxes are the eddy-correlation approach (McKay and Thurtell 1978) and detailed profile methods (de la Casiniere 1974). Unfortunately, both these methods require extensive and expensive instrumentation, and are not well suited to the conditions and environments often of interest to hydrologists. In addition, neither method is readily suitable for telemetry applications for real-time streamflow forecasting. In practice, therefore, hydrologists often resort to methods which require measurements of wind speed, temperature and humidity at one level and exploit the fact that the temperature and vapour pressure at a melting snow surface are 0°C and 6.11 mb.

One method for calculating the sensible and latent heat fluxes uses empirical wind functions (e.g., Anderson 1976). The wind function depends on stability, surface roughness and measurement height. The empirically-derived wind functions will represent the average surface and stability conditions prevailing during the calibration period, and will be biased. Anderson (1976) and Male and Gray (1981) attempted to compare coefficients derived by several workers by reducing the measurement levels to a standard height of 1 m. The choice of extrapolation formula is arbitrary, so comparisons cannot be conclusive. However, the comparisons indicate that the coefficients range greatly between environments, as would be expected.

Another method of estimating the turbulent exchanges over melting snow is the bulk aerodynamic method, which employs bulk transfer coefficients derived from flux-gradient relationships and semi-empirical profile forms for wind, temperature and humidity. These bulk transfer coefficients explicitly account for variable stability, surface conditions and measurement heights, and have been used by Anderson (1976), Price (1977), Heron and Woo (1978), Prowse and Owens (1982) and Moore and Owens (in press). However, several important assumptions underlying the bulk aerodynamic approach are not discussed adequately by any of these authors. This paper presents a derivation of the bulk aerodynamic transfer coefficients, discusses some of the assumptions and their practical implications, and reviews the field evidence for the validity of the bulk aerodynamic approach.

Theory

The exchanges of momentum (M), sensible heat (Q_H) and latent heat (Q_E) are often expressed in the surface layer by the familiar flux-gradient equations

$$M = \rho K_M \frac{du}{dz} \tag{1a}$$

$$Q_H = \rho c_p K_H \frac{dT}{dz} \tag{1b}$$

$$Q_E = \rho L_V K_E \frac{dq}{dz} \tag{1c}$$

where

M is in $N\ m^{-2}$, and Q_H and Q_E are in $W\ m^{-2}$
ϱ is the air density in $kg\ m^{-3}$
K_M, K_H and K_E are the eddy diffusivities for momentum, sensible heat and water vapour in $m^2\ s^{-1}$
c_p is the specific heat of air at constant pressure in $J\ kg^{-1}\ °C^{-1}$
L_V is the latent heat of vaporisation in $J\ kg^{-1}$
T is air temperature in °C
q is the specific humidity in $g\ g^{-1}$
z is the height above the surface in m

Contrary to micrometeorological convention, the fluxes are here considered positive when directed toward the surface. Eqs. (1) can be expressed in integrated form as (after Deardorff 1968)

$$M = \rho D_M U_\alpha \tag{2a}$$

$$Q_H = \rho c_p D_H (T_\alpha - T_s) \tag{2b}$$

$$Q_E = \rho L_V D_E (q_\alpha - q_s) \tag{2c}$$

where D_M, D_H and D_E are the bulk exchange coefficients for momentum, heat and water vapour in $m\ s^{-1}$ the subscripts s and a refer to the values at the surface and at height z_a.

In practice, the term $(q_a - q_s)$ is replaced by $(0.622/p)\ (e_a - e_s)$, where p is atmospheric pressure (mb) and e is the vapour pressure (mb).

The snow surface temperature has an upper limit of 0°C. During snowmelt, the air temperature is usually greater than 0°C, so atmospheric conditions over melting snow are generally stable (de la Casiniere 1974). Log-linear profiles for wind, temperature and humidity apply in this stability range (Webb 1970), and the gradients can be written

$$\frac{du}{dz} = \frac{u^*}{kz}\phi_M\left(\frac{z}{L}\right) \tag{3a}$$

$$\frac{dT}{dz} = \frac{T^*}{kz}\phi_H\left(\frac{z}{L}\right) \tag{3b}$$

$$\frac{dq}{dz} = \frac{q^*}{kz}\phi_E\left(\frac{z}{L}\right) \tag{3c}$$

$$\phi_i\left(\frac{z}{L}\right) = 1 + b_i\frac{z}{L}$$

where

u^* is the friction velocity $= (M/\varrho)^{1/2}$ in $m\ s^{-1}$
T^* and q^* are temperature and humidity scales analogous to friction velocity

k is von Karman's constant, equal to 0.4
b_i are empirical constants
L is the Monin-Obukov length scale in m.

The length scale, L, is defined by

$$L = \frac{T_k u^{*3} \rho c_p}{kgQ_H}$$

where

T_K is the mean temperature of the air layer in K
g is the gravitational acceleration in m s^{-2}

The eddy diffusivities can be assumed equal for near-neutral to stable conditions (Oke 1970). Equality of diffusivities implies that $\phi_M = \phi_H = \phi_E$; that is, $b_M = b_H = b_E = b$ (Dyer 1974). Dyer (1974) noted that available evidence suggests that $b = 5$. If the eddy diffusitivies are equal, Eqs. (3) can be integrated to yield

$$u_a = \frac{u^*}{k}\left(\ln\frac{z_a}{z_0} + b\frac{z_a}{L}\right) \tag{4a}$$

$$T_a - T_s = \frac{T^*}{k}\left(\ln\frac{z_a}{z_T} + b\frac{z_a}{L}\right) \tag{4b}$$

$$q_a - q_s = \frac{q^*}{k}\left(\ln\frac{z_a}{z_q} + b\frac{z_a}{L}\right) \tag{4c}$$

where

$z_a >> z_o, z_T, z_q$
z_o is the roughness length in m
z_T and z_q are scaling heights for T and q, analogous to z_o, in m.

and the quantities u^*, T^* and q^* are defined by the following expressions (Busch 1973)

$$M = \rho u^{*2} \tag{5a}$$

$$Q_H = \rho c_p u^* T^* \tag{5b}$$

$$Q_E = \rho L_V u^* q^* \tag{5c}$$

Male and Granger (1981) noted that consensus amongst micrometeorologists is divided as to the profile forms for temperature and humidity. Many investigators support an alternative formulation due to Businger, Wyngaard, Izumi and Bradley (1971), in which the right hand sides of Eqs. (4b) and (4c) are multiplied by a factor $R = 0.74$, b is replaced by b/R and $k = 0.35$. However, a re-analysis of the

data set used by Businger *et al.* and an analysis of a new data set support the more traditional formulation given by Eqs. (4b) and (4c), with $k = 0.4$ (Wieringa 1980; Dyer and Bradley 1982).

The bulk exchange coefficients are derived by combining Eqs. (2), (4) and (5); that is

$$D_M = \frac{k^2 u_\alpha}{(\ln \frac{z_\alpha}{z_0} + b \frac{z_\alpha}{L})^2} \tag{6a}$$

$$D_H = \frac{k^2 u_\alpha}{(\ln \frac{z_\alpha}{z_0} + b \frac{z_\alpha}{L})(\ln \frac{z_\alpha}{z_T} + b \frac{z_\alpha}{L})} \tag{6b}$$

$$D_E = \frac{k^2 u_\alpha}{(\ln \frac{z_\alpha}{z_0} + b \frac{z_\alpha}{L})(\ln \frac{z_\alpha}{z_q} + b \frac{z_\alpha}{L})} \tag{6c}$$

Before Eqs. (6) can be applied, the scale heights z_o, z_T and z_q and the stability parameter z_α/L must be known; or alternatively, if z_o is known and T and q are measured at two levels, the fluxes can be calculated iteratively, initially assuming $z_\alpha/L = 0$ (Berkowicz and Prahm 1982). For the case of measurements at only one level, another approach is to assume equality of the scale heights and relate z_α/L to a more readily computed stability parameter.

A commonly used stability parameter is the gradient Richardson number, defined by

$$Ri = \frac{g \frac{dT}{dz}}{T_K (\frac{du}{dz})^2} \tag{7}$$

If $z_T = z_o$ (or equivalently, if $T_o = T(z_o) = T_s$), the bulk form of Ri can be defined as

$$Rb = \frac{g(T_\alpha - T_s)(z_\alpha - z_0)}{T_K u_\alpha^2} \tag{8}$$

If $K_H = K_M$, then Oke (1970) shows that

$$\frac{z}{L} = \frac{Ri}{1 - b\,Ri} \tag{9}$$

From Eqs. (3), (4), (7) and (8), we derive

$$Ri = \frac{Rb\left(\ln \frac{z_\alpha}{z_0} + b \frac{z_\alpha}{L}\right)}{1 + b \frac{z_\alpha}{L}} \tag{10}$$

Combining Eqs. (9) and (10),

$$\frac{z_\alpha}{L} = \frac{Rb \ln \frac{z_\alpha}{z_0}}{1 - b\,Rb} \tag{11}$$

If $z_T = z_q = z_o$, then $D_H = D_E = D_M$. Under neutral conditions $z/L = 0$, so the ratio of the stable and neutral case transfer coefficients (D_S/D_N) is

$$\frac{D_S}{D_N} = \frac{\left(\ln \frac{z_\alpha}{z_0}\right)^2}{\left(\ln \frac{z_\alpha}{z_0} + b \frac{z_\alpha}{L}\right)^2} \tag{12}$$

Substituting Eq. (11) into Eq. (12) gives

$$\frac{D_S}{D_N} = (1 - b\,Rb)^2 \tag{13}$$

Therefore, the bulk exchange coefficients are given by

$$D_H = D_E = D_M = \frac{k^2 u_\alpha (1 - b\,Rb)^2}{\left(\ln \frac{z_\alpha}{z_0}\right)^2} \tag{14}$$

Deardorff (1968) derived ratios of the bulk transfer coefficients for the general case of $D_H \neq D_E \neq D_M$. Anderson (1976) noted that Deardorff's ratios are the same as Eq. (13) if the bulk transfer coefficients are equal. Price (1977) derived ratios of $1/(1 + 10\,Rb)$ for stable conditions and $(1 - 10\,Rb)$ for unstable conditions. These ratios are equivalent to Eq. (13) for small values of Rb, since his derivation assumed that z_α/L is small.

The only unknown quantity in Eq. (14) is z_o. The value of z_o can be calculated for neutral conditions from wind profiles or from wind measurements at two heights z_1 and z_2 according to

$$z_0 = \exp\left(\frac{u_2 \ln z_1 - u_1 \ln z_2}{u_2 - u_1}\right) \tag{15}$$

This formula is sensitive to errors in wind speed, so the scatter is usually large, and

Table 1 – Roughness lengths over melting snow

z_0 (mm)	Remarks	Source
2.5	glacier snow, 1	Sverdrup (1936)
0.9	glacier snow, 1	Wendler and Streten (1969)
0.9	glacier snow, 1	Wendler and Weller (1974)
5.0	seasonal snow, 2	Price (1977)
5.0	suncupped glacier snow, 2	Fohn (1973)
4.0	seasonal snow, 3	Moore and Owens (in press)
5.0	seasonal snow, 4	Anderson (1976)
4.0	seasonal snow, 1	Grainger and Lister (1966)
6.8	"undulating wet snow", 1	Grainger and Lister (1966)
3.0	seasonal snow, 3	Heron and Woo (1978)
.2-.8	level snow cover, 1	Konstantinov (1966)
1-5	average snow cover, 1	Konstantinov (1966)
5-20	weak friable snow, 1	Konstantinov (1966)

Notes:
1. Calculated from profiles.
2. Calculated from Lettau's (1969) formula.
3. Calculated from wind speeds at two heights.
4. Based on calibration of snowmelt model (with stability correction) with lysimeter outflow.

an average value from several runs is required (Berkowicz and Prahm 1982). Alternatively, z_0 has been calculated from Lettau's (1969) formula based on a description of the surface roughness elements (Fohn 1973; Price 1977). Table 1 shows values of z_0 over melting snow given in the literature. The values mostly lie in the range from 1 mm, corresponding to "smooth" snow, to 5 mm, for drifted or suncupped snow. Fig. 1 illustrates the dependece of the bulk transfer coefficients on z_0. The figure shows that if the roughness length can be estimated to within 1 or 2 mm, the resulting error in the calculated flux will be within about 20 %.

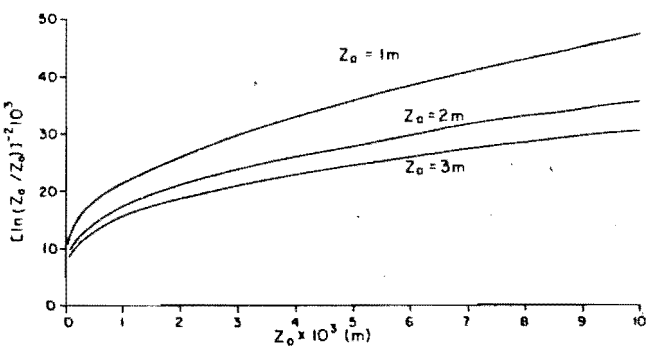

Fig. 1. The dependence of the bulk transfer coefficient on the roughness length.

Assumptions

Three assumptions, besides the validity of the flux-profile relationships, were made in the derivation of Eq. (14). These are the validity of log-linear profiles, the equality of the eddy diffusivities, and the equality of the scale heights for windspeed, temperature and humidity. These assumptions and their implications will be discussed in turn.

Log-Linear Profiles

The derivation of log-linear profiles assumes that there is no radiative or turbulent flux divergence in the atmospheric surface layer (Lumley and Panofsky 1964). During weather situations characterised by light winds, the profiles of wind, temperature and humidity deviate markedly from log-linear forms due to radiative flux divergence and the lack of vertical mixing (Halberstam and Schieldge 1981). However, under these conditions, the sensible and latent heat fluxes are less important than radiation, so inaccuracies in their estimation should not be critical to snowmelt computations. The constant turbulent flux assumption also requires a homogeneous surface and steady state conditions (Lumley and Panofsky 1964). The satisfaction of the steady state requirement is difficult. Brutsaert (1982) suggested the use of averaging times from 20 to 60 min as a compromise between achieving sampling stability and ensuring stationarity of atmospheric conditions. Joffre (1982) discussed stationarity problems in more detail. Homogeneous conditions are rarely met in the field. Fortunately, snowcover tends to smooth small-scale terrain inhomogeneity and produce a homogeneously rough surface. Despite this smoothing by snowcover, two types of inhomogeneity can still exist.

One common form of surface inhomogeneity is a leading edge between snow-free and snow-covered ground. In this situation, horizontal flux divergence occurs, violating one of the assumptions of the aerodynamic approach. However, a numerical analysis by Weisman (1977) indicates that most of the flux divergence occurs within several metres downwind of the leading edge, so that one-dimensional equations such as Eq. (2) should be applicable at the measurement site given a sufficient fetch. Male and Gray (1981) suggested that the height of the constant flux layer is one-hundredth the fetch. Thus, for instrument heights of 1 to 2 m, an upwind fetch of 100 to 200 m should be sufficient.

Terrain features such as slopes and hills affect the structure of turbulence. The analysis by Jackson and Hunt (1975) shows that these effects can be neglected for flow over hills with slopes on the order of 0.05. Furthermore, if the velocity profile upwind of the hill is logarithmic, then it remains logarithmic with the same roughness length in the inner layer as the flow passes over the hill, even though the airflow accelerates (Jensen and Peterson 1978). This statement does not apply to the separated-flow zone on the downwind side of the hill. Field observations by

Mason and Sykes (1979) suggest that the results of Jackson and Hunt apply to hills with slopes much greater than assumed by their theory. There is as yet no consensus as to the effect of flow over hills on a log-linear upwind profile (A. J. Bowen pers. comm.). These results suggest that the aerodynamic approach should be applicable even in the non-ideal field situations confronting most researchers, as long as the terrain is not too complex and the fetch is sufficient.

Equality of Diffusivities

The equality $K_H = K_E = K_M$ is supported in the stable range by several studies (Dyer 1974), but has been questioned by some workers (Male and Gray 1981). The equality of K_H and K_M is supported by most studies,at least for the range of stability in which turbulent exchange is important. However, as mentioned previously, many researchers support the profile formulations of Businger *et al.* (1971), which imply that $K_H/K_M = 1.35$ under neutral conditions, and that von Karman's constant equals 0.35. Unfortunately, the evidence supporting either set of formulations is still inconclusive. The equality of K_E and K_H in the stable range is supported by studies such as Oke (1970) and Webb (1970), while Male and Granger (1981) reported results that show $K_E/K_H = 0.5$ for most of the stable range. Lang, McNaughton, Fazu, Bradley and Ohtaki (1983) presented evidence that $K_E > K_H$ when Q_H is towards the surface and Q_E is away from the surface. However, during many rapid melt situations, Q_H and Q_E are both directed toward the surface, and there appear to be no detailed studies of this situation. Male and Granger (1981) suggest that this controversy might be explained by McBean and Miyake's (1972) statement that universal transfer laws for passive scalars such as moisture may not exist. The evidence against equality of the eddy diffusitivies in the stable range is inconclusive, so the assumption that $K_H = K_E = K_M$ is as reasonable as any other, but carries some degree of uncertainty.

Equality of Scale Heights

The equality of the scale heights is the most problematic assumption, despite the arguments by Joffre (1982) that $z_T = z_o$. Very few values for z_T over melting snow have been given in the literature. Sverdrup (1936) reported values from .072 to .32 mm (z_o = 2.5 mm), while Wendler and Streten (1966) reported $z_T = z_o$ = .9 mm. No values for z_q over melting snow were found, probably because of the difficulty of obtaining accurate measurements of humidity. Unlike z_o, which is primarily a function of surface characteristics, z_T and z_q depend upon the thickness of the laminar boundary layer, and vary with flow conditions. Webb (1975) stated that z_T and z_q equal $D/(nku^*)$, where D is the molecular diffusivity in air (m^2s^{-1}) and n is a parameter equal to 7 for water vapour. Substitution of typical values of u^* over melting snow into this expression yields scale heights one to two orders of magnitude smaller than z_o. Values for z_T and z_q calculated from an alternative expression due to Brutsaert (1975) are similar. Fig. 2 illustrates the dependence of the neu-

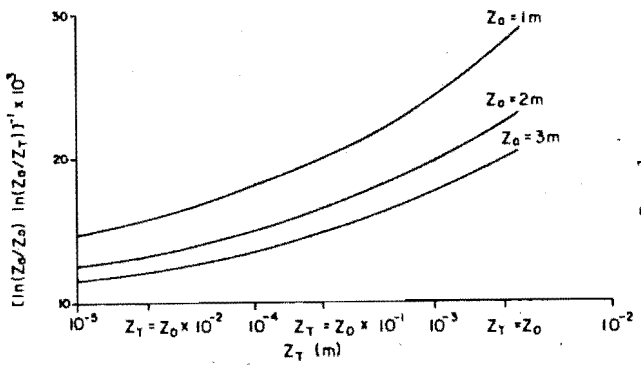

Fig. 2.
The dependence of the neutral case bulk transfer coefficient on the temperature scaling length for z_o = .0025.

tral-case bulk transfer coefficient on a variable z_T, given z_o = 2.5 mm. If $z_T = z_o/10$, assuming that $z_T = z_o$ will produce an overestimate of 30-40 %, depending on the measurement height; and if $z_T = z_o/100$, the overestimate will be 65-75 %. However, as discussed in the next section, the studies which have employed bulk aerodynamic formulae do not report a positive bias in the snowmelt computed from the energy budget, which would be expected from the considerations given above.

At least a partial answer to the problem posed by unequal scale heights can be found by examining their effect on the stability correction. Consider a situation in which the profiles of windspeed, temperature and humidity are given by Eqs. (4). The value of *Rb* which is calculated from the measurements and is used to compute the stability correction is given by

$$Rb_C = \frac{Ri\left(1+b\frac{z}{L}\right)\left(\ln\frac{z}{z_T} + b\frac{z}{L}\right)}{\left(\ln\frac{z}{z_0} + b\frac{z}{L}\right)^2}$$

where *Ri* and *z/L* are given for any height from the profiles. The value of *Rb* assumed by the derivation of the stability correction is given by

$$Rb_A = \frac{Ri\left(1+b\frac{z}{L}\right)}{\ln\frac{z}{z_0} + b\frac{z}{L}}$$

The ratio of Rb_C to Rb_A is

$$\frac{Rb_C}{Rb_A} = \frac{\ln\frac{z}{z_T} + b\frac{z}{L}}{\ln\frac{z}{z_0} + b\frac{z}{L}} \qquad (16)$$

Eq. (11) was solved to calculate Rb_A as a function of *z/L*; Rb_C was then calculated from Eq. (16). Fig. 3 shows the ratios of the stability correction calculated from Rb_C to that calculated from Rb_A as a function of Rb_C. As Rb_C and stability

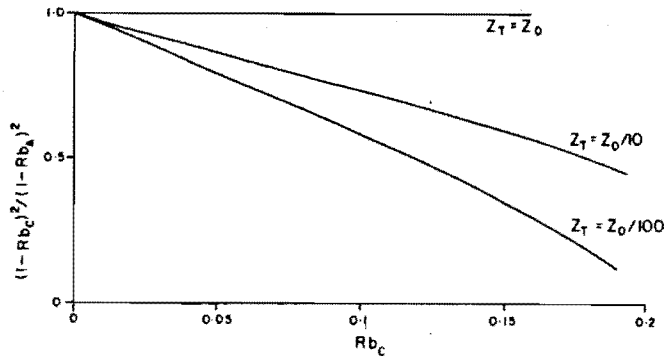

Fig. 3.
Ratio of the stability corrections using calculated and assumed values of *Rb*.

increase, the ratio of the corrections decreases, tending to compensate for the overestimation caused by assuming $z_T = z_q = z_o$. The point at which the bulk transfer coefficient overestimation and the correction factor underestimation compensate for each other is at $Rb_C = .095$ for $z_T = z_o/10$ and at $Rb_C = .098$ for $z_T = z_o/100$. Anderson (1976) found that turbulent exchange was most significant as an energy source for snowmelt for Rb_C in the range .05 to .09. In this range, the positive bias due to variations from $z_T = z_0$ would average on the order of 10 %, and could be masked by instrument error or uncertainty in the value of z_o. However, more research is required on the behaviour of z_T and z_q over melting snow, and the implications for heat and vapour transfer.

Field Experience

Several studies have employed bulk aerodynamic formulae in conjunction with measurements or estimates of the snow surface radiative exchange to compute snowmelt. Anderson (1976) compared computed snowmelt with lysimeter outflow for both daily and hourly periods. The agreement in both cases was good, with a negative bias of 6 %. Heron and Woo (1978) found on a daily basis that melt estimated from the energy budget agreed to within 25 % of melt computed from depth and density measurements, except during the initial melt period, when the snowpack was ripening, and during the late melt period, when the snowcover was patchy. Moore and Owens (in press) found that computed snowmelt over an eight day period agreed to within 3 % of that calculated from depth and density measurements. Price (1977) found good agreement between computed melt and runoff from a hillslope on a daily basis, with a standard error about the regression line (which was not significantly different from the 1:1 line) of 7 mm/d.

There are two problems associated with using these comparisons to verify the bulk aerodynamic formulae. First, errors in the computed melt may be caused by errors in the radiative exchange, which in most of the cases was the greatest source of energy for snowmelt. Second, the errors involved in determining daily ablation from depth and density are possibly of the same magnitude as the errors in daily

computed snowmelt.

Male and Granger (1979) compared daily values of Q_H and Q_E computed from bulk aerodynamic formulae with "measured" values. Their comparison indicates that the bulk aerodynamic formulae are not accurate, and overestimate evaporation. They attributed the scatter to the radiative heating of the lower air layers, which would cause profiles of windspeed, temperature and humidity to deviate from log-linear forms. It is difficult to assess this comparison because Male and Granger did not give details of their computation, such as the value of z_0 used and the averaging time for the values of windspeed, temperature and humidity; nor did they state how they measured Q_H and Q_E. In conditions similar to those for which this comparison was made, Q_H and Q_E are usually much less important than radiative exchange for snowmelt. The conditions in which Q_H and Q_E are important to the energy budget are often characterised by moderate to strong winds and low insolation – conditions in which log-linear profiles are most likely to apply.

Conclusions

Formulae relating the turbulent exchanges of sensible and latent heat over melting snow to measurements of windspeed, temperature and humidity at one level can be derived from flux-gradient relationships and assumed profile forms. These bulk aerodynamic formulae are superior to empirical wind functions because they can account for differences in stability, surface conditions and measurement heights, and do not have to be empirically calibrated. The main problem in their application is in specifying the roughness length. Fortunately, the roughness length ranges over less than an order of magnitude, and the formulae are not critically sensitive to changes in the roughness length. Field experience indicates that the bulk aerodynamic formulae are adequate for use in energy budget computations of daily or shorter-term snowmelt. However, bulk aerodynamic computations of Q_H and Q_E need to be tested directly against more accurate methods under a variety of conditions to make clear their limitations.

The most problematic assumption underlying the bulk aerodynamic approach is the equality of the scale heights for wind, temperature and humidity. More research needs to be carried out on the behaviour of the scale heights for temperature and humidity over melting snow, and the implications for heat and vapour transfer.

Acknowledgements

I would like to thank Professor Hans Panofsky for several stimulating conversations. Dr. Colin Taylor read and made useful comments on the manuscript. The comments made by the anonymous referee are also appreciated.

References

Anderson, E. A. (1976) A point energy and mass balance model of a snow cover. Tech Memo. NWS 19 NOAA, Washington, D.C. [illegible]

Berkowicz, R., and Prahm, L. P. (1982) Evaluation of the profile method for estimation of surface fluxes of momentum and heat. *Atmospheric Environment, Vol. 16,* pp. 2809-2819.

Brutsaert, W. (1975) The roughness length for water vapour, sensible heat and other scalars. *J. Atmos. Sci., Vol. 32,* pp 2028-2031.

Brutsaert, W. (1982) *Evaporation into the Atmosphere.* D. Reidel, Dordrecht.

Busch, N. E. (1973) On the mechanics of atmospheric turbulence. In: *Workshop on Micrometeorology,* edited by D. A. Haugen, American Meteorological Society, Boston, pp. 1-65.

Businger, J. A., Wyngaard, J. C., Izumi, Y., and Bradley, E. F. (1971) Flux-profile relationships in the atmospheric surface layer. *J. Atmos. Sci., Vol. 28,* pp 181-189.

Deardorff, J. W. (1968) Dependence of air-sea transfer coefficients on bulk stability. *J. Geophys. Res., Vol. 73,* pp 2549-2557.

de la Casiniere, A. C. (1974) Heat exchange over a melting snow surface. *J. Glaciol., Vol. 13,* pp 55-72.

Dyer, A. J. (1974) A review of flux-profile relationships. *Boundary-Layer Meteorol., Vol. 7,* pp 363-372.

Dyer, A. J., and Bradley, E. F. (1982) An alternative analysis of flux-gradient relationships at the 1976 ITCE. *Boundary-Layer Meteorol., Vol. 22,* pp 3-19.

Fohn, P. M. B. (1973) Short-term snow melt and ablation derived from heat- and mass-balance measurements. *J. Glaciol., Vol. 12,* pp 275-289.

Grainger, M. E., and Lister, H. (1966) Windspeed, stability and eddy viscosity over melting ice surfaces. *J. Glaciol., Vol. 6,* pp 101-127.

Halberstam, I., and Schieldge, J. P. (1981) Anomalous behaviour of the atmospheric surface layer over a melting snow pack. *J. Appl. Meteorol., Vol. 20,* pp 255-265.

Hendrick, R. L., Filgate, B. D., and Adams, W. D. (1971) Application of environmental analysis to watershed snowmelt. *J. Appl. Meteorol., Vol. 10,* pp 418-429.

Heron, R., and Woo, M.-K. (1978) Snowmelt computations for a high Arctic site. Proceedings, 35th Eastern Snow Conference, Hanover, New Hampshire, pp 162-172.

Jackson, P. S., and Hunt, J. C. R. (1975) Turbulent wind flow over a low hill. *Quart. J. Roy. Meteorol. Soc., Vol. 101,* pp 929-955.

Jensen, N. O., and Peterson, E. W. (1978) On the escarpment wind profile. *Quart. J. Roy. Meteorol. Soc., Vol. 104,* pp. 719-728.

Joffre, S. M. (1982) Momentum and heat transfers in the surface layer over a frozen sea. *Boundary-Layer Meteorol., Vol. 24,* pp 211-229.

Konstantinov, A. R. (1966) *Evaporation in Nature.* Israel Program for Scientific Translations, Jerusalem.

Lang, A. R. G., McNaughton, K. G., Fazu, C., Bradley, E. F., and Ohtaki, E. (1983) Inequality of eddy transfer coefficients for vertical transport of sensible and latent heat during advective inversions. *Boundary-Layer Meteorol., Vol. 25,* pp 25-42.

Lettau, H. (1969) Note on aerodynamic roughness-parameter estimation on the basis of roughness-element description. *J. Appl. Meteorol., Vol. 8,* pp 828-832.

Light, P. (1941) Analysis of high rates of snow melting. *Trans. Am. Geophys. Union, Vol. 22,* pp 195-205.

Lumley, J. L., and Panofsky, H. A. (1964) *The Structure of Atmospheric Turbulence.* John Wiley and Sons, New York.

Male, D. H., and Granger, R. J. (1979) Energy and mass fluxes at the snow surface in a Prairie environment. In: Proceedings, Modeling of Snow Cover Runoff, edited by S. C. Colbeck and M. Ray, CRREL, Hanover, New Hampshire, pp 101-124.

Male, D. H., and Granger, R. J. (1981) Snow surface energy exchange. *Water Resour. Res., Vol. 17,* pp 609-627.

Male, D. H., and Gray, D. M. (1981) Snowcover ablation and runoff, In: *Handbook on Snow,* edited by D. M. Gray and D. H. Male, Pergamon Press, Toronto, pp 360-436.

Mason, P. J., and Sykes, R. I. (1979) Flow over an isolated hill of moderate slope. *Quart. J. Roy. Meteorol. Soc., Vol. 105,* pp 383-395.

Moore, R. D., and Owens, I. F. (in press) Controls on advective snowmelt in a maritime alpine basin. *J. Climate Appl. Meteorol.*

McKay, D. C., and Thurtell, G. W. (1978) Measurements of the energy fluxes involved in the energy budget of a snow cover. *J. Appl. Meteorol., Vol. 17,* pp. 339-349.

Oke, T. R. (1970) Turbulent transfer near the ground in stable conditions. *J. Appl. Meteorol., Vol. 9,* pp. 778-786.

Price, A. G. (1977) Snowmelt runoff processes in a subarctic area. Climatology Research Series No. 10, McGill University, Montreal.

Prowse, T. D., and Owens, I. F. (1982) Energy balance over melting snow, Craigieburn Range, New Zealand. *J. Hydrol. (N.Z.), Vol. 21,* pp 133-147.

Sverdrup, H. U. (1936) The eddy conductivity of the air over a smooth snow field. *Geofys. Publikasjoner, Vol. 11,* pp. 1-69.

Webb, E. K. (1970) Profile relationships: the log-linear range and extension to strong stability. *Quart. J. Roy. Meteorol. Soc., Vol. 96,* pp 67-90.

Webb, E. K. (1975) Evaporation from catchments, In: *Prediction in Catchment Hydrology,* edited by T. G. Chapman and F. X. Dunin, Australian Academy of Science, Sydney, pp 203-236.

Weisman, R. N. (1977) Snowmelt: a two-dimensional turbulent diffusion model. *Water Resour. Rs., Vol. 13,* pp 337-342.

Wendler, G., and Streten, N. A. (1969) A short term heat balance study on a Coast Range glacier. *Pure and Applied Geophysics, Vol. 77,* pp 68-77.

Wendler, G., and Weller, G. (1974) A heat balance study of the McCall Glacier, Brooks Range, Alaska: A contribution to the International Hydrological Decade. *J. Glaciol., Vol. 13,* pp 13-26.

Wieringa, J. (1980) A re-evaluation of the Kansas mast influence on measurements of stress and cup anemometer everspeeding. *Boundary-Layer Meteorol., Vol. 18,* pp 411-430.

Received: 5 August, 1983

Address:
Geography Department,
University of Canterbury,
Private Bag,
Christchurch, New Zealand.

Appendix B - Listing of runoff model.

```
      CHARACTER*12 JUDAY1
      CHARACTER*40 LABEL
      REAL ELEV(10),FST(10),GL(10),AREA(10)
      REAL PCS(2000)
      REAL ASWE(10),PET(12),QM(2000),QOBS(2000),FSWE(10)
     1,SLW(10)
      COMMON /BLK1/ TB,A1,A2,RMF,CRF,WRC
      COMMON /BLK2/ FC,CL,BETA
      COMMON /BLK3/ PERC,C0,C1,C2,UZL,SUZ,SLZ,WET
      COMMON /BLK4/ SUZIN,SLZIN
      COMMON /BLK5/ CR,LMAX
      COMMON /BLK6/ PCS
      OPEN(5,FILE='SIM82',STATUS='OLD')
      OPEN(6,FILE='INVER',STATUS='OLD')
      OPEN(8,FILE='QOUT',STATUS='OLD')
      OPEN(9,FILE='OUTSIM',STATUS='OLD')
C
C     READ IN BASIN PARAMETERS: NZ=# OF ELEVATION ZONES;
C     IDAY,LDAY,JUDAY1=JULIAN DAY NUMBERS OF FIRST AND LAST
C     DAYS AND DATE OF FIRST DAY; BAREA=BASIN AREA (KM**2);
C     ELEV=ZONE MEAN ELEVATION (M); GL=FRACTION OF ZONE IN
C     TUSSOCK; PET=POTENTIAL EVAPOTRANSPIRATION (MM/D);
C     AREA=ZONE AREA (KM**2); FST=FRACTION OF ZONE IN
C     FOREST.
      READ(6,100) LABEL
      READ(6,101) NZ,IDAY,LDAY,JUDAY1
      READ(6,102) BAREA,WET
      READ(6,102) (ELEV(I),I=1,NZ)
      READ(6,102) (AREA(I),I=1,NZ)
      READ(6,102) (FST(I),I=1,NZ)
      READ(6,102) (GL(I),I=1,NZ)
      READ(6,102) (PET(I),I=1,12)
  100 FORMAT(A40)
  101 FORMAT(I3,2I6,A12)
  102 FORMAT(20F6.1)
  103 FORMAT(3I2,5F6.1,F4.1)
C
C     READ IN SNOW ROUTINE PARAMETERS: TB=RAIN/SNOW
C     DISCRIMINATION TEMPERATURE (C); A1,A2=WIND FUNCTION
C     PARAMETERS; RMF=RADIATION MELT FACTOR;
C     CRF=REFREEZING COEFFICIENT; WRC=WATER
C     RETENTION CAPACITY.
C
      READ(6,102) TB,A1,A2,RMF,CRF,WRC
C
C     READ IN SOIL AND RESPONSE FUNCTION PARAMETERS;
C     SET INITIAL VALUES.
C
      READ(6,102) FC,CL,BETA,PERC,C0,C1,C2,UZL,SUZIN,SLZIN
      SM=FC
      SUZ=SUZIN
```

```
      SLZ=SLZIN
C
C     INITIALIZE SNOW STORAGE: ASWE=OPEN ZONE STORAGE;
C     FSWE=FOREST STORE;
C     SLW=LIQUID WATER CONTENT OF SNOW.
C
      DO 1 J=1,NZ
       ASWE(J)=0.
      SLW(J)=0.
    1  FSWE(J)=0.
C
C     READ IN DATA FOR EACH DAY
C
      DO 2 I=IDAY,LDAY
       READ(5,103) NY,M,ND,TCF,TSB,DP,PCS(I),QOBS(I)
      TG=(TSB-TCF)/636.
      IF(DP.LT.0.) DP=0.
      VAREA=0.
      DRO=0.
      P=PCS(I)
C
C     LOOP THROUGH EACH ELEVATION ZONE
C
      DO 3 IZ=1,NZ
C
C     COMPUTE ZONE TEMPERATURE AND CALL SNOW ROUTINE
C
      T=TCF+(ELEV(IZ)-914.)*TG
      CALL SNOW(T,P,DP,M,ND,ASWE,SLW,FSWE,FST,GL,VFRAC,
     1IZ,ZRO)
      DRO=DRO+ZRO*AREA(IZ)
    3 VAREA=VAREA+VFRAC*AREA(IZ)
C
C     CALCULATE BASIN WATER INPUT, EVAPORATING AREA,
C     ROUTE THROUGH SOIL MOISTURE AND STORAGES.
C
      VAREA=VAREA/BAREA
      W=DRO/BAREA
      CALL SOIL(M,SM,VAREA,W,DUZ,PET)
      CALL RESFUN(DUZ,RO,PET,M)
C
C     CONVERT RO IN MM/D TO L/S
C
      QM(I)=RO*BAREA*10.**6/86400.
    2 WRITE(9,111) NY,M,ND,(ASWE(K),K=1,6),SUZ,SLZ,PCS(I),W
     1,QOBS(I),QM(I),SM
  111 FORMAT(3I2,13F6.1)
      CALL OUTPUT(QM,QOBS,IDAY,LDAY,JUDAY1,BAREA,LABEL)
      STOP
      END
C
C
      SUBROUTINE SNOW(TA,P,DP,M,ND,ASWE,SLW,FSWE,FST,GL,
     1VFRAC,IZ,ZRO)
      REAL ASWE(10),FSWE(10),FST(10),GL(10),SLW(10)
      COMMON /BLK1/ TB,A1,A2,RMF,CRF,WRC
```

```
      ARO=0.
      FRO=0.
      IF(TA.GT.TB) GO TO 10
C
C     TA LE TB: CHECK FOR NEW SNOW AND ADD TO PACK
C
      IF(P.EQ.0..AND.TA.GT.0.) GO TO 10
      ASWE(IZ)=ASWE(IZ)+P
      FSWE(IZ)=FSWE(IZ)+P*.7
      TR=TA
      IF(TR.GT.0.) TR=0.
      RFR=CRF*(0.-TR)
      IF(RFR.GT.SLW(IZ)) GO TO 1
      SLW(IZ)=SLW(IZ)-RFR
      ASWE(IZ)=ASWE(IZ)+RFR
      GO TO 20
    1 ASWE(IZ)=ASWE(IZ)+SLW(IZ)
      SLW(IZ)=0.
      GO TO 20
C
C     NO NEW SNOW; CALCULATE ALPINE ZONE CONDITIONS
C
   10 IF(FST(IZ).EQ.1.) GO TO 40
      IF(ASWE(IZ).EQ.0.) GO TO 30
      IF(P.GT.10.) AMELT=RMELT(TA,P,DP,A1,A2)
      IF(P.LE.10.) AMELT=CWMELT(TA,DP,A1,A2,M,ND,RMF)
      IF(AMELT.GT.ASWE(IZ)) GO TO 2
      ASWE(IZ)=ASWE(IZ)-AMELT
      WCAP=ASWE(IZ)*WRC
      IF(AMELT+P+SLW(IZ).LT.WCAP) GO TO 3
      ARO=(AMELT+P+SLW(IZ)-WCAP)*(1.-FST(IZ))
      SLW(IZ)=WCAP
      GO TO 4
    3 SLW(IZ)=SLW(IZ)+P+AMELT
      ARO=0.
      GO TO 4
    2 ARO=(ASWE(IZ)+SLW(IZ)+P)*(1.-FST(IZ))
      ASWE(IZ)=0.
      SLW(IZ)=0.
    4 IF(FST(IZ).EQ.0.) GO TO 20
      GO TO 40
C
C     NO SNOW IN ALPINE; CALCULATE NET PRECIPITATION
C
   30 ARO=P*(1.-FST(IZ)-.2*GL(IZ))
      IF(FST(IZ).EQ.0.) GO TO 20
C
C     NO NEW SNOW; CALCULATE FOREST ZONE CONDITIONS
C
   40 FMELT=TA*(1.5+P*.7/79.7)
      IF(FMELT.GT.FSWE(IZ)) FMELT=FSWE(IZ)
      FSWE(IZ)=FSWE(IZ)-FMELT
      FRO=(FMELT+P*.7)*FST(IZ)
C
C     CALCULATE NET WATER INPUT AND EVAPORATING AREA
C
```

```
 20     ZRO=FRO+ARO
       VFRAC=FST(IZ)
       IF(ASWE(IZ).EQ.0.) VFRAC=1.
       RETURN
       END
C
       FUNCTION RMELT(TA,P,DP,A1,A2)
       E=6.11*10.**(7.5*TA/(TA+237.3))
       QN=4.6*TA
       QTURB=(A1+A2*DP)*(.56*TA+(E-6.11))
       QP=P*TA/20.65
       RMELT=(QN+QTURB+QP)*.259
       RETURN
       END
C
       FUNCTION CWMELT(TA,DP,A1,A2,M,ND,RMFX)
       RMF=RMFX*(1.+COS((30*(M-1)+ND+9)*6.28/365.))/2.
       CWMELT=RMF*TA+.56*TA*(A1+A2*DP)*.259
       RETURN
       END
C
C
       SUBROUTINE SOIL(M,SM,VAREA,W,DUZ,PET)
       REAL PET(12)
       COMMON /BLK2/FC,CL,BETA
C
C      ADD WATER INPUT MM BY MM
C
       DUZ=0.
       NW=IFIX(W)
       SM=SM+W-NW
       IF(SM.LE.FC) GO TO 50
       Y=SM-FC
       SM=FC
       DUZ=DUZ+Y
 50    DO 1 J=1,NW
        SM=SM+1.
        IF(SM.GE.FC) DUZ=DUZ+1.
  1     IF(SM.LT.FC) DUZ=DUZ+(SM/FC)**BETA
C
C      TAKE AWAY THROUGHFLOW AND EVAPORATION
C
       SM=SM-DUZ
       EVAP=PET(M)
       IF(SM.LT.CL) EVAP=(SM/CL)*PET(M)
       SM=SM-EVAP*VAREA
       IF(SM.LT.0.) SM=0.
       RETURN
       END
C
C
       SUBROUTINE RESFUN(DUZ,Q,PET,M)
       COMMON /BLK3/PERC,C0,C1,C2,UZL,SUZ,SLZ,WET
       REAL PET(12)
C
C       ADD WATER FROM SOIL TO UPPER ZONE, SUBTRACT PERC
```

```
C
      SUZ=SUZ+DUZ
      PERC1=PERC
      IF(SUZ.LT.PERC) PERC1=SUZ
      SUZ=SUZ-PERC1
C
C     RELEASE WATER FROM STORAGES; Q UNITS ARE MM/D
C
      Q0=0.
      IF(SUZ.GT.UZL) Q0=C0*(SUZ-UZL)
      Q1=0.
      SUZ=SUZ-Q0
      IF(SUZ.GT.0.) Q1=C1*SUZ
      SUZ=SUZ-Q1
      Q2=0.
      IF(SLZ.GT.0.) Q2=C2*SLZ
      SLZ=SLZ-Q2+PERC1
      SLZ=SLZ-PET(M)*WET
      IF(SLZ.LT.0.) SLZ=0.
      Q=Q0+Q1+Q2
      RETURN
      END
C
C
      SUBROUTINE OUTPUT(QM,QOBS,IDAY,LDAY,JUDAY1,BAREA,
     1LABEL)
      COMMON /BLK4/SUZIN,SLZIN
      COMMON /BLK1/ TB,A1,A2,RMF,CRF,WRC
      COMMON /BLK5/ CR,LMAX
      COMMON /BLK2/FC,CL,BETA
      COMMON /BLK3/PERC,C0,C1,C2,UZL,SUZ,SLZ,WET
      REAL QM(LDAY),QOBS(LDAY)
      CHARACTER*40 LABEL
      CHARACTER*12 JUDAY1
      WRITE(8,101) LABEL
  101 FORMAT(10X,A40)
      WRITE(8,110) TB,A1,A2,RMF
  110 FORMAT(10X,'TB = ',F4.1,' A1 =',F6.1,' A2 =',F6.1,
     1' RMF =',F6.1)
      WRITE(8,120) CRF,WRC
  120 FORMAT(10X,'CRF = ',F6.2,'; WRC = ',F6.2)
      WRITE(8,102) FC,CL,BETA
  102 FORMAT(10X,'FC =',F5.0,2X,'CL = ',F5.0,2X,'BETA = ',
     1F4.1)
      WRITE(8,103) C0,C1,C2,PERC
  103 FORMAT(10X,'C0 = ',F5.3,2X,'C1 = ',F5.3,2X,'C2 = '
     1,F5.3,2X,'PERC = ',F4.1)
      WRITE(8,111) WET,CR,LMAX
  111 FORMAT(10X,' WET =',F4.2,' CR =',E8.3,' LMAX =',I3)
      WRITE(8,104) UZL,SUZIN,SLZIN
  104 FORMAT(10X,'UZL = ',F5.1,2X,'INIT. STORES:',
     1 ' SUZ = ',F5.1,2X,'SLZ = ',F5.1)
      CALL MODEFF(QOBS,QM,IDAY,LDAY,FSQ,F0SQ,E)
      WRITE(8,105) FSQ,F0SQ,E
  105 FORMAT(10X,'FSQ = ',E10.4,4X,'F0SQ = ',E10.4,4X,
     1'E = ',F6.4)
```

```
      CALL REGRES(QOBS,QM,IDAY,LDAY,A,B,SEA,SEB,RSQ,F,NDF,
     1CUMERR,BAREA)
      WRITE(8,106) CUMERR
106   FORMAT(10X,'CUMULATIVE ERROR = ',F6.0)
      WRITE(8,107) A,B
107   FORMAT(10X,'REGRESSION  QM = A + B*QOBS, A = ',F7.2,
     12X,'B = ',F7.4)
      WRITE(8,108) RSQ,SEA,SEB
108   FORMAT(10X,'RSQ = ',F6.4,2X,'STD ERRORS, A:',F7.2,2X,
     1'B:',F7.4)
      WRITE(8,109) F,NDF
109   FORMAT(10X,'F = ',F8.2,3X,'DF = ',I5)
      CALL PLOT(QM,QOBS,IDAY,LDAY,JUDAY1,BAREA)
      RETURN
      END

      SUBROUTINE PLOT(QM,QOBS,IDAY,LDAY,JUDAY1,BAREA)
      DIMENSION QM(LDAY),QOBS(LDAY),PCS(2000)
      CHARACTER*12 JUDAY1
      CHARACTER*1 CHAR(130)
      COMMON /BLK6/ PCS
      WRITE(8,101) JUDAY1
101   FORMAT(10X,'JULIAN DAY 1 = ',A12)
      WRITE(8,102)
102   FORMAT('JULIAN',T21,'DISCHARGE (L/S)   M=MODEL',T71,
     1'ACC. DIFF.  (MM)',T105,'PRECIPITATION (MM)')
      WRITE(8,103)
103   FORMAT(' DAY',T39,'O = OBSERVED')
      WRITE(8,104) 100,200,300,400,500,-500,0,500,0,100,200
104   FORMAT('(DOWN)',T11,'0',1X,5(7X,I3),6X,I4,8X,I1,8X,I3,
     1T100,I1,T109,I3,T119,I3)
      WRITE(8,105) IDAY-1
105   FORMAT(6X,I3,1X,'+',5('*********+'),9X,'+',
     12('*********+'),9X,'+',3('*********+'))
      ACCDIF=0.
      DO 2 I=IDAY,LDAY
       DO 1 J=1,130
1       CHAR(J)=' '
      CHAR(11)='I'
      CHAR(81)='I'
      CHAR(100)='I'
      JMOD=IFIX((QM(I)+5.)/10.)+11
      JOBS=IFIX((QOBS(I)+5.)/10.)+11
      ACCDIF=ACCDIF+(QM(I)-QOBS(I))*86400./(BAREA*10.**6)
      JAD=81+IFIX((ACCDIF+SIGN(25.,ACCDIF))/50.)
      IF(JMOD.GT.100) JMOD=100
      IF(JAD.GT.100) JAD=100
      IF(JOBS.GT.100) JOBS=100
      JRAIN=IFIX((PCS(I)+5.)/10.)+100.
      IF(JRAIN.GT.130) JRAIN=130
      DO 4 J=101,JRAIN
4      CHAR(J)='R'
      N10=I-10*(I/10)
      CHAR(JMOD)='M'
      CHAR(JOBS)='O'
      CHAR(JAD)='X'
```

```
      IF(N10.EQ.0) GO TO 3
      WRITE(8,106)  (CHAR(J),J=1,130)
 106  FORMAT(130A1)
      GO TO 2
  3   CHAR(11)='+'
      CHAR(81)='+'
      CHAR(100)='+'
      WRITE(8,107)I,(CHAR(J),J=10,130)
 107  FORMAT(5X,I4,121A1)
  2   CONTINUE
      RETURN
      END
C
C
      SUBROUTINE MODEFF(X,Y,IN,LN,FSQ,F0SQ,E)
      REAL X(LN),Y(LN)
      SUMX=0.
      SUMX2=0.
      SUMY=0.
      FSQ=0.
      N=LN-IN+1
      DO 1 I=IN,LN
       SUMX=SUMX+X(I)
       SUMX2=SUMX2+X(I)**2
       SUMY=SUMY+Y(I)
 1     FSQ=FSQ+(Y(I)-X(I))**2
      F0SQ=SUMX2-SUMX**2/N
      E=(F0SQ-FSQ)/F0SQ
      RETURN
      END
C
C
      SUBROUTINE REGRES(X,Y,IN,LN,A,B,SEA,SEB,R2,F,NDF,
     1CUMERR,BAREA)
      REAL X(LN),Y(LN)
      SUMX=0.
      SUMX2=0.
      SUMY=0.
      SUMY2=0.
      SUMXY=0.
      N=LN-IN+1
      DO 1 I=IN,LN
       SUMX=SUMX+X(I)
       SUMX2=SUMX2+X(I)**2
       SUMY=SUMY+Y(I)
       SUMY2=SUMY2+Y(I)**2
  1    SUMXY=SUMXY+X(I)*Y(I)
      XM=SUMX/N
      YM=SUMY/N
      CUMERR=(SUMY-SUMX)*86400./(BAREA*10.**6)
      NDF=N-2
      B=(SUMXY-SUMX*SUMY/N)/(SUMX2-(SUMX**2)/N)
      A=YM-B*XM
      SSREG=B*(SUMXY-SUMX*SUMY/N)
      SSTOT=SUMY2-(SUMY**2)/N
      R2=SSREG/SSTOT
```

```
      SEY=SQRT((SSTOT-SSREG)/NDF)
      F=SSREG/SEY**2
      SEB=SEY/SQRT(SUMX2-SUMX**2/N)
      SEA=SEY*SQRT(SUMX2/(N*SUMX2-SUMX**2))
      RETURN
      END
C
C
      SUBROUTINE CHANNL(QG,I,QM)
      COMMON /BLK5/CR,LMAX
      REAL QM(1000),F(50)
C
C     DETERMINE BASE OF TRANSFER FUNCTION
C
      L=LMAX-CR*QG
      L=(L/2)*2+1
      IF(L.LT.1) L=1
C
C     COMPUTE TRANSFER FUNCTION
C
      IF(L.EQ.1) GO TO 1
      N=L/2+1
      SUM=0.
      DO 2 J=1,L
       F(J)=FLOAT(J)
       IF(J.GT.N) F(J)=FLOAT(L+1-J)
   2   SUM=SUM+F(J)
C
C     CONVOLUTE QG WITH TF
C
      DO 3 J=1,L
   3   QM(I+J-1)=QM(I+J-1)+QG*F(J)/SUM
      GO TO 4
   1  QM(I)=QG
   4  RETURN
      END
```